Study of Geological and Morphological Controls on the Occurrence of Natural Terrain Landslide Clusters in Selected Catchments in Hong Kong

GEO Report No. 362

D.L.K. Tang, C.C.J. Wong, Y.M. Sin, A.H.Y. Wong, S.H.S. Leung & K.L.H. Lo

Geotechnical Engineering Office
Civil Engineering and Development Department
The Government of the Hong Kong
Special Administrative Region

[Blank Page]

Study of Geological and Morphological Controls on the Occurrence of Natural Terrain Landslide Clusters in Selected Catchments in Hong Kong

GEO Report No. 362

D.L.K. Tang, C.C.J. Wong, Y.M. Sin, A.H.Y. Wong, S.H.S. Leung & K.L.H. Lo

This report was originally produced in March 2021 as GEO Geological Report No. GR 1/2021

First published, December 2022

Prepared by:

Geotechnical Engineering Office,
Civil Engineering and Development Department,
Civil Engineering and Development Building,
101 Princess Margaret Road,
Homantin, Kowloon,
Hong Kong.

Preface

In keeping with our policy of releasing information which may be of general interest to the geotechnical profession and the public, we make available selected internal reports in a series of publications termed the GEO Report series. The GEO Reports can be downloaded from the website of the Civil Engineering and Development Department (http://www.cedd.gov.hk) on the Internet.

Raymond WM Cheung
Head, Geotechnical Engineering Office
December 2022

Foreword

This report synthesises the findings of an investigation on the occurrence of natural terrain landslide clusters in seven selected catchments in Hong Kong, including a pilot study catchment above Keung Shan Road in West Lantau which was documented in GEO Geological Report No. GR1/2018. The objective of the project is to study the potential links between natural terrain landslides and geological/geomorphological settings. The ultimate goal is to offer possible physical explanations for the observed spatial landslide distribution, to support the territory-wide landslide susceptibility model established by the GEO.

This study was carried out by Dr Denise L.K. Tang, Ms Clio C.J. Wong, Ms Y.M. Sin, Ms Aries H.Y. Wong, Mr Simon S.H. Leung and Mr Kevin L.H. Lo of the Planning Division. Dr Julian S.H. Kwan provided comments on an earlier draft of this report. Mr Steven Williamson, of AECOM China Ltd., is thanked for his valuable discussions on the geomorphology and landslide characteristics of the catchment above Fan Kam Road. Technical officers, Ms S.M. Chan, Messrs C.S. Chung, K.W. Pau and Y.H. Tang provided resourceful support in the ArcGIS spatial analyses and manipulation of LiDAR data. All their contributions are gratefully acknowledged.

Jeffrey C F Wong
Chief Geotechnical Engineer/Planning

Abstract

Understanding the distribution of natural terrain landslides, in particular when and where they occurred in clusters, is vital for managing the landslide risk. Previous rainfall and landslide susceptibility analyses revealed the connections between intense rainstorms and general slope gradient with landslide frequency. Yet, the observed spatial distribution of landslide clusters requires more specific physical, geological and/or geomorphological explanation. This study investigated seven catchments, located in west Lantau Island (4 nos.), central New Territories (2 nos.) and east Kowloon (1 no.), all with notable landslide clusters but of various morphological settings and underlying geology. Detailed review of catchment characteristics, geomorphological mapping, spatial analysis of relict and recent failures were conducted. The clustered landslides were generally small, shallow failures in thin colluvium or saprolite, which suggest that they were primarily caused by continuing weathering on over-steepened slopes. Based on our findings, mature bowl-shaped drainage depressions, break-in-slopes associated with geological contacts and over-steepened incised slopes have been recognised as prime locations of multiple, repeated landslides. Potential influence of human disturbance and catchment characteristics on landslide clustering has been reviewed, although no conclusive correlation could be identified from the seven studied catchments.

Contents

List of Tables

List of Figures

1 Introduction

In order to understand the occurrence of landslide clusters and investigate the potential underlying geological and geomorphological controls, the Planning Division has conducted a review study on natural terrain catchments with notable landslide clusters. The ultimate goal of this project is to offer possible physical explanation for the observed spatial distribution of landslides, to support the territory-wide landslide susceptibility model (Lo et al, 2015). The background and methodology adopted on catchment selection for review, together with the findings of a pilot review, are detailed in Tang et al (2018).

Subsequent to the pilot study (Tang et al, 2018), six additional catchments were selected for comprehensive review. In addition, further refinement of the geomorphological model of the pilot study catchment has been conducted. This synthesis report summarises the findings and observations from all the seven study catchments and highlights any geological and geomorphological features that are common in these catchments and might have contributed to landslide clustering. For individual catchments, detailed evaluation of site geology and geomorphological conditions, characterisation of relict and recent landslides, and spatial cluster analysis were carried out. The findings of the detailed review of individual catchments are presented in Appendix A to E.

2 Catchment Characteristics

2.1 Location and General Characteristics

The seven selected catchments (Figure 2.1) for this study included:

(a) Above Upper Keung Shan Road, west Lantau - catchment 58, i.e. the pilot study catchment (hereafter catchment KSR58; Tang et al, 2018);

(b) Above Upper Keung Shan Road, west Lantau - catchment 56, and its adjacent catchment (hereafter catchments KSR56 and KSR56A);

(c) Coastal catchment to the north of Tai O Cemetery, Lantau - including catchment 50 and two adjacent catchments (hereafter catchment TO);

(d) Pak Tai To Yan, within Lam Tsuen Country Park, Tai Po - Catchment 25 (hereafter catchment PTTY);

(e) Fei Ngo Shan, east Kowloon - Catchment 46 and its nearby catchment (hereafter catchment FNS); and

(f) Fan Kam Road, within Lam Tsuen Country Park, Tai Po - (hereafter catchment FKR).

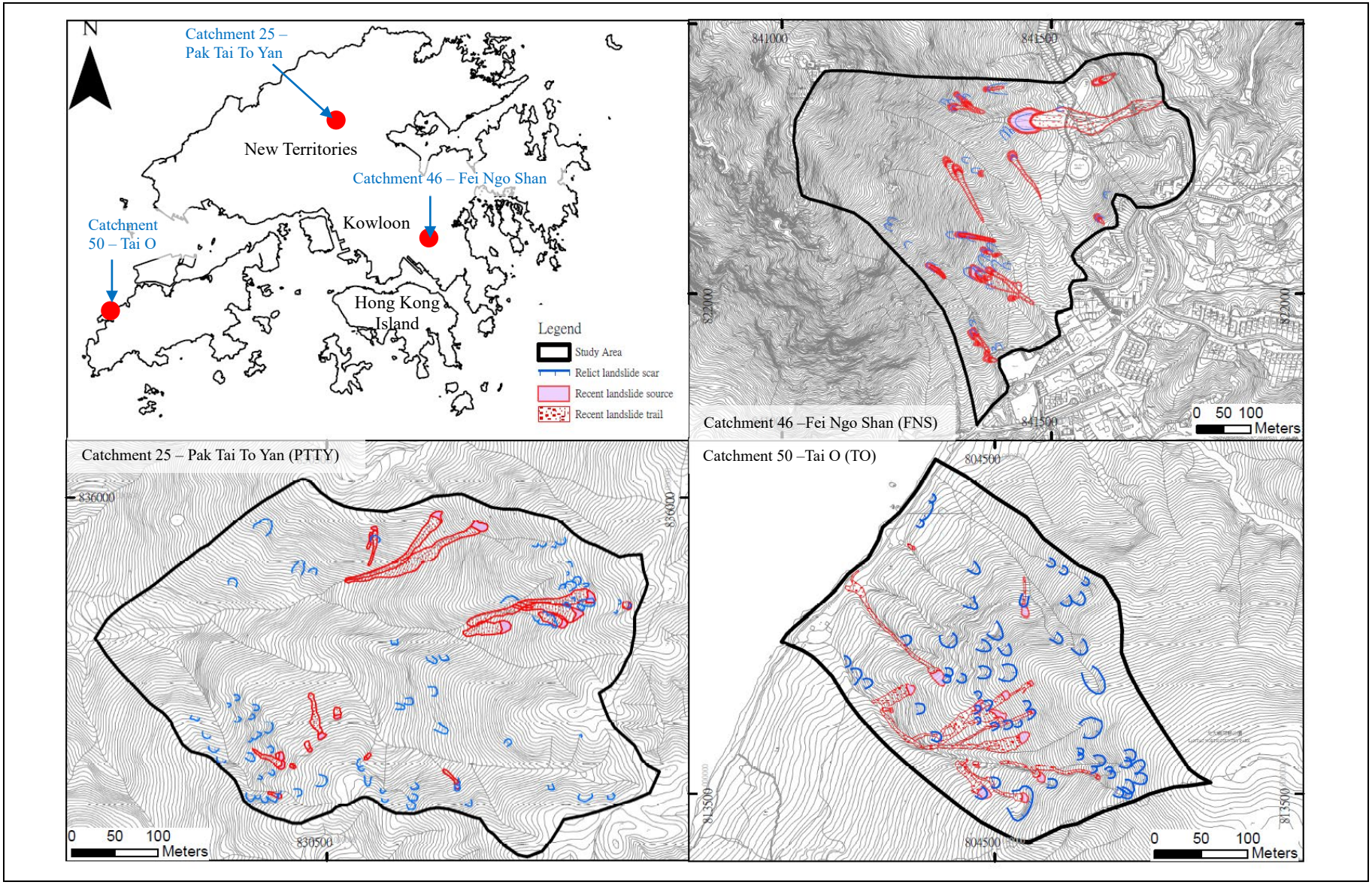

Figure 2.1 Location Plan of the Study Catchments (Sheet 1 of 2)

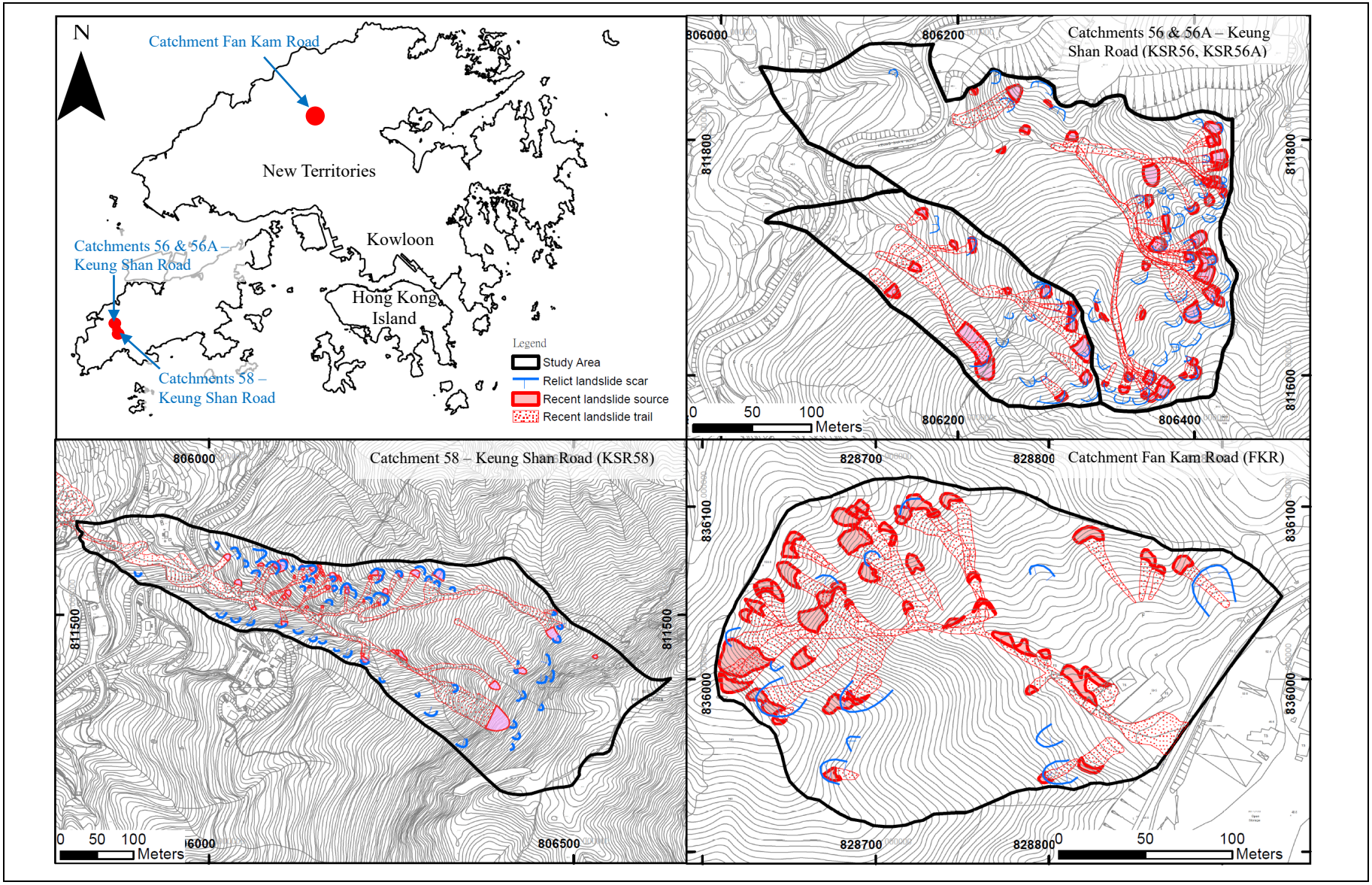

Figure 2.1 Location Plan of the Study Catchments (Sheet 2 of 2)

The general characteristics of individual catchments are summarised in Table 2.1. The plan area of these catchments vary from 0.024 to 0.26 km^2, with elevation differences range from approximately 100 to 400 m. These catchments are in sub-circular to elongate shapes and the aspect ratio varies from 1.2 to 3. The compactness factors for these catchment range from 1.17 to 1.57. Drainages are present in all catchments with total length of 0.5 - 5.5 km and give a range of drainage density from 5.2 to 29.2 per km. All catchments exhibit a certain degree of human disturbance. Significant human activities were observed in catchment PTTY and minor disturbance in catchments TO, KSR56, KSR56A, KSR58 and FKR.

Table 2.1 Characteristics of the Study Catchments

Catchment ID	PTTY	TO	KSR56	KSR56A	KSR58	FNS	FKR
Location	Pak Tai To Yan	Tai O	Keung Shan Road	Keung Shan Road	Keung Shan Road	Fei Ngo Shan	Fan Kam Road
Plan Area (km^2)	0.19	0.10	0.06	0.02	0.12	0.26	0.05
Elevation Difference (m)	~ 290	~ 260	~ 160	~ 140	~ 320	~ 400	~ 100
Aspect Ratio (Long Axis: Short Axis)	1.8	1.5	1.8	2.9	3	1.2	1.3
Total Length of Drainage Lines (km)	5.5	1.8	0.7	0.5	2.2	1.4	1.0
Compactness Factor (1)	1.2	1.2	1.5	1.3	1.5	1.4	1.1
Drainage Density (km^{-1})(2)	29.2	18.4	12.3	20.4	18.7	5.2	21.7
Presence of Human Disturbance	Plantation Terraces ~32% of Catchment Area	Minor Footpath and Graves	Cut Slopes along Keung Shan Road			Minor Footpath and Cut Slopes at the Lower Part	Trenches along Ridgeline and at the Middle Part; Terraces

Notes: (1) Compactness factor is obtained from the ratio of the perimeter (P) of the catchment to the circumference of a circle whose area (A) is equal to that of the catchment. i.e Compactness = $P/2\sqrt{\pi A}$.

(2) Drainage density is the ratio of the total length of drainages to the basin area.

2.2 Previous Studies

Previous studies that were carried out at or in the vicinity of the study catchments are summarised below:

(a) Sin (2006, unpublished report) conducted a study to investigate geological features that are related to the natural terrain landslides in Fei Ngo Shan. The study included desk study, field mapping and review of ground investigation works for landslide incident no. 2005/08/0381 (i.e. ENTLI feature no. 11NEB0566E within Catchment FNS).

(b) Under the LI consultancy Agreement No. CE 15/2004 (GE), Maunsell Geotechnical Services Limited (MGSL) conducted a landslide investigation of the 21 August 2005 debris flow (i.e. ENTLI feature no. 11NEB0566E within Catchment FNS) occurred on the natural terrain near Fei Ngo Shan Service Reservoir (MGSL, 2008). Detailed desk study and field mapping were carried out.

(c) Cheung (2008) reported the findings from the desk study and design of mitigation measures at Catchment KSR58.

(d) Under LPMit Agreement No. CE 62/2008 (GE), Arup Fugro Joint Venture (AFJV) conducted a natural terrain hazard review, which included a detailed aerial photograph interpretation on landslides occurred in west Lantau, including Catchments TO, KSR56, KSR56A and KSR58, at a regional scale supplemented by site reconnaissance on selected areas (AFJV, 2010). In addition, a detailed geomorphological mapping for the nearby catchments above Tai O Cemetery was reported by AFJV (2010).

(e) Detailed field mapping of the June 2008 landslides in Catchment KSR58 was conducted by a GEO in-house team (Lee et al, 2010). They mapped the dimension and characteristics of landslide sources, zones of depletion/accumulation, debris volumes and material properties, entrainment characteristics, and signs of distress (e.g. tension cracks). Based on the field observations, Lee et al (2010) carried out a mass balance exercise of the debris flow and interpreted the failure mechanism of the landslide event.

(f) Under LPMit Agreement No. CE 17/2008 (GE), a natural terrain hazard assessment covering the natural hillsides above Windsor Castle at Fei Ngo Shan (i.e. HLC Nos. 11NE-B/DF1, 11NE-B/DF1a and 11NE-B/DF7) was conducted. The

findings were reported in Stage 2(H) Report No. S2(H)R005/2013 (OAP, 2011).

(g) Under the Landslip Investigation (LI) consultancy Agreement No. CE 40/2007 (GE), Fugro Scott Wilson Joint Venture (FSWJV) conducted an aerial photograph interpretation to map and characterise the landslides occurred on Lantau Island in June 2008. The study area covered Catchments TO, KSR56, KSR56A and KSR58. A summary report was prepared to document their findings (FSWJV, 2014).

(h) Under LPMit Agreement No. CE 27/2012 (GE), a natural terrain hazard assessment covering catchments KSR56 and KSR56A was carried out by AECOM. A detailed engineering geomorphological mapping, field inspections of the 2008 landslides and site-specific ground investigation were conducted under the study. The findings were reported in Stage 2(H) Report No. S2(H)R11/2015 (AECOM, 2015).

(i) Under the LI consultancy, AECOM carried out an investigation of landslide clusters on hillsides above Fan Kam Road occurred during the August 2018 rainstorm (AECOM, 2019). The landslide investigation study covered part of Catchment FKR. Detailed field mapping of the landslide clusters and analysis of the cause of landslides were carried out.

2.3 Slope Angle Distribution

For each catchment, the distribution of slope angle class is derived from a 5-m grid based on the DEM generated from the 2010 airborne LiDAR data (Figure 2.2). The distribution of slope angle class provides a useful proxy of the overall steepness of individual catchments. Catchments PTTY, TO, KSR58 and FNS, with over 50% to 70% of the hillside with gradient > 30°, are generally steeper than catchments KSR56 and KSR56A, with only 30% of catchment area steeper than 30°. About half of the area of catchment FKR is steeper than 30°. The steeper nature of catchments PTTY, TO, KSR58 and FNS is contributed by the presence of rocky cliffs within these catchments.

2.4 Geology and Regolith

According to the published 1:20,000-scale geological maps, the solid geology of the study catchments are mostly volcanic rocks (tuff or tuffites) of various formations, including the Tai Mo Shan, Shing Mun, undifferentiated Lantau and Mount Davis formations, and sedimentary rocks of the Tai O Formation (Table 2.2).

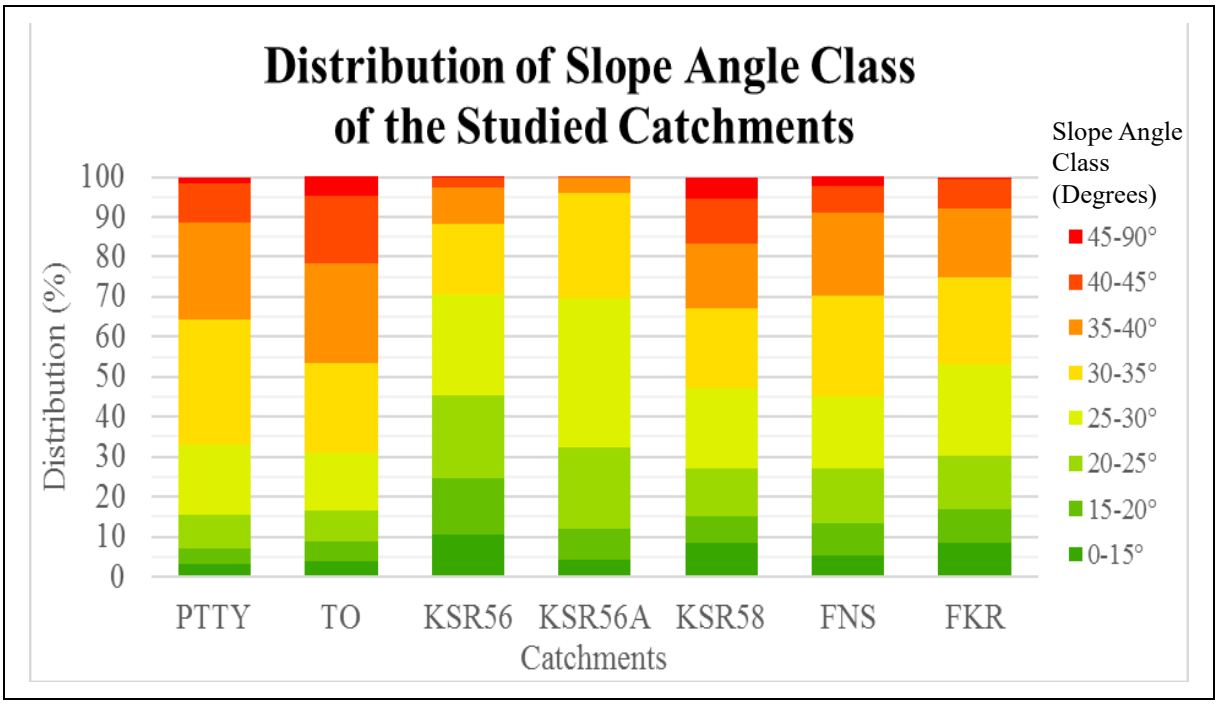

Figure 2.2 Slope Angle Distribution of the Catchments

Table 2.2 Summary of Solid Geology of the Catchments

Catchment	Solid Geology	Geological Maps
PTTY	Lapilli lithic-bearing coarse ash crystal tuff of the Tai Mo Shan Formation with some NE-trending altered tuff bands	3 & 7 (GCO, 1986b, 1991; GEO, 2008)
TO	Fine ash tuff of the Shing Mun Formation at the upper portion, overlying siltstone and sandstone layers of the Tai O Formation at the lower portion	9 (GEO, 1994)
KSR56 & KSR56A	Undifferentiated rhyolite lava and tuff of the Lantau Formation	13 (GEO, 1995)
KSR58	Layers of siltstone, tuffite and tuff (Pak Kok Member of Lantau Formation) form the upper portion and undifferentiated rhyolite lava and tuff of the Lantau Formation in the lower portion	13 (GEO, 1995)
FNS	Fine to coarse ash crystal tuff, tuff breccia and tuffite of the Mount Davis Formation, cut by an N-E trending quartzphyric rhyolite dyke	11 (GCO, 1986a;GEO, 2012)
FKR	Lapilli lithic-bearing coarse ash crystal tuff of the Tai Mo Shan Formation	2 & 6 (GCO, 1988, 1989; GEO, 2018)

Site-specific aerial photograph interpretation (API) was carried out for individual catchments to identify the distributions and types of regolith. The majority of the catchments PTTY, KSR56, KSR56A, KSR58, FNS and FKR are underlain by volcanic rock outcrops, intermittent rock outcrops or saprolite. About 30% of catchment TO and 11% of catchment KSR58 are underlain by sedimentary rocks.

Transported materials (i.e. superficial deposits) also cover significant portions of the study catchments. Taluvium was found accumulated below some rock cliffs in catchment KSR58 and FNS. Colluvial deposits are commonly found along drainages at catchments PTTY, KSR56, KSR56A, KSR58 and FNS, and as debris lobes at the lower part of catchments TO, KSR56A and KSR58. At catchment PTTY, colluvium with thickness up to 3 m was locally observed on open side slope. Alluvium and beach deposits are less common, but are present at catchments PTTY and TO, respectively.

2.5 Terrain Units

Each of the study catchments was sub-divided into various terrain units, for reflecting specific geology, geomorphology, regolith types and dominant processes. Given that the individual catchments have differing geology and geomorphology settings, the types of terrain units present in each catchment are inevitably varied. In addition, since the geomorphological interpretations of the catchments were conducted separately by individual geologists, the classification and nomenclature of terrain units also differ. As a result, direct comparison of the relative distribution and other aspects of the terrain units of separate catchments is difficult. Nonetheless, we have proposed a unified nomenclature system for the terrain units, which are summarized in Table 2.3.

Catchment PTTY could be sub-divided into three main terrain units, namely, ‘Ridge’, ‘Rocky Terrain’, ‘Drainage Depressions’, ‘Valley Side Slope’, ‘Open Side Slope’ and ‘Valley Deposit’ (see Appendix A for details). The ‘Open Side Slope’ terrains represent relatively open, planar hillslopes without obvious influence from drainage line, and are further sub-divided according to slope gradients. On the other hand, the ‘Valley Side Slope’ terrains are those deeply-incised hillslopes located on the sides of stream courses, and consist of a series of topographic/drainage depressions. Intermittent ‘Rocky Terrain’, inferred to be bands of more resistant, altered tuff, are also present within various terrain units.

The terrain unit classification for catchment KSR58 have been further refined subsequent to the pilot study (see Appendix F for details). Catchment KSR58 is characterized by the presence of prominent rock cliffs (‘Middle Fall Face’) above the relatively planar ‘Middle Transportation’ unit at the mid-slope, and deeply-incised, steep ‘Middle Incised’ unit in the lower part of the catchment. The ‘Middle Fall Face’, defined by relatively continuous convex and concave break-in-slopes at the upper and lower limits of the terrain unit, probably reflects the underlying geology, i.e. metamorphosed tuff and tuffaceous layers, which are more resistant to weathering and erosion. The ‘Middle Incised’ unit consist of a series of topographic depressions, interpreted to be associated with relict landslide clusters.

Table 2.3 Summary of Terrain Units in the Study Catchments and Proposed Unified Nomenclature

Unified Name and Typical Characteristics	PTTY	TO [Note 1]	KSR56/56A	KSR58	FNS	FKR
Ridge and Spur (Gradient 0 - 20°; Shallow Saprolite, Sometimes Intermittent Outcrops or Exhumed Tors; Weathering)	Ridge	Upper Spur	Ridge	Ridge / Spur	Ridge	Ridge/Spur
Fall Face (Gradient ≥ 40°; Rock or Intermittent Outcrops; Mass Wasting and Weathering)	Rocky Terrain	Middle Fall Face	(Not present or undifferentiated)	Middle Fall Face	Fall Face	(Not present or undifferentiated)
Drainage Depression (Gradient 25 - 40°; Bowl-Shaped Depressions Containing Drainage Heads; Saprolite and Colluvium; Mass Wasting)	Drainage Depressions	(Not present or undifferentiated)	Drainage Depressions	(Not present or undifferentiated)	Middle Incised	Drainage Depression
Open Side Slope with Drainage Incision (Gradient 25 - 40°; Moderately-Incised Terrain; Colluvium and Saprolite; Mass Wasting)	Valley Side Slope	Middle Incised	Valley Side Slope	Middle Incised	Upslope Incised	Open Hillslope
				Upper Transportation	Upslope Transportation	
Open, Planar Side Slope with no obvious Drainage Incision (Gradient 25 - 40°; Planar Slope; Colluvium and Saprolite; Mass Wasting And Weathering)	Open Side Slope	Middle Transportation	Planar Side Slope	Middle Transportation	Middle Transportation	
					Downslope Transportation	
Drainage Channel (Gradient 30 - 40°; Incised Channel Wall along River Course; Mass Wasting)	(Not present or undifferentiated)	Incised Drainage Channel	(Not present or undifferentiated)	Incised Drainage Channel	(Not present or undifferentiated)	Drainage Channel
Depositional (Gradient < 20°; Colluvium and Alluvium; Deposition)	Valley Deposit	Lower Deposition	Deposition Lower Slopes	Lower Deposition	Deposition	Depositional

Note: "Lower Coastal Erosion" and "Lower Coastal Deposition" units are present in catchment TO only and are excluded from this summary table.

Catchments KSR56 and KSR56A, although located adjacent to catchment KSR58, have a significant different geomorphology owing to two factors. First, most of the catchment areas are underlain by volcanic saprolite with the absence of rock cliffs, which accounts for an overall gentler slopes comparing with catchment KSR58 (see Section 2.3). Second, the catchments are characterised by well-developed, bowl-shaped 'Drainage Depressions' at the upper slope and incised drainages bounded by 'Valley Side Slopes' (Appendix D). For catchment KSR56, about a quarter of the catchment area has been classified as 'Planar Side Slope' unit, which has moderate gradient (9 - 37°) and shows no obvious influence from the drainages.

Catchment TO is a coastal catchment, which could be sub-divided into eight terrain units (Appendix C). The dominant terrain units include the mid-slope 'Middle Fall Face', relatively steep 'Middle Incised' with well-defined drainage lines, and planar 'Middle Transportation' that are underlain by volcanic / sedimentary saprolite and with minimal influence of drainage lines. The lower portion of the catchment is characterised by the presence of debris lobes, and coastal erosional and deposition units. Similar to catchment KSR58, the presence of rock cliffs is a manifestation of the underlying geology, and in this case, the geological contact between underlying layered sandstones and the volcanic rocks above.

Catchment FNS is located on the eastern flank of Kowloon Peak, and consists of the N-S trending ridge down to the mid-slope region of Fei Ngo Shan. The study catchment could be subdivided into eight terrain units (Appendix B). The catchment is characterized by steep (generally > 40°), prominent rock cliffs (i.e. "Fall Face" unit) at the upper part, and two "Transportation" units (30 - 45°) at upslope and mid-slope regions, which are represented by extensive, linear areas of intermittent rock outcrops/talus deposits. In addition, two "Incised" units, of upslope and mid-slope region, could be defined for generally steep hillslopes that are adjacent to and influenced by incised drainages. The lower part of the catchment could be subdivided into "Transportation" and "Deposition" units, based on the dominant processes, regolith types and slope gradient. The foothill region, which has been largely modified by urban development, was not included in the review.

Catchment FKR is relatively small, and is characterized by a series of drainage depressions with the head of drainage lines located relatively close to the catchment boundary. The catchment could be sub-divided into seven terrain units, including 'Ridge/Spur', 'Drainage Depression', 'Open Hillslope', 'Depositional Slope', 'Channel Wall', 'Valley Floor' and 'Man-made Terrace' (Appendix E). The 'Drainage Depression' unit is generally steep (>3 5°) with shallow regolith and contributes to over 50% of both relict and recent landslides. The 'Open Hillslope' unit consists of mostly planar to slightly divergent hillslopes of generally 30 - 40° in gradient. The 'Depositional Slope' unit is found at the lower part of the catchment with a gentle gradient (< 25°) and mantled by colluvial deposits. The 'Channel Wall' and 'Valley Floor' units are located immediately adjacent to the present stream course, and are directly influenced by the fluvial processes of erosion and deposition.

2.6 Drainage Patterns and Drainage Depressions

Well-defined drainages are present in all the study catchments. Catchments TO, KSR56A, FNS and KSR58 commonly consist of second order drainage with few individuals in first order. A third order drainage is present in each of the catchments TO, KSR56 and

FKR while a fourth order drainage in catchment PTTY. The total length of drainage lines in these catchments varies from 0.74 to 5.54 km and gives the ratio of drainage lengths to catchment area from 5.2 to 29.2 km^{-1} (refer to Table 2.1).

First order open drainage is present in catchments TO and KSR56A while incised drainages are observed in catchments TO and FNS. The lengths of these drainages vary from 38 to 232 m. The second to fourth order incised drainages in the studied catchments are all in dendritic pattern, with lengths from 227 to 5536 m. The heads of these drainages are equally distributed near ridge in catchments KSR56, KSR56A, FKR, mid-slope in catchments PTTY, FNS or at/immediately below rock outcrops in catchments TO and KSR58. Drainages in these catchments are confined and have steep side slopes at gradient of at least 35°. Undercutting along drainage is commonly observed in the studied catchments. The orientations of sub-drainages/major drainage in catchments PTTY and KSR58 respectively, were identified to have been controlled by faults.

Broad depressions are observed at all of the heads of drainages in catchments KSR56, KSR56A and FKR as well as in several drainages in catchments PTTY. Distance between head of drainage in these depressions were measured to the nearest catchment fringe (i.e. ridge/spur lines). The average distances are 60 m, 42 m for the first, second order drainage lines in catchment KSR56A respectively. Average distance of 23 m and 28 m for third order drainage lines in catchments FKR and KSR56 respectively. The forth order drainage lines in catchment PTTY has a distance of 75 m to the fringe. It is observed that in a well-defined, apparently more mature, drainage depression, the distance between head of drainage line to catchment fringe is general shorter.

2.7 Human Disturbance

All study catchments have been affected by various degrees of human disturbance (Table 2.1). The lower portions of catchments KSR56, KSR56A and KSR58 were modified by the construction of Keung Shan Road and the associated cut slopes. Similarly, a series of cut slopes, a service reservoir and Fei Ngo Shan Road were constructed at the lower part of catchment FNS. Abandoned terraces in herringbone pattern were observed from 1963 aerial photographs in the upper to middle portions of catchment PTTY (i.e. ~ 32% of the catchment area). For catchment FKR, extensive small excavations were found near the ridge and possibly related to military activities such as fox holes and defensive positions (AECOM, 2019). In addition, a series of man-made terraces (now abandoned) are present at the lower part of catchment FKR.

2.8 Sign of Distress

Tension cracks were reported in API and field mapping records in catchments PTTY and KSR56A respectively. At the southern part of catchment PTTY, three sign-of-distress features (about 30 - 40 m in length), likely to be associated with the human activities (Section 2.7) and/or slope failures, were observed on the NW-facing slope. In addition, a tension crack, with length up to 110 m was found along the sides of a broad topographic depression catchment PTTY. For the tension crack in catchment KSR56A, its mapped length was 5 m, and was probably associated with the detached landslide materials.

3 Landslide Characteristics

3.1 ENTLI Records

Detailed API was carried out for individual catchments to verify the landslide records in the ENTLI database (up to 2016) for compiling a site-specific landslide inventory. The dimensions, source volumes, runouts, failure modes and other characteristics of the landslides were also assessed based on the API and review of previous landslide mapping records or studies. Table 3.1 shows the number of landslides in the existing ENTLI dataset (up to 2016) and site-specific landslide inventory for each catchment.

Table 3.1 ENTLI and Site-specific Landslide Inventory of Each Catchment

Catchment	No. of ENTLI Features (up to 2016)			No. of Confirmed Landslides		
	Relict	Recent	Total	Relict	Recent	Total
PTTY	64	15	79	74	18	92
TO	85	17	102	56	18	74
KSR56	43	49	92	49	54	103
KSR56A	16	14	30	17	16	33
KSR58	72	50	122	54	49	103
FNS	31	27	58	35	27	62
FKR	14	17	31	9	51*	60

Note: Asterisk denotes the number of recent landslides for Catchment FKR is reviewed up to year 2018.

3.2 Landslide Characteristics

In this study, reviewing the landslide characteristics have depended largely on the available mapping records (e.g. Lee et al., 2010 for catchment KSR58) or published natural terrain hazard study reports (e.g. AECOM, 2015 for catchment KSR56) or landslide investigation reports (e.g. MGSL, 2008, for catchment FNS). The major limitation of this review is that except for catchment FKR, it is not possible to visit and directly observe the landslide sites. For catchments PTTY and TO, which have no previous mapping records or detailed reports, the landslide characteristics could only be inferred from the interpretation of aerial photographs. Having said the above limitations, the landslide characteristics of the recent landslides, either directly observed or inferred, are summarized below.

Most of the recent landslides in the study catchments were small in size, shallow in depth (generally 0.5 - 2.0 m), with source dimensions vary from 1 to 17 m wide and approximately 1 to 37 m long. Over 90% of the recent landslides in the study catchments had source volume less than 150 m^3. These shallow landslides failed within thin colluvial or saprolitic soils, or at the interface between them in catchments KSR56, KSR56A, KSR58 and FKR. (e.g. Lee et al, 2010; AECOM, 2015; 2019). For these shallow failures, the material

exposed along the slip planes were usually less weathered materials. In addition, soil pipes and tension cracks were commonly observed at the source regions at catchments KSR56, KSR56A, KSR58 and PTTY. AECOM (2019) postulated that for the landslide clusters above Fan Kam Road, the failures were probably induced by infiltration through the shallow colluvium, resulting in a perched water table at the interface between colluvium and underlying weathered tuff.

The characteristics of these shallow landslides suggest that the underlying reason of the failures was probably continuous deterioration and weathering of in-situ materials on over-steepened slopes, which failed as a consequent of rise in pore water pressure during a rainstorm. The process of continuous weathering means that these shallow failures would probably be a cyclic phenomenon. Therefore, the rate of weathering of in-situ materials is a key factor of the frequency of landslide occurrence.

Two larger recent landslides occurred in catchments KSR58 and FNS, with source volumes of approximately 730 and 3,500 m^3, respectively. Both of these two landslides were considered to be controlled by underlying geological structures, including adversely-oriented joints (Sin, 2006 unpublished; MGSL, 2008; Lee et al, 2010). The largest landslide (ENTLI No. 13NWB2728E) in catchment KSR58 occurred in year 2008, with source dimension of 33 m long, 35 m wide, 1.2 m deep and source volume of about 730 m^3. The steepest slope gradient of the source area is 49°. Lee et al (2010) reported that the surface rupture of the landslide was along adversely oriented, daylighting sheeting joints in metamorphosed volcanic bedrock. This landslide was also initiated close to the contact between a tuffaceous layer and the underlying metamorphosed volcanic rocks, which might also have influenced the occurrence of failure.

In Catchment FNS, the source dimension of the largest recent landslide (ENTLI No. 11NEB0566E, 2005) was 40 m long, 37 m wide and 4.5 m deep. The source volume of this landslide is approximately 3,500 m^3. The landslide initiated in a rounded, scoop-shaped depression, which subsequently inferred as a degrade relict landslide (MGSL, 2008). The recent landslide had runout distance of 291 m and occurred at slope gradient of 34°. Field mapping of the landslide found that the rupture surface was largely controlled by persistent, adversely-oriented, undulating to slickensided, clay-infilled relict joints (MGSL, 2008).

The other confirmed relict landslides were shallow in depth and most of them were of relatively small volume (Table 3.2). For relict landslides, the dimensions of source vary from 2.5 - 33 m wide, 2 - 24 m long and 0.5 - 4 m depth, with source volumes ranging 2 - 1,244 m^3. The largest relict landslide occurred within catchment TO (with source volume of 1,244 m^3) has been interpreted as probably formed by multiple failures or had been enlarged by continuous, post-failure erosion. It is also worth noting that quite some numbers of relatively wide Type C relict ENTLI features have been verified as being not related to single large-scale failures. Instead, these features probably represent broad, bowl-shaped topographic/drainage depressions that are formed by continuous erosion at and above the head of drainage lines.

Table 3.2 Landslides in Each Catchment

Catchment	Landslide Type	Source Width (m)	Source Length (m)	Source Depth (m)	Source Volume (m^3)
PTTY	Relict	3 - 20	2 - 19	0.5 - 3	2 - 408
	Recent	4 - 16	3 - 12	1 - 2	8 - 189
TO	Relict	3 - 33	2 - 24	0.5 - 4	2 - 1,244
	Recent	1 - 17	1 - 18	0.5 - 2	< 1 - 211
KSR56	Relict	5 - 30	3 - 11	0.5 - 2	6 - 178
	Recent	2 - 17	1 - 17	0.5 - 2	1 - 152
KSR56A	Relict	5 - 25	5 - 13	1 - 1.5	17 - 180
	Recent	5 - 17	3 - 37	0.5 - 1.5	5 - 252
KSR58	Relict	3 - 33	2 - 35	1 -2	1 - 725
	Recent	4 - 22	3 - 18	0.5 - 2	5 - 391
FNS	Relict	6 - 17	6 - 33	1 - 2	31 - 338
	Recent	3 - 37	2 - 40	0.5 - 4.5	2 - 3,500
FKR	Relict	7 - 22	3 - 25	2 - 3	40 - 320
	Recent	4 - 22	3 - 24	0.5 - 1.5	3 - 230

The overall frequency of recent landslide occurrence in the study catchments is about three landslides/year over 46 years (from 1963 to 2008), although most landslides cluster occurred during intense rainstorms at specific years. About 10% and 55% of these clusters occurred in years 1982 and 2008 respectively. About 6% of clusters each occurred in years 1993 and 1999. Over 58% of these landslides were channelised debris flows. Since all the landslides occurred in or prior to year 2008, the slope angle of these landslides (derived from 5-m grid year 2010 LiDAR data) would represent the post-failure slope angle. Overall, approximately 60% of these landslide clusters formed on steep landform with gradient over 35°.

3.3 Distribution of Landslides with Respect to Slope Gradient Class

About half of the relict landslides in catchments PTTY, TO, KSR58 and FNS occurred on slopes at slope gradient > 35°. Relict landslides in catchments KSR56 and KSR56A tend to occur at gentler slope (i.e. only about 33% and 17% of landslides at slopes at gradient > 35°). Over 70% of recent landslides were found at slope with gradient > 35° in catchments PTTY, TO and FNS. About 18 - 53% of recent landslides in catchments KSR56, KSR56A and KSR58 occurred at slope gradient > 35°. Figure 3.1 shows a summary of slope angle distribution of recent landslides in each catchment.

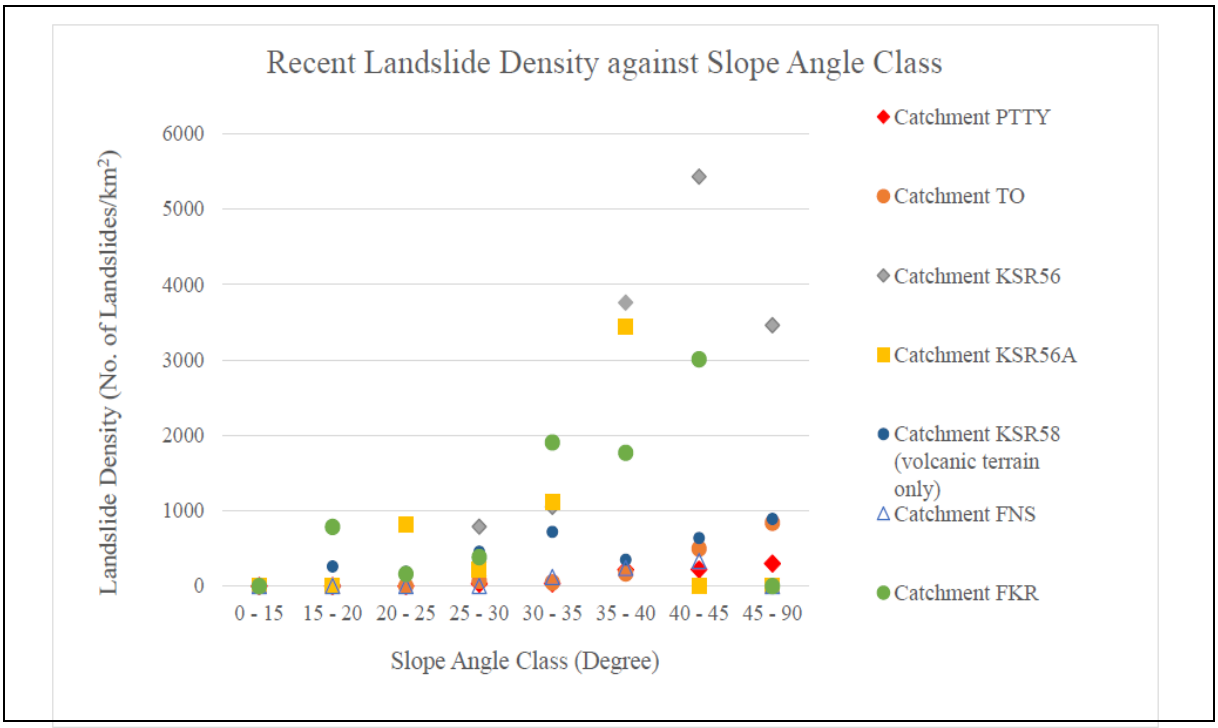

Figure 3.1 Distribution of Recent Landslide Density in Each Slope Angle Class

In general, landslide density increases with increasing slope angle classes for all catchments, except that no landslide was found on terrain with gradient > 40° or no terrain area has slope angle ≥ 45° in catchment KSR56A and decreased in landslide densities at slope angle class of 45 - 90° in catchments KSR56, FNS and FKR. Lo et al (2015) suggested that under the same rainfall and slope angle classes, areas underlain by sedimentary rocks are generally as susceptible to landslide activities as the areas underlain by volcanic rocks in territory-wide. Among the six study catchments, only catchments KSR58 and TO are underlain by both volcanic and sedimentary rocks. Our analysis shows that the landside densities in areas underlain by sedimentary rocks are as susceptible to landslide activities as in volcanic terrains in catchment TO. In particular, the landslide density in areas underlain by sedimentary rocks at slope angle class of 45 - 90° is one order of magnitude higher than the one in areas underlain by volcanic rocks. However, for catchment KSR58, no landslide occurred in areas underlain by the tuffaceous sedimentary rocks, which are present at the upper most part of the catchment.

4 Spatial Distribution of Landslide Clusters

4.1 Classification of Landslide Clusters

For each of the study catchments, the spatial distribution of the recent landslide with respect to the relict landslides have been reviewed and analysed according to the eight-fold classification scheme proposed by Tang et al (2018) (Table 4.1). Under this scheme, Types 1 to 4 clusters represent retrogressive failures at over-steepened terrains on open hillslopes to broad topographic depressions; Types 5 to 6 are retrogressive or multiple failures clustering at drainage heads; Type 7 is defined as landslide clusters along incised drainage

channels; and Type 8 clusters are those initiated at well-defined break-in-slope. A more detailed description of the proposed classification is presented in Tang et al (2018; Table 6.1 and Appendix B).

Table 4.1 Classification of Recent Landslide Clusters in Each Catchment

Type of Landslide Clusters	Numbers of Recent Landslide Clusters (% in bracket)						
	PTTY (n=18)	TO (n=18)	KSR56 (n=54)	KSR56A (n=16)	KSR58 (n=49)	FNS (n=27)	FKR (n=51)
1	2 (11%)	5 (28%)	1 (2%)	0	13 (27%)	1 (4%)	3 (6%)
2	1 (5.5%)	0	0	0	10 (20%)	1 (4%)	1 (2%)
3	3 (17%)	0	1 (2%)	0	3 (6%)	3 (11%)	1 (2%)
4	1 (5.5%)	1 (5.5%)	0	0	9 (18%)	0	8 (16%)
5	0	3 (17%)	0	0	1 (2%)	9 (33%)	19 (37%)
6	1 (5.5%)	1 (5.5%)	38 (70%)	9 (56%)	0	3 (11%)	4 (8%)
7	1 (5.5%)	5 (28%)	8 (15%)	2 (13%)	5 (10%)	0	6 (12%)
8	0	0	1 (2%)	0	2 (4%)	2 (7%)	0
Not in Cluster	9 (50%)	3 (17%)	5 (9%)	5 (31%)	6 (12%)	8 (30%)	9 (17%)

The review found that about 9 - 50% of the recent landslides within the study catchments did not occur in cluster based on the proposed classification scheme. About 73% and 39% of the recent landslide clusters in catchments KSR58 and PTTY respectively were classified as Types 1 to 4, and interpreted to be related to retrogressive failures, destabilised past landslide debris and over-steepened slopes at previous failure scars. These landslide clusters were mostly likely controlled by geomorphological factors, such as slope gradients (cf. Tang et al, 2018). The occurrence of landslide clusters in topographic and/or drainage depressions (i.e. Type 5 to 7) are notable in catchments TO (50%), FNS (44%), KSR56 (85%), KRS56A (69%) and FKR. In particular, approximately 85% and 69% of landslide clusters in catchments KSR56 and KSR56A, respectively were concentrated in Types 6 and 7. Type 8 clusters occurred in catchments KSR56, KSR58 and FNS, and only account for 2 - 7% of the recent landslides.

4.2 Spatial Analysis

In the previous study by Lo & Ko (2017), a landslide cluster was defined as where there were three or more landslides occurring within a 30 m buffer. In this study, we have re-evaluated the occurrence of landslide clustering, adopting the "multi-distance spatial cluster" analysis tool in ArcGIS. Apart from the seven study catchments under this review, those 80 catchments identified by Lo & Ko (2017) as containing significant occurrence of landslide clusters have also been analysed using ENTLI data (Appendix G).

We conducted the "multi-distance spatial cluster" analysis, which is based on Ripley's K-function (Ripley, 1981), to determine whether the occurrence of relict and recent landslides is clustered, dispersed, or randomly-distributed throughout the study catchments. One key feature of the method is that it provides information on the spatial dependence, either clustering or dispersion of landslides, over a range of distances (i.e. at different scale). In essence, the K-function calculates the average number of neighbouring landslides within the evaluated distance of each landslide. As the evaluated distance increases, the number of neighbouring landslides would typically increase. If the average number of landslides for a particular evaluation distance is higher than the landslide density of the study catchment, the distribution of the landslides is considered clustered at that distance.

Figure 4.1 shows the output diagram from ArcGIS of the analytical result for catchment FKR, for illustration purpose. Apart from determining the observed K-values of the feature of interest (i.e. landslides for this study), the tool also computes the expected K-values for random spatial distribution at different distances (blue line in Figure 4.1), with the lower and upper confidence envelops (grey, dashed lines in Figure 4.1). The red line in Figure 4.1 indicates the observed K-values and the result suggested that for catchment FKR, spatial clustering of recent landslides starting from 4 m is statistically significant.

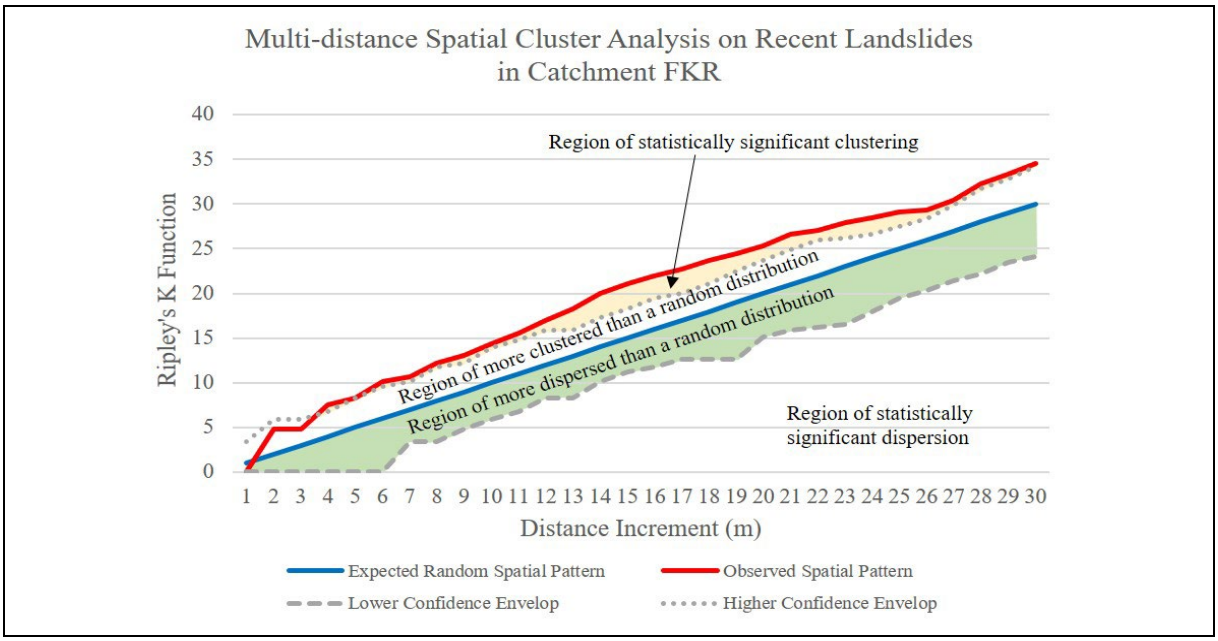

Figure 4.1 An Example of the Output of Multi-Distance Spatial Cluster Analysis on Recent Landslides in Catchment FKR

Among the 80 catchments analysed, 20 catchments statistically contain clusters of both relict and recent landslides, while another 30 catchments have clusters for either relict or recent landslides based on the results of Ripley's K-function analysis (Appendix G). For the six study catchments, catchments PTTY, FNS, TO, KSR56 and KSR58 have both relict and recent landslide clusters, catchment FKR has clusters of recent landslides, while statistically there was no landslide clustering in catchment KSR56A. For catchments PTTY, TO, KSR56, KSR58 and FNS, relict landslides start to cluster from a range of distance of 3 - 22 m; whilst for recent landslides, clusters occur from a range of distance of 1 - 32 m in all catchments except catchment KSR56A (Table 4.2).

Table 4.2 Minimum Distance of Relict and Recent Landslides Forming Clusters

Catchment ID	Minimum Distance of Relict Landslide Clusters (m)	Minimum Distance of Recent Landslide Clusters (m)
PTTY	11	6
TO	16	32
KSR56	17	1
KSR56A	(Statistically no clustering)	(Statistically no clustering)
KSR58	22	1
FNS	3	1
FKR	(Statistically no clustering)	4

5 Discussion

5.1 Potential Controls on Landslide Clustering

5.1.1 Maturity of Drainage and Valley Development

The maturity of drainage and the stage of valley development have an important influence on landslide clustering. Hansen (1984) presented an evolutionary terrain model linking the rate of geomorphological activities (including landslides) with various landforms formed in different stages of valley development. He reviewed > 800 natural terrain failures occurred during the 1982 rainstorms in Hong Kong and recognised that a large number of these landslides were developed retrogressively from incised drainage lines, and/or at locations with previous failures.

As pointed out by Hansen (1984), deep, bowl-shaped valleys/depressions are more susceptible to multiple failures than less well-developed valleys. These bowl-shaped depressions are generally located at the upper part of catchments, where drainage heads extended close to the catchment fringes, indicating that the drainage systems are mature. Multiple failures tend to occur simultaneously as clusters in the drainage depressions. For

instance in catchments KSR56, KSR56A and FKR, a substantial proportion of recent landslides (45 - 80%) clustered within these drainage depressions, and most of which occurred during the same rainstorm events. It is noted that some of the bowl-shape depressions, although probably developed through continuous drainage incision and repetitive, multiple failures, have been registered in the ENTLI database as single relict features. Similar observations were made by Halcrow (2007), who recognised that the large curved depressions in Cloudy Hill might have been misinterpreted as previous large-scale relict ENTLI features (particularly Type C relict landslides; see descriptions in Section 3.2 above).

Broad topographic depressions represent the intermediate stage of valley development. An example is the "Middle Incised" unit delineated in catchment TO (see Appendix C). Within this unit, a higher percentage of landslides, clustered around the heads of drainage, has been observed. The clustering of landslide is considered to be related to generally steeper slope gradient and also direct influence of drainage lines, including concentration of surface runoff and erosional alluvial processes.

5.1.2 Geological Contacts

We noted that some landslide clusters in catchments KSR58, PTTY, TO and FNS occurred close to geological contacts, or where more resistance rocks have formed prominent rock cliffs and outcrops. The presence of geological contacts could have either a direct or indirect influence to the distribution of landslides.

The change in lithology, such as the volcanic/sedimentary contact as observed in catchment TO and KSR58, might imply the presence of a structural plane, a change in rock mass properties, material strengths, porosity, etc, which directly influence slope stability. In some cases, the variation in lithologies may be less tangible. For instance, in catchment PTTY, several individual recent landslides were initiated at the bands of altered tuff with the crystal tuff unit. Similarly, the presence of altered layers with prominent quartz veining at the source of many recent landslides in catchment FNS may have led to the inference that these geological features have at least partly controlled the concentration of some recent landslides.

The underlying solid geology commonly controls catchment morphologies, which indirectly influence the distribution of landslides. Rock units that are more resistant to weathering and erosion, tend to form prominent steep (general > 35°) rock cliffs, with well-defined break-in-slopes. The observed landslide clusters at the fall face unit (e.g. in catchments TO and KSR58) might reflect the generally steeper gradient in rocky terrains, which are primarily more susceptible to landslide activities. In fact, some previous notable landslides (e.g. 1993 and 2008 debris flows from Shek Pik) also occurred in similar geomorphological settings. A rock cliff might also act as an "erosion barrier", which limits retrogressive failures to advance uphill crossing the cliff ("barrier"). As a result, repetitive failures tend to concentrate along the concave break-in-slope below the fall face. Talus (rock/boulder fall deposit) accumulated below a rock cliff may become unstable and contribute to further failures. Furthermore, the less permeable nature of the rock cliffs may increase infiltration into the saprolite/superficial deposits below, causing landslides at the base of the rock cliffs.

5.1.3 Catchment Characteristics

The geometric charcteristics of the study catchments, including catchment size, elevation difference, aspect ratio, compactness factor, drainage density and slope gradient distribution (Table 2.1 and Figure 2.2), have been reviewed in this study. However, given the limited data from only seven selected catchments, no obvious connection between these characteristics with landslide susceptibility can be inferred. In addition, although the maturity of drainage depressions and valley development have been identified as a key factor controlling the occurrence of landslide clustering (Section 5.1.1 above), a quantitative measure is yet to be established for future analysis of such features. In fact, the potential connections between catchment characteristics and landslide susceptibility have rarely been investigated in Hong Kong. Some recent works (Wong et al, 2020) observed that there might be possible connections of catchment shape and drainage density with the entrainment potential of debris flows, but the findings were not conclusive. It is therefore worthy to review additional catchments with notable landslide clusters to identify various aspects of natural terrain catchments that may link to higher susceptibility of failures and debris flow events.

5.1.4 Human Disturbance

All the study catchments have been affected to various degrees by human disturbance, including formation of cut slopes, footpaths, agricultural trenches / terraces or military trenches (see Table 2.1). Some of the observed landslides occurred in close proximity to these anthropogenic features in the study catchments. For instance, in the central part of catchment PTTY, four recent landslides, with signs of distress and tension cracks, were spatially clustered and initiated close to some planation trenches/terraces that were adjacent to a drainage line. This observation might suggest that these landslides were caused by, or at least had been partly controlled by, human activities. The herringbone-shaped trenches/terraces might have concentrated surface runoff, leading to higher landslide susceptibility close to these features. It is worthy to note, however, that apart from the above-mentioned four recent landslides, no failure occurred in other areas affected by similar planation terraces, which covered about 32% of the catchment area of catchment PTTY.

Human disturbance at catchment FKR was obvious in the 1963 aerial photographs, from which military trenches and foxholes (now abandoned) were clearly evidence, especially at the catchment crest. Most of the relict and recent landslides in catchment FKR were concentrated in the drainage depressions formed immediately below the crest. The abandoned trenches could have influenced the infiltration of surface water and thereby adversely affect the slope stability (c.f. AECOM, 2019). However, there is insufficient evidence to suggest that human disturbance was a direct controlling factor for the observed failures. In summary, the actual effects of anthropogenic activities on natural terrain landslide susceptibility and their distribution remain uncertain and are worthy for further investigation.

5.2 Classification of Landslide Clusters

As discussed by Tang et al (2018), the proposed eight-fold classification for landslide clusters was developed largely based on observation of landslide distributions and characteristics from the pilot study catchment (i.e. catchment KSR58). As such, the proposed scheme might not be adoptable for other catchments with dissimilar geomorphological conditions. Another limitation is that the scheme does not consider the terrain evolution processes that complicate the geomorphological setting of landslide clustering. In addition, the system only considers the spatial relationships of recent landslides with respect to relict landslides, and the relationship of repeated recent landslide failures are not assessed. Besides, where landslides in a cluster were located very close, or even overlapped with each other, the classification might become subjective. For instance, in catchment KSR56 the landslides clusters were spatially concentrated at the boundary of drainage depressions. Individual landslides were located so closely that it was unable to distinguish, especially where landslides were closely clustered, or even overlapped, such that their spatial relationships with each other could not be easily distinguished.

In view of the drawbacks discussed above, we have modified the classification scheme to better categorize landslide clusters with respect to the terrain units (Figure 5.1; Table 5.1).

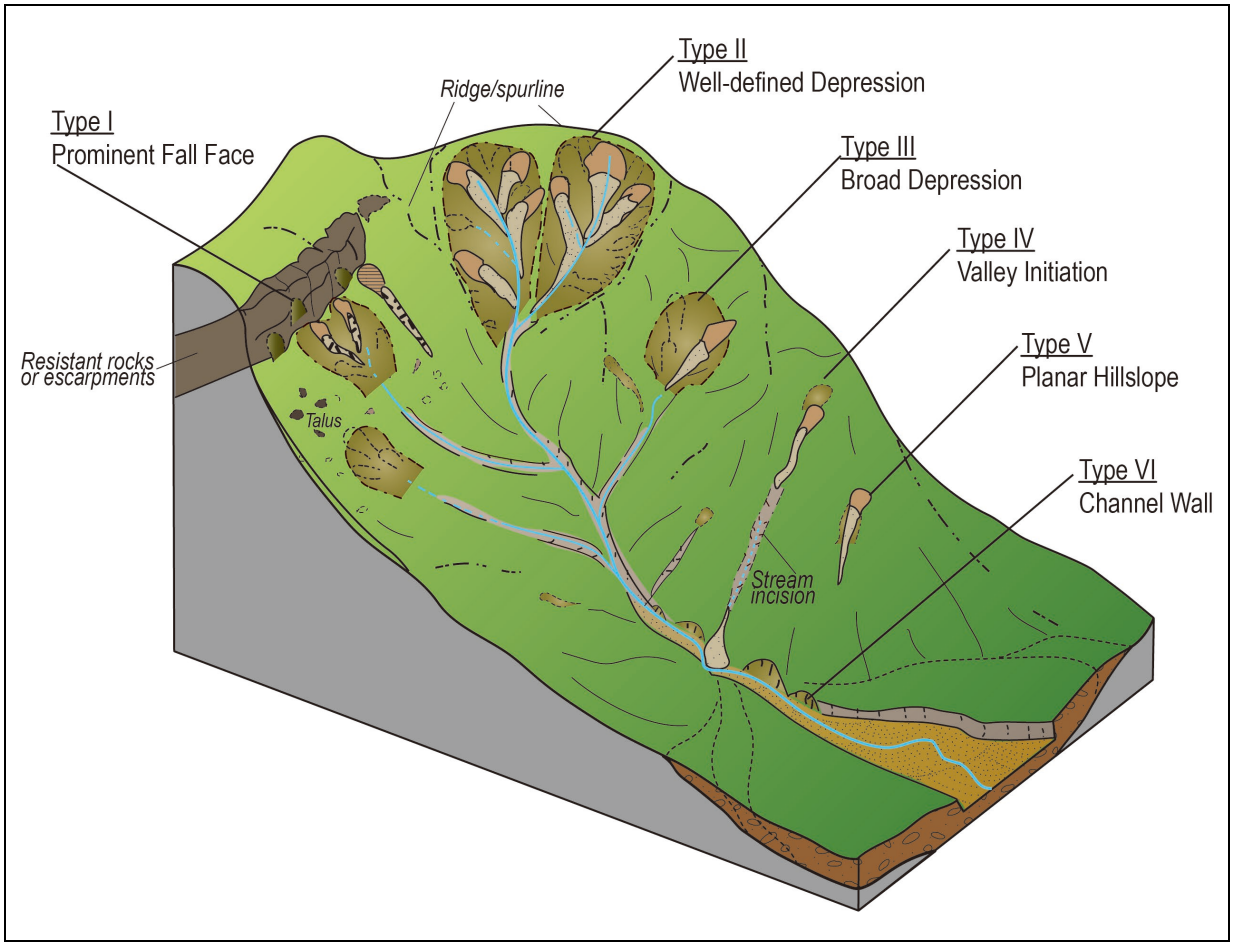

Figure 5.1 Proposed Terrain Type-based Classification of Landslide Clusters (Detailed Descriptions in Table 5.1 below)

Table 5.1 Descriptions of Geomorphological Setting of the Proposed Terrain Type-based Classification of Landslide Clusters

Type	Descriptions of Geomorphological Setting for Occurrence of Landslide Clusters
Type I	Group of landslides occurred on a prominent fall face (e.g. associated with the presence of geological contacts, more resistant rock layers or escarpments), and immediately from the concave break-in-slope below. Failures are possibly structurally controlled (e.g. adverse joint sets). Talus accumulated immediately below the fall face is potentially unstable.
Type II	Repeated, multiple failures within a well-defined (i.e. "mature"), bowl-shaped topographic depression between spurs. Failures are associated with strong erosion/undercutting at and above heads of drainage extending close to the topographic depression boundary.
Type III	Repeated failures within a broad topographic depression/valley; failures cause broadening stream incision and further valley development.
Type IV	Repeated failures on a mostly open, planar hillslope; failures create local topographic depressions that concentrate surface runoff and result in initiation of stream incision and valley development.
Type V	Retrogressive landslides on an open, planar or divergent hillslope with no apparent stream incision; failures may result in oversteepening at sources or destabilizing slope materials for future failures.
Type VI	Repeated failures on steep channel walls along incised drainage line; failures are associated with undercutting/erosional action of fluvial or debris flow.

The definition of terrain units under the revised scheme are broadly based on the slope model proposed by Dalrymple et al (1968), with further consideration of the stages of stream incision and valley development proposed in Hansen (1984)'s landform model of Hong Kong. The revised scheme aims at distinguishing the occurrence of landslide clusters in hilly terrains at various stages of valley development. Types II to V settings denote terrain evolution phases starting from generally open planar hillslopes (Type V) that gradually develop into a local topographic depressions (Type IV) through stream incision and retrogressive failures. Landslides from these setting are mostly controlled by slope gradient. Local topographic depressions begin to widen and deepen into broad topographic depressions and valleys (Type III). Type II setting represents well-defined drainage depressions that are developed through continue headward erosion of the drainages and repeated failures. Over-steepened slopes, which are susceptible for repeated failures, are formed at the upper boundary of the bowl-shaped depressions that have migrated close to the catchment fringe.

6 Conclusions

In this study, seven notable catchments with relict and recent landslide clusters, including four in west Lantau (catchments KSR56, KSR56A, KSR58 and TO), two in the central New Territories (catchments PTTY and FKR) and one in East Kowloon

(catchment FNS) have been selected for investigating the potential geological and geomorphological controls on those landslide clusters. For each catchment, we reviewed catchment characteristics, geology and geomorphological settings, the characteristics of relict and recent landslides, and spatial analysis of landslide clusters. The key findings are summarised below:

(a) Most of the recent landslides clusters in the study catchments were small-scale, shallow (generally 0.5 - 2.0 m) failures. Over 90% of the recent landslides in the study catchments had source volume < 150 m^3. These shallow landslides commonly failed within thin colluvial or saprolitic soils, or at the interface between them, and usually exposing less weathered bedrock along the slip planes. The failures were probably induced by infiltration through the shallow soil strata, resulting in a perched water table at the interface between colluvium/saprolite and underlying weathered rock. The observed repetitive nature of these landslides could be explained by the fact that they were primarily caused by continuous, progressive weathering of in-situ materials on over-steepened slopes.

(b) During the review of ENTLI features of individual catchments, quite some numbers of relatively broad, Type C relict ENTLI features have been verified as being not related to single large-scale failures. Instead, these features probably represent broad, bowl-shaped topographic or drainage depressions that are formed by continuous erosion at and above the head of drainage lines.

(c) We conducted "multi-distance spatial cluster" analysis, using Ripley's K-function (Ripley, 1981), of 80 natural terrain catchments which are identified by Lo & Ko (2017) as containing notable landslide clusters of both relict and recent landslides. The results of Ripley's K-function analysis show that among the 80 catchments, 20 catchments statistically contain clusters of both relict and recent landslides, while another 30 catchments have clusters for either relict or recent landslides.

(d) For each study catchments, the spatial distribution of landslide clusters have been reviewed and categorised using the classification scheme proposed by Tang et al (2018). Limitations of Tang et al (2018)'s scheme have been identified. A modified terrain type-based landslide clusters classification system is introduced, which is partly referenced to Hansen (1984)'s landform model on the stages of stream incision and valley development. Under the modified scheme, six types of terrain units/morphological

settings (Type I to VI) with various likelihoods of occurrence of landslide clustering are classified.

(e) The study has recognised that (1) feature-forming geological contacts; (2) mature bowl-shaped drainage depressions, and (3) over-steepened incised slopes are the prime locations of multiple, repeated landslides. It is expected that catchments with any of, or a combination of these features may have higher potential of repetitive, multiple failures. On the other hand, potential influence of human disturbance and catchment characteristics on landslide clustering has been reviewed, although no conclusive correlation of these factors with landslide susceptibility could be identified from the seven studied catchments.

7 References

AECOM Asia Company Limited (AECOM) (2015). *Stage 2(H) Study Report - Study Area 13NW-B/SA6 Keung Shan Road Near Sham Wat Road, Lantau Island (LPMitP Agreement No. CE 27/2012 (GE) Landslip Prevention and Mitigation Programme, 2012, Package D, Landslip Prevention and Mitigation Works - Investigation, Design and Construction)*. Geotechnical Engineering Office, Hong Kong, 440 p.

AECOM Asia Company Limited (AECOM) (2019). *Detailed Study of the 29 August 2018 Landslides on the Natural Hillside Above Fan Kam Road, Pat Heung (Landslide Study Report LSR 2/2019)*. Geotechnical Engineering Office, Hong Kong, 84 p.

Arup Fugro Joint Venture (AFJV) (2010). *Natural Terrain Hazard Review Report (LPMitP Agreement No. CE62/2008(GE) Landslip Prevention and Mitigation Programme, 2008, Package N, Natural Terrain Mitigation Works, West Lantau - Investigation, Design and Construction).* Geotechnical Engineering Office, Hong Kong, 405 p.

Cheung, H. (2008). *Medium Term Mitigation Measures for KS3 at Keung Shan Road, Lantau - Design Report.* Geotechnical Engineering Office, Hong Kong, 82 p.

Dalrymple, J., Long, R. & Conacher, A. (1968). A hypothetical nine-unit land-surface model. *Zeitschrift fur Geomorphologie*, Germany, vol. 12, pp 71-78.

Fugro Scott Wilson Joint Venture (FSWJV) (2014). *Summary Report on the Identification of June 2008 Natural Terrain Landslides on Lantau Island (Agreement No. CE 40/2007 (GE) Study of Landslides Occurring in Hong Kong Island and Outlying Islands in 2008 and 2009 - Feasibility Study*. Geotechnical Engineering Office, Hong Kong, 35 p.

Geotechnical Control Office (GCO) (1986a). *Hong Kong and Kowloon.* Hong Kong Geological Survey Sheet 11, Solid and Superficial Geology, 1:20,000 Series HGM20. Geotechnical Control Office, Hong Kong.

Geotechnical Control Office (GCO) (1986b). *Sha Tin.* Hong Kong Geological Survey Sheet 6, Solid and Superficial Geology, 1:20,000 Series HGM20. Geotechnical Control Office, Hong Kong.

Geotechnical Control Office (GCO) (1988). *Yuen Long.* Hong Kong Geological Survey Sheet 6, Solid and Superficial Geology, 1:20,000 Series HGM20. Geotechnical Control Office, Hong Kong.

Geotechnical Control Office (GCO) (1989). *San Tin.* Hong Kong Geological Survey Sheet 2, Solid and Superficial Geology, 1:20,000 Series HGM20. Geotechnical Control Office, Hong Kong.

Geotechnical Control Office (GCO) (1991). *Sheung Shui.* Hong Kong Geological Survey Sheet 3, Solid and Superficial Geology, 1:20,000 Series HGM20. Geotechnical Control Office, Hong Kong.

Geotechnical Engineering Office (GEO) (1994). *Tung Chung.* Hong Kong Geological Survey Sheet 9, Solid and Superficial Geology, 1:20,000 Series HGM20. Geotechnical Engineering Office, Hong Kong.

Geotechnical Engineering Office (GEO) (1995). *Shek Pik.* Hong Kong Geological Survey Sheet 13, Solid and Superficial Geology, 1:20,000 Series HGM20. Geotechnical Engineering Office, Hong Kong.

Geotechnical Engineering Office (GEO) (2008). *Sha Tin.* Hong Kong Geological Survey Sheet 7 (Edition II), Solid and Superficial Geology, 1:20,000 Series HGM20. Geotechnical Engineering Office, Hong Kong.

Geotechnical Engineering Office (GEO) (2012). *Hong Kong and Kowloon.* Hong Kong Geological Survey Map Sheet 11, Solid and Superficial Geology, 1:20,000 Series HGM20 (Edition II) Geotechnical Engineering Office, Hong Kong.

Geotechnical Engineering Office (GEO) (2018). *Yuen Long.* Hong Kong Geological Survey Map Sheet 6, Solid and Superficial Geology, 1:20,000 Series HGM20 (Edition II) Geotechnical Engineering Office, Hong Kong.

Halcrow China Limited (Halcrow) (2007). *Detailed Study of Selected Natural Terrain Landslides at Cloudy Hill (GEO Report No. 207)*. Geotechnical Engineering Office, Hong Kong, 95 p with 7 appendices.

Hansen, A. (1984). Engineering geomorphology: The application of an evolutionary model of Hong Kong's terrain. *Zeitschrift fur Geomorphologie*, supplementary vol. 51, pp 39-50.

Lee, C.W., Ho, S.Y. & Shek, W.C. (2010). *2008 Landslide Field Mapping Records - Landslide Mapping Report at Kwun Yum Temple (Landslide No. LS08-0228).* Geotechnical Engineering Office, Hong Kong, 214 p.

Lo, F.L.C., Law, R.P.H. & Ko, F.W.Y. (2015). *Territory-wide Rainfall-based Landslide Susceptibility Analysis (Special Project Report SPR 1/2015)*. Geotechnical Engineering Office, Hong Kong, 27 p.

Lo, F.L.C. & Ko, F.W.Y. (2017). *Rainfall-based Correlation of Recent Landslides with Clusters of Relict Landslides (Discussion Note DN 2/2017)*. Geotechnical Engineering Office, Hong Kong, 10 p.

Maunsell Geotechnical Services Limited (MGSL) (2008). *Detailed Study of the 21 Augus 2005 Debris Flow on the Natural Hillside near Fei Ngo Shan Service Reservoir (GEO Report No. 233).* Geotechnical Engineering Office, Hong Kong, 123 p. plus 1 drawing.

Maunsell Geotechnical Services Limited (MGSL) (2009). *Stage 3 Study Report on Feature No. 11NE-B/C960 Access Road to WSD Service Reservoir at Fei Ngo Shan (Agreement No. CE28/2006 (GE) 10-Year Extended LPM Project Phase 7, Package F - The New Territories and Outlying Islands Landslip Preventive Works on Government Slopes and Related Studies - Investigation, Design and Construction) (Stage 3 Report S3R 1/2009).* Geotechnical Engineering Office, Hong Kong, 396 p.

Ove Arup & Partners Hong Kong Limited (OAP) (2011). *Natural Terrain Hazard Study for Study Area A (Hillside Catchment Nos. 11NE-B/DF1, 11NE-B/DF1a, 11NE-B/DF7) Hillside above Windsor Castle, Fei Ngo Shan (LPMit Agreement No. CE17/2008(GE) - Natural Terrain Hazard Mitigation Works, New Territories East and West - IDC) (Stage 2(H) Report S2(H)R 5/2013).* Geotechnical Engineering Office, Hong Kong, 536 p.

Ripley, B.D. (1981). *Spatial Statistics*. Wiley, New York, 272 p.

Sin, Y.M. (2006). *Study on Geological Features Related to Landslides in Fei Ngo Shan (Unpublished Report).* Geotechnical Engineering Office, Hong Kong, 31 p.

Tang, D.L.K., Wong, C.C.J., Sin, Y.M. & Mok, S.C. (2018). *Study of Geological Controls on the Occurrence of Natural Terrain Landslide Clusters - A Pilot Study at a Catchment above Keung Shan Road, West Lantau (Geological Report GR 1/2018).* Geotechnical Engineering Office, Hong Kong, 45 p.

Wong, E.K.L., Law, R.P.H. & Li, I. (2020). *Modelling of Entrainment and Development of an Improed Debris Mobility Modelling Program "2d-DMM". (Technical Note TN 3/2020)*. Geotechnical Engineering Office, Hong Kong, 28 p.

Appendix A

Geological and Geomorphological Review of Landslide Clusters in Catchment 25 - Pak Tai To Yan

(Prepared by C.C.J. Wong)

Contents

List of Tables

List of Figures

List of Plates

A.1 Location and Catchment Characteristics at Pak Tai To Yan

Catchment No. 25 is located at Pak Tai To Yan within Lam Tsuen Country Park in Tai Po (Figure A1.1). It is sub-circular, west-oriented and covers an area of ~0.19 km^2. The elevation difference is 292 m, varies from 197 mPD to 489 mPD. The aspect ratio of the catchment (i.e. width of long axis to width of short axis) is about 1.8 to 1. A fourth order drainage system, in dendritic pattern, runs in east to west direction. The drainage system is incised at the head of drainage to the east and become a broad stream course to the west. According to the ENTLI records (updated to 2016), a total of 79 numbers of natural terrain landslides occurred in Catchment No. 25. However, no previous landslide-related study has been carried out for this catchment.

A.2 Site Geology

According to the published 1:20,000-scale geological map sheet nos. 3 (GCO, 1991) and 7 (second edition; GEO, 2008), the catchment is underlain mainly by lapilli lithic-bearing coarse ash crystal tuff with several NE-trending bands of thermally altered tuff (Figure A2.1). These volcanic rocks have been assigned to the Middle Jurassic Tai Mo Shan Formation (~ 164 Ma) in the Tsuen Wan Volcanic Group. Addison (1986) reported that the tuff is massive and welded, consisting mainly of lapilli-to-coarse ash crystal and scattered, small, sub-angular lithic lapilli of mudstone and siltstone. Secondary calcite and biotite were also reported in the tuff.

The altered tuff is pale grey, fine-grained, common with relict glassy quartz lapilli up to 5 mm. The altered tuff may also contain lithic lapilli of sandstone and microcrystalline volcanic rocks, or volcanic lapilli that appear as fiammes aligning parallel to the margins of the tuff body. The steeply-inclined bands of altered tuff are mostly less than 5 m wide but extending in some cases more than 1 km in length. Field observations (Addison, 1986) suggested that the altered tuff usually formed sharp ridges of jagged crags. Secondary biotite and deeply altered feldspar grains have been recorded. The altered tuff is interpreted to be associated with hydrothermal process, and possibly related to the intrusion of subvolcanic exhalative origin (Addison, 1986).

Few E-trending and one SE-trending faults have been mapped at the upper part of the catchment (GCO, 1991; GEO, 2008). One of the E-trending and the SE-trending faults appear to have controlled on the orientations of sub-drainages.

There is no existing ground investigation data found within and in the vicinity of the Study Area.

A.3 Slope Angle Distribution

The slope angle class distribution of the catchment is derived from 5-m grid based on the DEM generated from the 2010 airborne LiDAR data (Figure A3.1) and summarised in Table A3.1. Over 67% of the catchment has a slope angle > 30°.

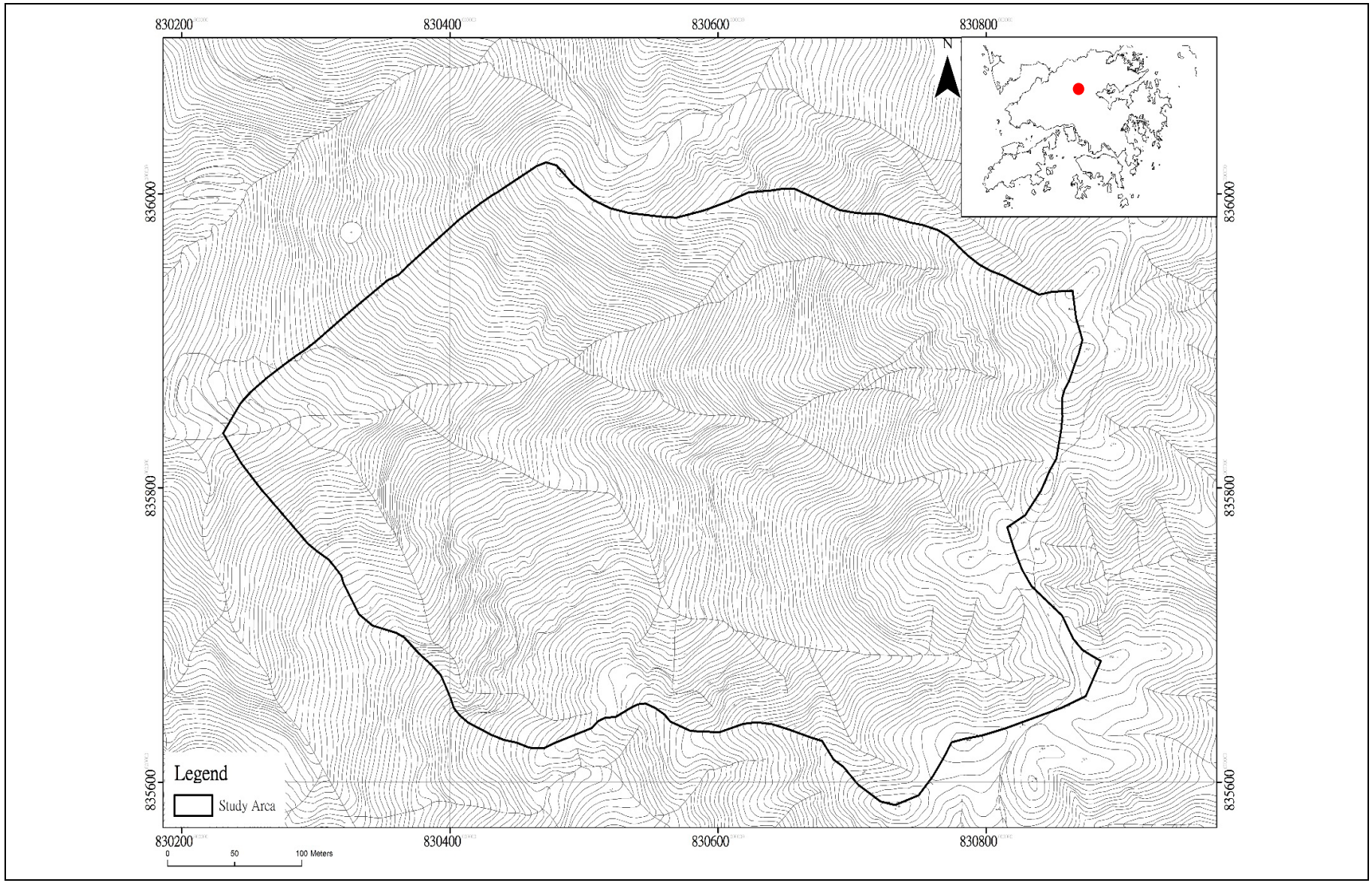

Figure A1.1 The Study Catchment (the Study Area) at Pak Tai To Yan, Tai Po

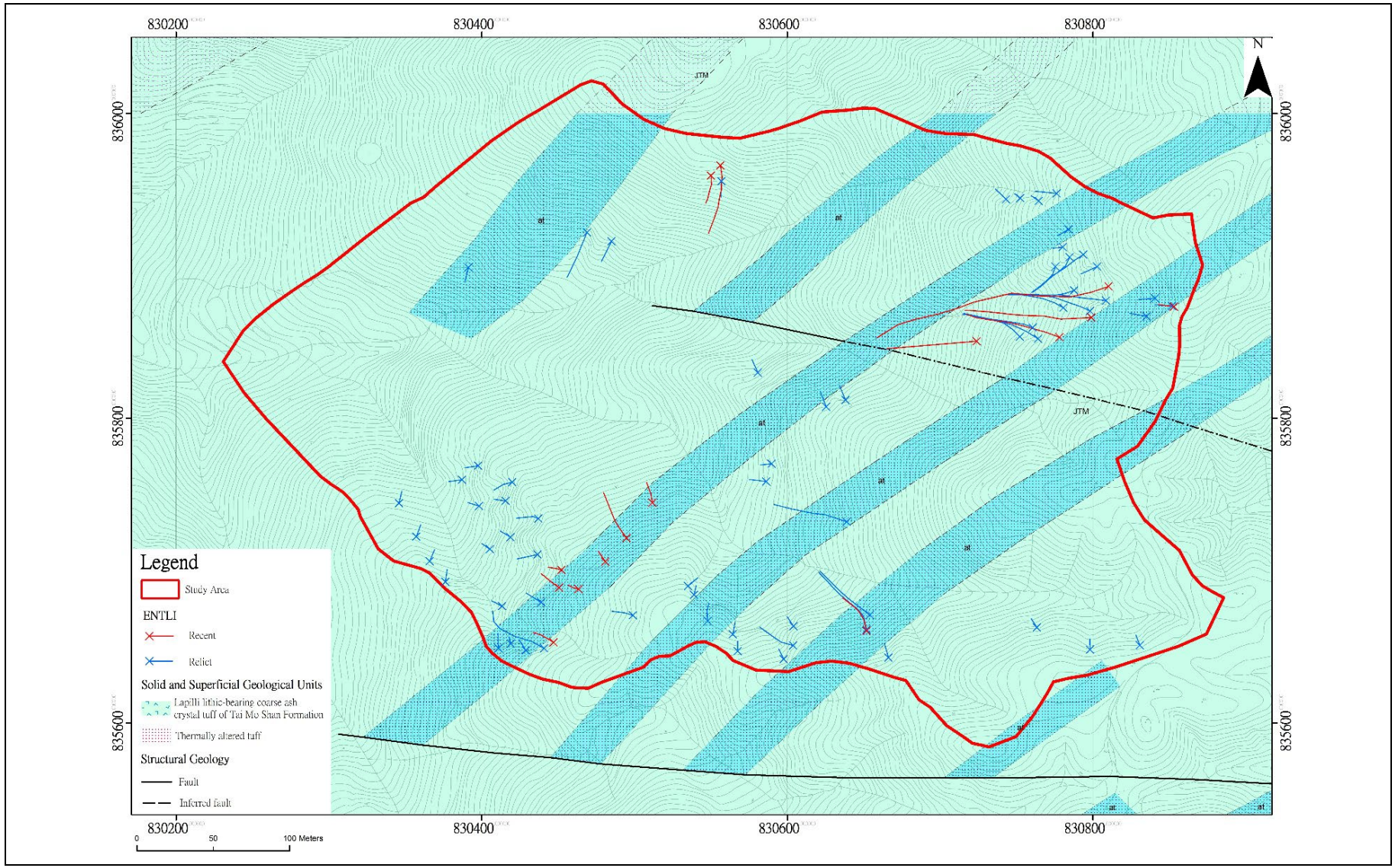

Figure A2.1 Solid and Superficial Geology of the Study Area Adopted from the Published 1:20,000-scale Geological Map Sheet Nos. 3 (GCO, 1991) and 7 (Second Edition; GEO, 2008)

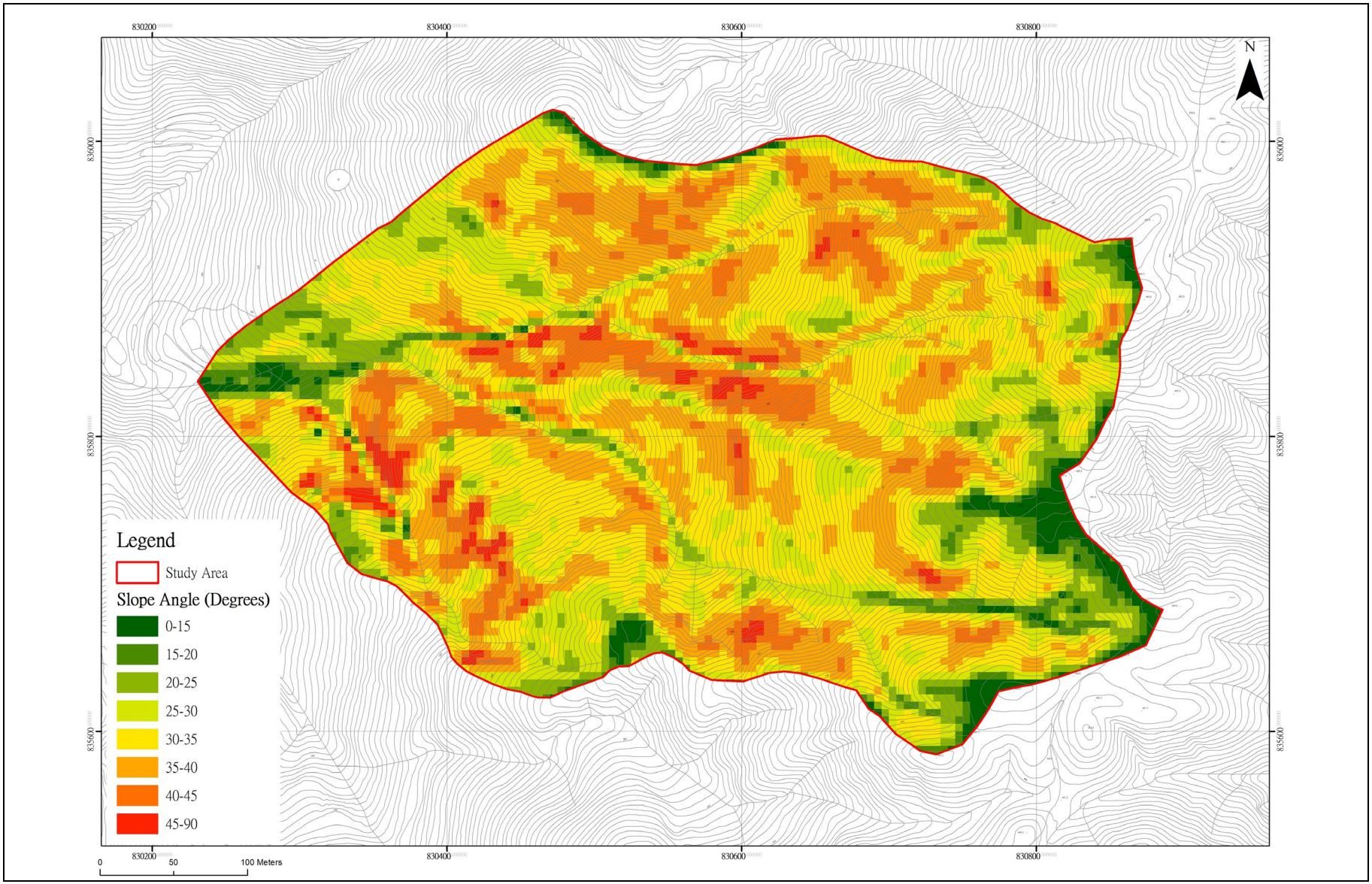

Figure A3.1 Slope Angle Classes of the Study Area Based on the DEM Generated from the 2010 Airborne LiDAR Data

Table A3.1 Distribution of Slope Angle Class in the Catchment

Slope Angle Class (Degrees)	Area (km^2)	Area (%)
0 - 15	0.0062	3.3
15 - 20	0.0075	3.9
20 - 25	0.0153	8.1
25 - 30	0.0336	17.7
30 - 35	0.0596	31.4
35 - 40	0.0462	24.3
40 - 45	0.0183	9.6
45 - 90	0.0034	1.7

A.4 Site-specific Landslide Inventory

According to the existing ENTLI database (up to 2016), there are 79 landslides, including 64 relict and 15 recent landslides, occurred in the Study Area. Of the 64 relict landslides, 50 (78.1%) landslides are classified as Class A relict, six (9.4%) as Class B relict and eight (12.5%) as Class C relict. For the recent landslides, 13 of those are open hillside failures (OHL) and two are channelised debris flows (CDF).

Past instabilities of the Study Area have been reviewed based on the available aerial photographs taken between 1945 and 2018. All landslides in the ENTLI database are confirmed and additional ten relict and three recent landslides are identified based on the API observations under this study. A total of 92 landslides, including 74 relict and 18 recent landslides are identified in the catchment. Of those recent landslides, 15 (83%) are classified as OHL and three (17%) are CDF. These landslides occurred in 1963, 1994, 1999, 2001 and 2005.

Relict and recent OHL landslides in the Study Area are relative small in size, with an average of about 8 m wide and 6 m long, and are shallow in depth (~ 1 m). The CDF in the Study Area have larger source areas compared with those for relict and recent OHL landslides. The average source area for CDF is about 15 m wide and 10 m long. Details and the characteristics of relict and recent landslides are summarised in Table A4.1.

Most of the recent and relict landslides occurred on slopes at slope angle class of 35 - 40°. In Table A4.2, about 94% of recent and 96% of relict landslides occurred on steeper terrain with slope gradient over 30°.

Table A4.1 Characteristics of Landslides in the Catchment

Type	Source Width (m)	Source Length (m)	Source Depth (m)	Est. Source Vol. (m^3) (1/6 π x W x L x D)	Runout Distance (m)
Relict Landslide (74 Landslides)					
	3 - 19.5 (average 7.6)	2 - 19 (average 6.2)	0.5 - 3 (average 1.4)	2 - 408 (average 42)	N/A
Recent Landslide (18 Landslides)					
OHL (15 nos.)	3.5 - 16 (average 8.2)	2.5 - 12 (average 5.6)	1 - 1.5 (average 1.1)	8 - 129 (average 41)	4 - 74 (average 24.4)
CDF (3 nos.)	14.5 - 16 (average 15.1)	8 - 11.5 (average 9.7)	1 - 2 (average 1.5)	80 - 181 (average 113)	133 - 166 (average 147.3)

Table A4.2 Distribution of Landslides in Slope Angle Classes in the Catchment

Slope Angle Class (Degrees)	No. of Recent Landslides	No. of Recent Landslides (%)	No. of Relict Landslides	No. of Relict Landslides (%)	Recent Landslide Density (No. of Landslide /km^2)	Relict Landslide Density (No. of Landslide /km^2)
0 - 15	0	0	0	0	0	0
15 - 20	0	0	0	0	0	0
20 - 25	0	0	0	0	0	0
25 - 30	1	5.6	3	4	29.8	89.2
30 - 35	2	11.1	16	21.5	33.6	268.5
35 - 40	10	55.5	30	41.0	216.5	649.5
40 - 45	4	22.2	16	21.5	218.9	875.5
45 - 90	1	5.6	9	12.0	296.3	2666.7

Three relict and four recent landslides are likely associated with geological structures. One of the relicts (ENTLI no. 7NWA0060E) has the initiation point immediately below the altered tuff bands. The other two relict scars (ENTLI no. 7NWA1160E and L54) are located at the geological boundary between crystal tuff and altered tuff bands. Four recent landslides (ENTLI nos. 7NWA1697E, 7NWA1698E, 7NWA1767E and 7NWA1776E) occurred across the mapped boundary between crystal tuff and altered tuff bands.

A.5 Human Activities

Based on observations from the year 1963 aerial photographs, about 32% of the catchment shows evidence of human disturbance (Figure A5.1). Series of linear features, possibly related to tea terraces activities, were observed, most of which were located at the mid-slope of the Study Area (Plate A6.1). The linear features, up to 50 m long and with varying spacing of about 6 - 10 m, were in herringbone pattern, cutting across contour lines. Some of these terraces might be related to local signs of distress in the catchment (see Section A.6 below).

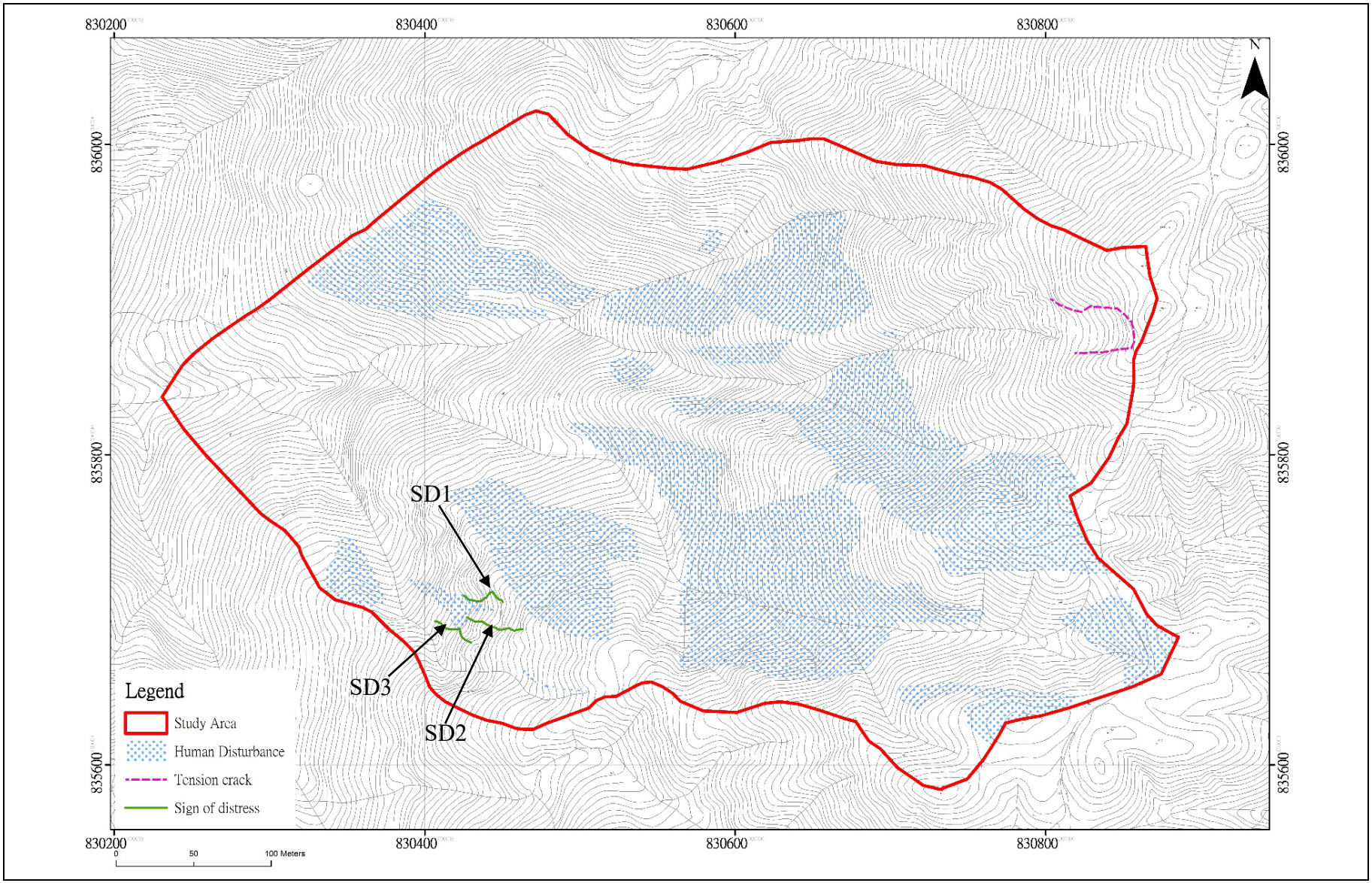

Figure A5.1 Distribution of Human Activities and Instability in the Study Area

A.6 Tension Crack and Signs of Distress

One tension crack and three sign of distress features were identified in year 1963 aerial photographs (Plates A6.1, A6.2 and Figure A5.1). The tension crack is observed near the ridge (830856E 83578N) and within a broad topographic depression up to 28 m wide. A landslide, ENTLI no. 07NWA1804E, is found to locate immediately below the tension crack. The length of the tension crack is approximate 110 m. In addition, three sign of distress features in curve shape (SD1 to SD3), with varying lengths from 29 m to 39 m. They are located in the NW-facing slope of the southern part of the catchment. The distress features SD1 and SD2 are partly located within the human disturbance area and likely associated with terraces activities. The distress feature SD2 further extends to the southern portion of landslide scars. The occurrence of distress feature SD3 may possibly be related to progressive failure.

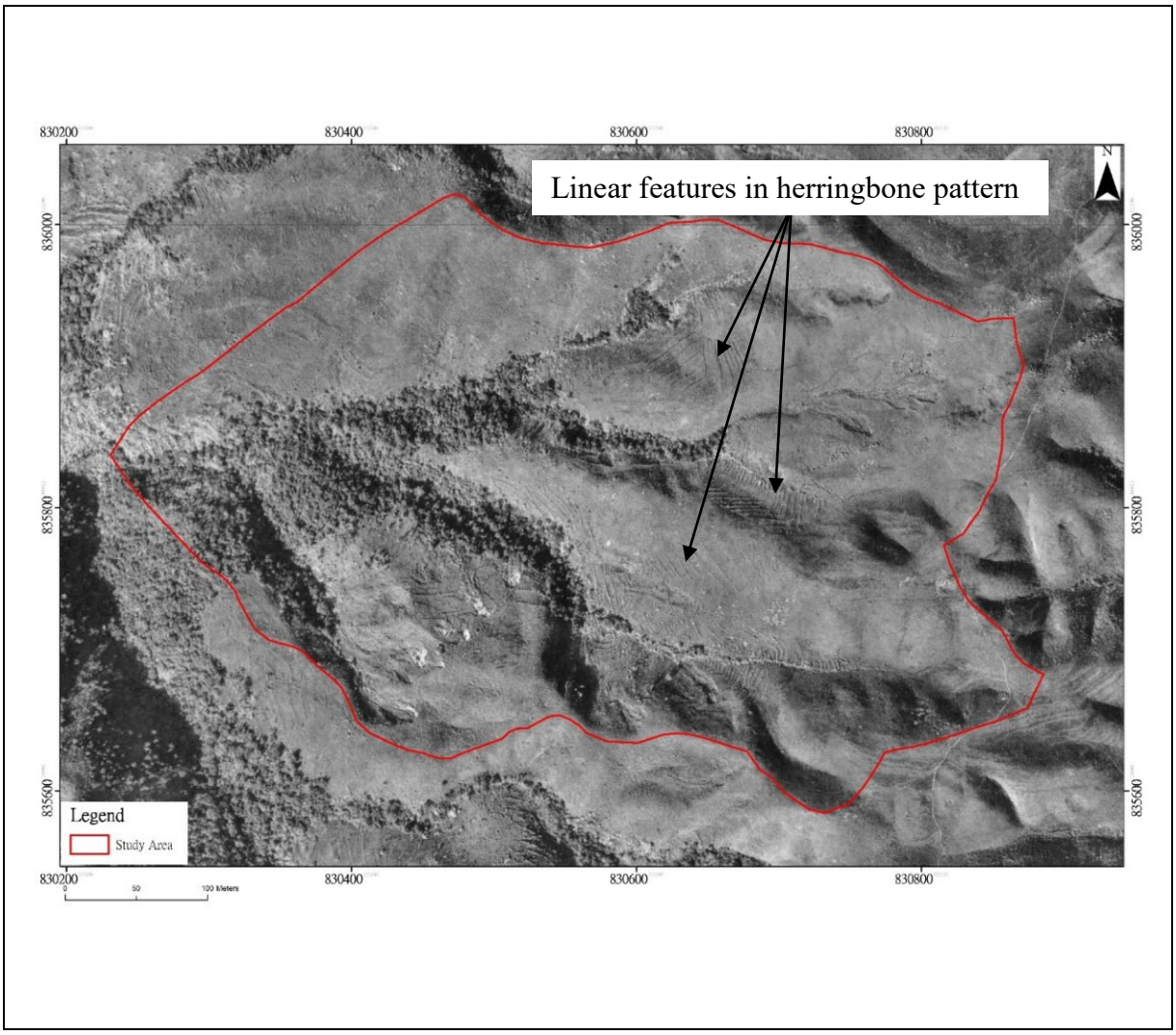

Plate A6.1 Location of Human Activities in the Study Area

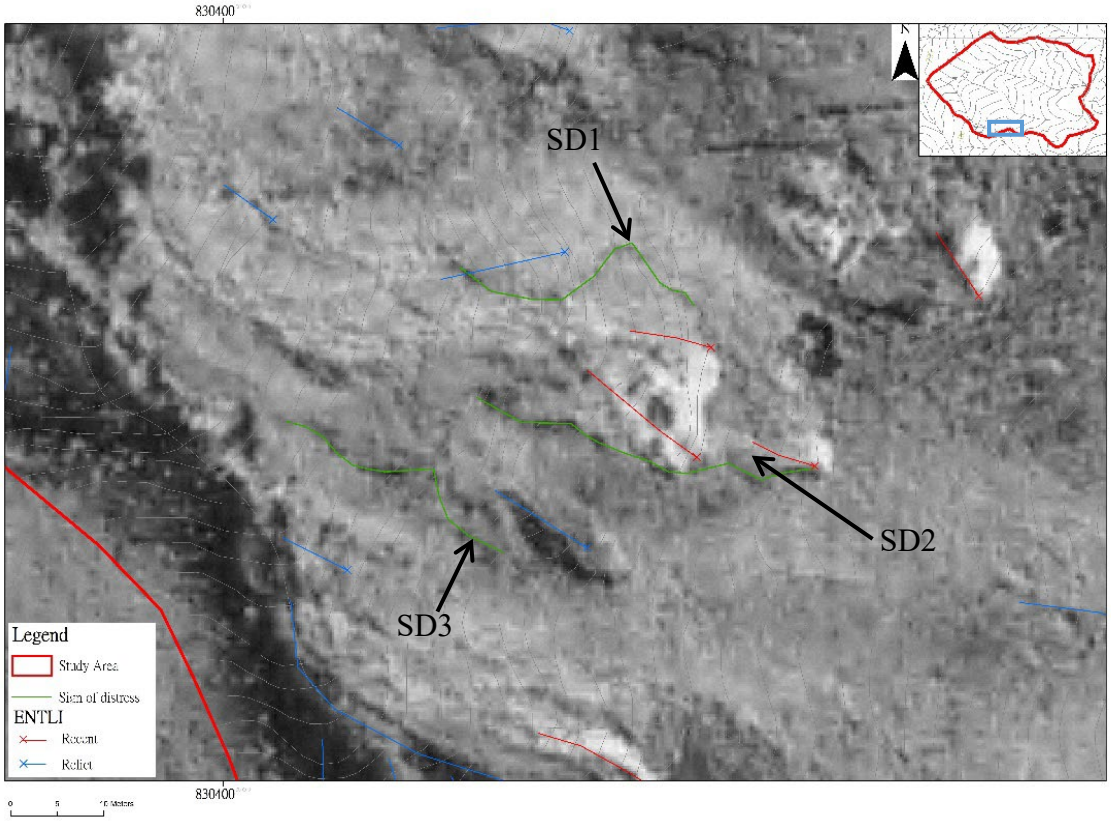

Plate A6.2 Sign of Distress Features in the Study Area

A.7 Site Geomorphology

The geomorphology of the Study Area was interpreted from year 1963 aerial photograph with aid of LiDAR data. The Study Area can be subdivided into six geomorphological units, namely 'Ridge', 'Open side slope', 'Rocky terrain', 'Drainage depression', 'Valley side slope' and 'Valley deposit' (Figure A7.1).

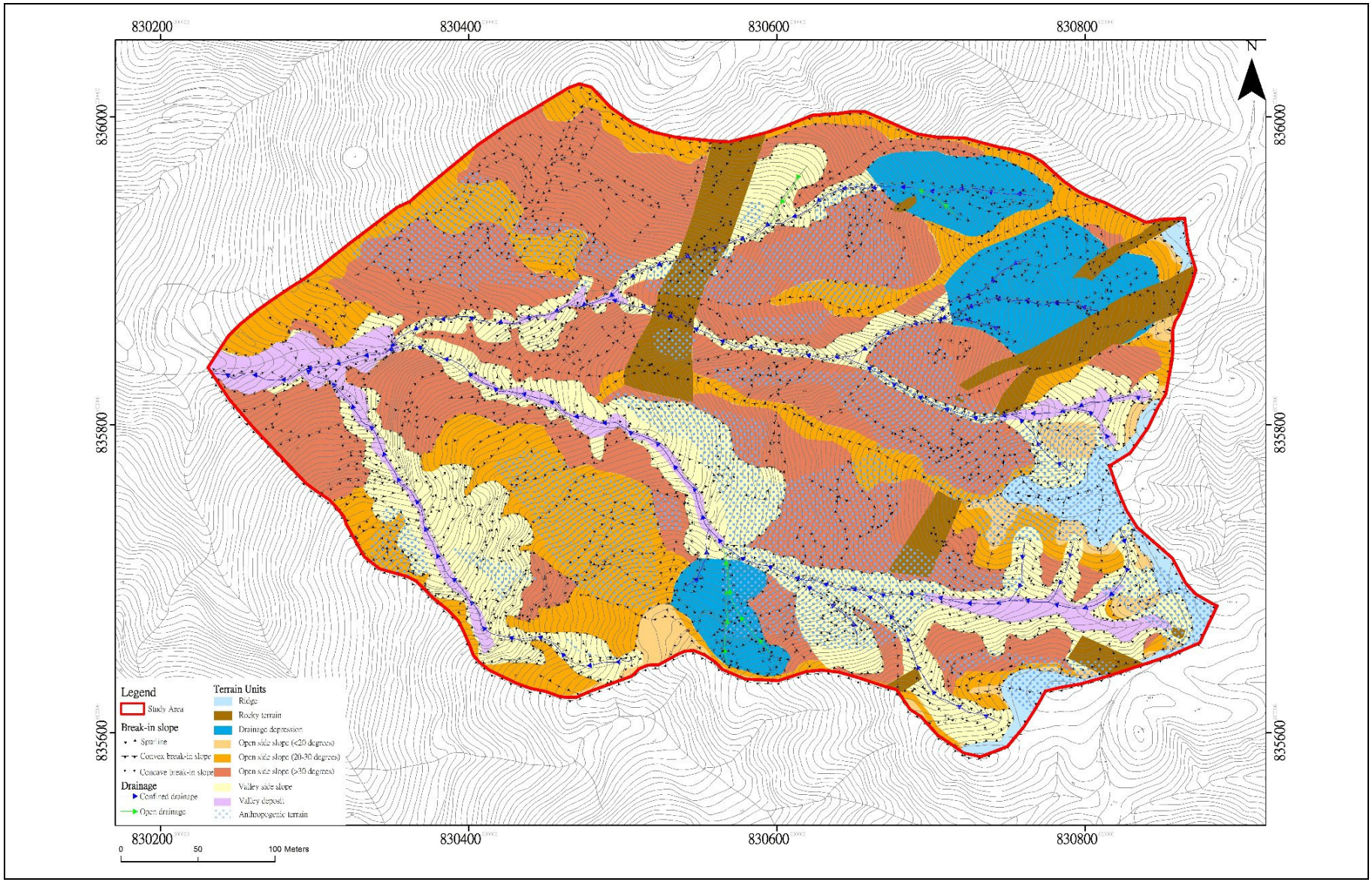

Figure A7.1 Geomorphological Units of the Study Area

A.7.1 'Ridge' Unit

This unit is located at the uppermost portions of the Study Area, mostly between 448 mPD and 489 mPD. It is predominately bounded by a series of rounded peaks along northeast to southwest-trending ridgeline, and with slope gradient of generally less than 15°. The unit is separated from the lower part of the catchment by a well-defined convex break-in slope. The regolith is interpreted as saprolite of crystal tuff and altered tuff. No landslide is found within this terrain unit.

A.7.2 'Open Side Slope' Unit

The 'Open side slope' unit comprises relatively planar slopes of the catchments. This terrain unit can be divided into 3 sub-units based on the slope angles < 20°, 20 - 30° and > 30°. The change in slope angle possibly reflects a transition from erosion to transportational terrains.

(i) 'Open side slope (< 20°)' is located immediately below 'Ridge' and extends to approximate 436 mPD. It represents broad, gently-sloping interfluves. The boundary of this sub-terrain unit is confined by secondary convex break-in slope. No landslide is found within this sub-terrain unit. The regolith is interpreted as saprolite of crystal tuff and altered tuff.

(ii) 'Open side slope (20 - 30°)' covers the planar slope with moderately steep gradient and locates immediately below 'Open side slope (< 20°)'. The lower boundary of this sub-terrain unit is bounded by secondary convex break-in slope. Some human activities have been identified within this unit. A total of eight landslides (including four relict and four recent) occurred within this sub-unit. The regolith is interpreted as thin layer of colluvium (up to 2 m) overlay saprolite of crystal tuff and altered tuff.

(iii) 'Open side slope (> 30°)' is located below 'Open side slope (20 - 30°)' and is characterised by hummocky surface, and locally steeper slope of > 45°. This unit covers most of the mid-slope area of the catchment. Past human activities are common in this terrain unit. Twelve relict and five recent landslides are found in this sub-unit. The regolith is interpreted as thin layer of colluvium (locally up to 3 m) overlay saprolite of crystal tuff and altered tuff.

A.7.3 'Rocky Terrain' Unit

The 'Rocky Terrain' unit refers to the terrains with intermittent rock outcrops that are inferred to be underlain by the N- to NE-trending altered tuff bands. One of these altered

tuff bands appears as a continuous band across several spurs for over ~ 170 m, while most of them are appeared partly on slope faces. Slope angle usually at 30 - 40° and locally > 45°. The slope gradient becomes shallower (< 25°) near the ridge where some exhumed corestones (tors) are present. A total of twelve landslides (including six relict and six recent) occurred in this unit.

A.7.4 'Drainage Depression' Unit

The 'Drainage depression' unit includes concave terrains that are located at the head of drainages and immediately below 'Open side slope (20 - 30°)'. This is an erosional unit with slope gradient of 30 - 40° and locally 40 - 45°. This area associates with head of drainages in the Study Area. Based on year 1963 aerial photograph, this unit comprise thin layer of colluvium (depth up to 2 m) overlay alluvium. A tension crack (mentioned in Section A.6) is located in one of the depression at the east of the Study Area. Human activities are found in the depression locates at the south of the Study Area. Twenty-five relict and three recent landslides are found in this terrain unit.

A.7.5 'Valley Side Slope' Unit

The 'Valley side slope' unit comprises deeply-incised terrains with general gradient of 35 - 40° and locally > 45° on both sides of well-defined stream courses. This terrain unit have been formed due to fluvial erosion along the drainages. The boundary between 'Open side slope' and 'Valley side slope' units is delineated by steepened heads of stream course and a convex break-in slope. This terrain unit is steep and narrow, with span up to 80 m. It consists of series of topographic depressions and many discontinuous and complex break-in slopes. The regolith for this terrain unit is interpreted as a thin layer of colluvium (2 - 3 m thick), overlying the saprolite of crystal tuff and altered tuff. This terrain unit may also represent reactivation of landslide debris, in particular at the southern part of the Study Area, which also indicate a change in erosion rate. Twenty-seven relict landslides are found in this unit but no recent landslide is observed. In particular, some topographic depressions with slope gradient > 45° at the southern portion of the catchment are associated with relict landslides. This terrain unit has locally affected by human disturbance.

A.7.6 'Valley Deposit' Unit

The 'Valley deposit' is a depositional unit and associates with the alluvium deposits along drainage. This unit has slope gradient of < 25°. Long and elongate deposit is found at the upper stream with slope gradient of 20 - 25°. It concentrates at the outlet of the drainage, locates at west of the study area when the slope gradient becomes shallow (i.e. < 15°). No landslide is found in this unit. This terrain unit has partly affected by human disturbance at the eastern part of the Study Area.

A.8 Landslide Density

The locations and extent of altered tuff bands have been refined based on the API

observations. The distribution of landslides in each slope angle class of different rock types (i.e. crystal tuff and altered tuff) is shown in Tables A8.1 and A8.2. In general, about 92% (68 of 74) of relict and 67% (12 of 18) of recent landslides occurred in crystal tuff. Most of the recent and relict landslides are distributed at slope angle class of 35 - 40° in both crystal tuff and altered tuff. For crystal tuff, slope angle class of 45 - 90° has the highest landslide densities for both relict and recent landslides. For altered tuff, equal distribution of relict and recent landslide at all slope angle classes and slope angle class of 35 - 40° has the highest landslide densities for both relict and recent landslides.

The landslide distribution and densities of relict and recent landslides for geomorphological units are shown in Table A8.3 and Figure A8.1. The recent and relict landslides occurred within the anthropogenic terrain has a combination factor of human activities on the respective terrain. The result shows that the 'Valley side slope' has the highest landslide density for the relict landslide whereas the 'Drainage depression' for recent landslide**.**

Table A8.1 Distribution of Landslides in Slope Angle Classes in Crystal Tuff of Tai Mo Shan Formation

Slope Angle Class (Degrees)	Area (km^2)	Area (%)	No. of Recent Landslides	No. of Relict Landslides	Recent Landslide Density (no. of Landslide /km^2)	Relict Landslide Density (no. of Landslide /km^2)
0 - 15	0.00607	3.4	0	0	0	0
15 - 20	0.00723	4.1	0	0	0	0
20 - 25	0.0145	8.1	0	0	0	0
25 - 30	0.0316	17.7	1	3	31.7	95.0
30 - 35	0.0563	31.6	1	15	17.8	266.6
35 - 40	0.0426	23.9	6	26	141.0	611.0
40 - 45	0.0167	9.4	3	15	179.5	897.3
45 - 90	0.0033	1.9	1	9	302.4	2721.2

Table A8.2 Distribution of Landslides in Slope Angle Classes in Altered Tuff

Slope Angle Class (Degrees)	Area (km^2)	Area (%)	No. of Recent Landslides	No. of Relict Landslides	Recent Landslide Density (No. of Landslide /km^2)	Relict Landslide Density (no. of Landslide /km^2)
0 - 15	0.0000964	0.8	0	0	0	0
15 - 20	0.000220	1.9	0	0	0	0
20 - 25	0.000816	6.9	0	0	0	0
25 - 30	0.00202	17.2	0	0	0	0
30 - 35	0.00334	28.4	1	1	299.5	299.5
35 - 40	0.00364	30.9	4	4	1099.6	1099.6
40 - 45	0.00156	13.2	1	1	642.1	642.0
45 - 90	0.0000677	0.6	0	0	0	0

Table A8.3 Distribution of Landslide Density in Geomorphological Settings

Geomorphological Setting (Terrain Unit)	Area (km^2)	No. of Recent Landslides	No. of Relict Landslides	Recent Landslide Density (No. of Landslide /km^2)	Relict Landslide Density (no. of Landslide /km^2)
Ridge	0.00531	0	0	0	0
Open Side Slope (< 20°)	0.00439	0	0	0	0
Open Side Slope (20 - 30°)	0.0348	4 (3*) (22.2%)	4 (1*) (5.4%)	114.9	114.9
Open Side Slope (> 30°)	0.0698	5 (1*) (27.8%)	12 (5*) (16.2%)	71.6	171.9
Rocky Terrain	0.0118	5 (27.8%)	6 (8.1%)	508.5	508.5
Drainage Depressions	0.0149	6 (33.3%)	25 (33.8%)	201.3	1677.9
Valley Side Slope	0.0406	3 (1*) (16.7%)	27 (9*) (36.5%)	0	665
Valley Deposit	0.00871	0	0	0	0

Note: Asterisk denotes as the number of landslide overlaps with anthropogenic terrain. Percentage in bracket indicates the distribution of landslide in each terrain unit.

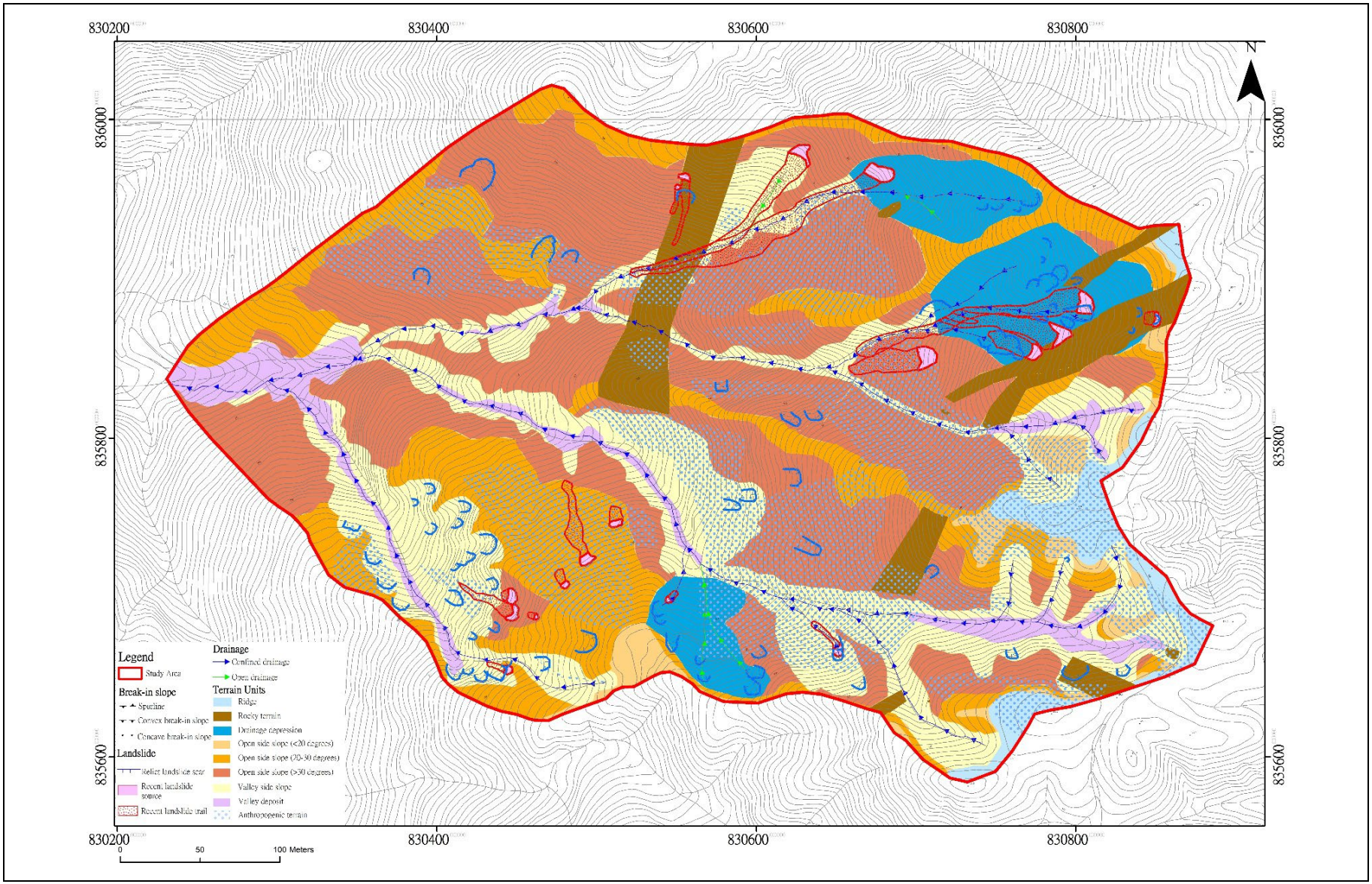

Figure A8.1 Distribution of Landslides in Geomorphological Units

A.9 Landslide Clusters

The distribution and the characteristics of landslide clusters at the Study Area have been reviewed according to the eight-fold classification scheme proposed by Tang et al (2018). The results are summarised in Table A9.1 below.

Table A9.1 Summary of Characteristics of Landslide Clusters at the Study Area

Type of Landslide Cluster	No. of Recent Landslides	Range of Distance to the Closest Related Relict (Older) Landslides (m)
1	2[(1)] (11%)	2 - 7
2	1* (5.5%)	2
3	3[(2)] (17%)	5 - 10
4	1[(1)] (5.5%)	13
5	0	N/A
6	1 (5.5%)	10
7	1 (5.5%)	5
8	0	N/A
Not in Clusters	9 (50%)	N/A

Note: Number in the upper bracket denotes as the number of landslide locates across boundary between crystal tuff and altered tuff. Asterisk denotes as the landslide is also affected by human disturbance.

The review found that about 50%, 39% and 11% of recent landslides in the catchment were not in cluster, Type 1 to 4 and Type 5 to 8, respectively.

Half (9 out of 18) of the recent landslides are considered not related to previous landslides and do not form landslide clusters. These landslides are located in the 'Rocky' (1 landslide), 'Open side slope (20 - 30°)' (2 landslides), 'Open side slope (> 30°)' (5 landslides) and 'Drainage depression' (1 landslide) units. Only two (~ 11%) of these landslides are associated with drainage erosion and might be indirectly related to the underlying geological structures (i.e. fault). Four (~ 22%) out of these nine landslides occurred in the human disturbance area, and three (~ 17%) of these were associated with signs of distress (Figure A3.3, SD1 and SD2).

For recent landslides belong to Type 1 to 4 clusters, the range of distance to the closest related relict landslides are up to 13 m. As suggested by Tang et al (2018), Type 1 to 4 landslide clusters are more likely to be related to geomorphological factors. However, there are four landslides under Types 1, 3 and 4 that were initiated across the boundary between crystal tuff and altered tuff bands. The occurrence of these four landslides could have been affected by the geological contacts.

Only 11% recent landslides were related to erosion at the head of drainage lines or to undercutting processes along drainage lines (i.e. Types 5 to 7 clusters). The distribution of these landslide clusters are thus considered to be related to the drainage pattern of the catchment, which in-turn might be indirectly related to the underlying geological structures (e.g. fault).

A.10 Conclusion

In this study, the geological and geomorphological settings of Catchment PTTY have been reviewed to identify any potential geological and geomorphological factors that may contribute to concentration of landslide activities. The key observations are summarised below:

(a) A total of 92 landslides were identified in the Study Area. Eighteen of them are recent landslides and 74 are relict. About 92% of relict and 67% of recent landslides occurred in crystal tuff. About 32% of the Study Area had been modified by human activities that formed series of linear trenches for terraces purposes. Furthermore, a tension crack and three features associated with sign of distress were identified. Two of the distress features were associated with terraces activities and one might be related to progressive failure.

(b) The Study Area is broadly defined into six geomorphological terrain units, namely 'Ridge', 'Open side slope', 'Rocky terrain', 'Drainage depression', 'Valley side slope' and 'Valley deposit'. About 37% of relict landslides occurred on 'Valley side slop' and 33% of recent landslides on 'Drainage depressions'.

(c) Based on the observations from the study, about 39% recent landsides were in clusters related to retrogressive failures, destabilised past landslide debris, over-steepened slopes or topographic depressions (i.e. Types 1 to 4 clusters; Tang et al, 2018). Four landslides under Types 1 to 4 clusters are also controlled by geological factor that their occurrence were across geological boundary between crystal tuff and altered tuff bands. About 11% recent landslides were related to erosion/undercutting along drainage lines (i.e. Types 5 to 7). Half of the recent landslides (nine numbers) were not in cluster, and four of which were likely to be associated with past human activities. Approximately 22% recent landslides (four numbers) are related to the geological boundaries between crystal tuff and altered tuff bands.

A.11 References

Addison, R. (1986). *Geology of Sha Tin. Geological Survey Memoir No. 1*. Geotechnical Control Office, Hong Kong, 85 p.

Geotechnical Control Office (GCO) (1991). *Sheung Shui.* Hong Kong Geological Survey Sheet 3, Solid and Superficial Geology, 1:20,000 Series HGM20. Geotechnical Control Office, Hong Kong.

Geotechnical Engineering Office (GEO) (2008). *Sha Tin.* Hong Kong Geological Survey Sheet 7 (Edition II), Solid and Superficial Geology, 1:20,000 Series HGM20. Geotechnical Engineering Office, Hong Kong.

Tang, D.L.K., Wong, C.C.J., Sin, Y.M. & Mok, S.C. (2018). *Study of Geological Controls on the Occurrence of Natural Terrain Landslide Clusters - A Pilot Study at a Catchment above Keung Shan Road, West Lantau (Geological Report No. GR 1/2018).* Geotechnical Engineering Office, Hong Kong, 45 p.

Appendix B

Geological and Geomorphological Review of Landslide Clusters in Catchment 46 - Fei Ngo Shan

(Prepared by K.L.H. Lo)

Contents

List of Tables

List of Figures

B1 Location and Catchment Chara

The Study Area is a southeast-facing hillside, located to the east of Fei Ngo Shan summit, Kowloon. The catchment covers an area of approximately 0.262 km^2, with an elevation arise from +196 mPD to +600 mPD at the crest (Figure B1.1). The aspect ratio of the catchment (i.e. width of long axis to width of short axis) is about 6 to 5. The Study Area has been modified by developments, including Fei Ngo Shan Fresh Water Service Reservoir, Fei Ngo Shan Road and the associated man-made features at the toe of the Study Area. Three Historical Landslide Catchments (HLCs), HLC Nos. 11NE-B/DF 1, 11NE-B/DF 7 and 11NE-B/OH 13 are located within the Study Area.

B.2 Geology

According to the published 1:20,000-scale geological map (Figure B2.1; GEO, 2012) and the accompanying geological reports, the Study Area is underlain largely by coarse ash crystal tuff of the Mount Davis Formation. A band of NNW-trending tuff breccia was mapped along the access road to Fei Ngo Shan Fresh Water Service Reservoir. A NNE-trending band of eutaxitic crystal-bearing fine ash vitric tuff is shown along the ridge of Fei Ngo Shan. A subordinate quartzphyric rhyolite dyke is shown to the east of the eutaxite band, near the summit. Colluvial deposits (> 2 m) are shown in the eastern flank of the catchment. No major fault intersects the Study Area but the NE-trending Jordon Valley Fault is shown to the southeast of the catchment.

Limited ground investigation data is available in the Study Area, at the foothill to the southeast of Fei Ngo Shan, mainly for previous LPMitP works and residential developments along Fei Ngo Shan Road (Figure B2.2). The previous ground investigation data revealed that the area is mainly underlain by lapilli-bearing coarse ash crystal tuff.

At the hillside to the east of Fei Ngo Shan, ground investigation works were carried out between February and April 2006 for investigation of a major landslide occurred on the natural hillside near the Fei Ngo Shan Service Reservoir on 21 August 2005. Weak to strong eutaxitic foliations occurred within the tuffs and were observed in the drillcores. Manganese-stained, polished and occasionally slickensided relict joint surfaces were observed in one of the trial pits (Trial Pit No. 43184/TP 7). These features were thought to be the possible geological controls of the major landslide occurred in 2005 (MGSL, 2008).

A few existing drillholes for extension works of a transposer station is also available. Colluvial deposits up to 8.5 m (Drillhole No. 41532/B-1) thick are present at the drainage line diverting towards Windsor Castle.

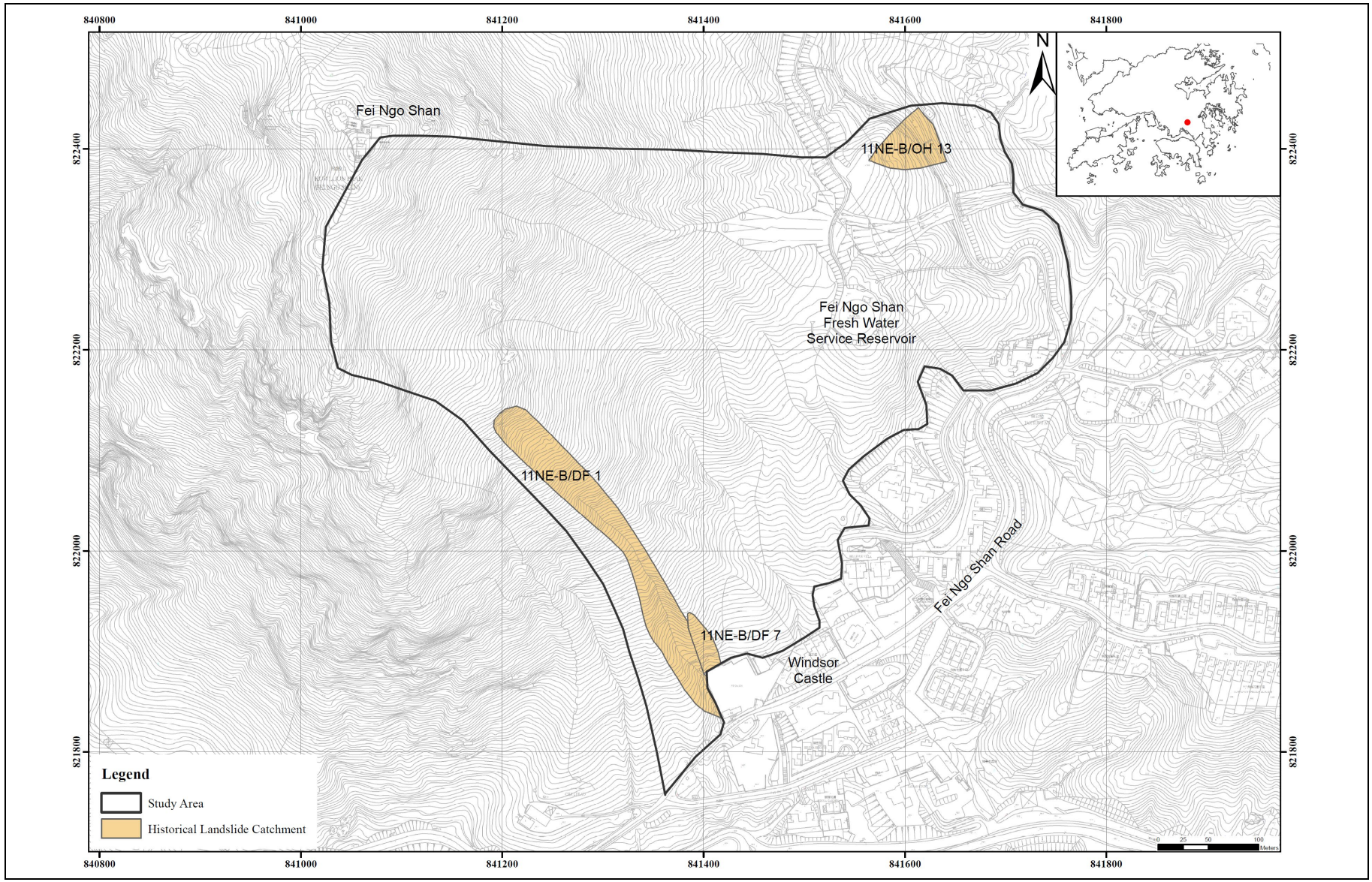

Figure B1.1 Location of the Study Area

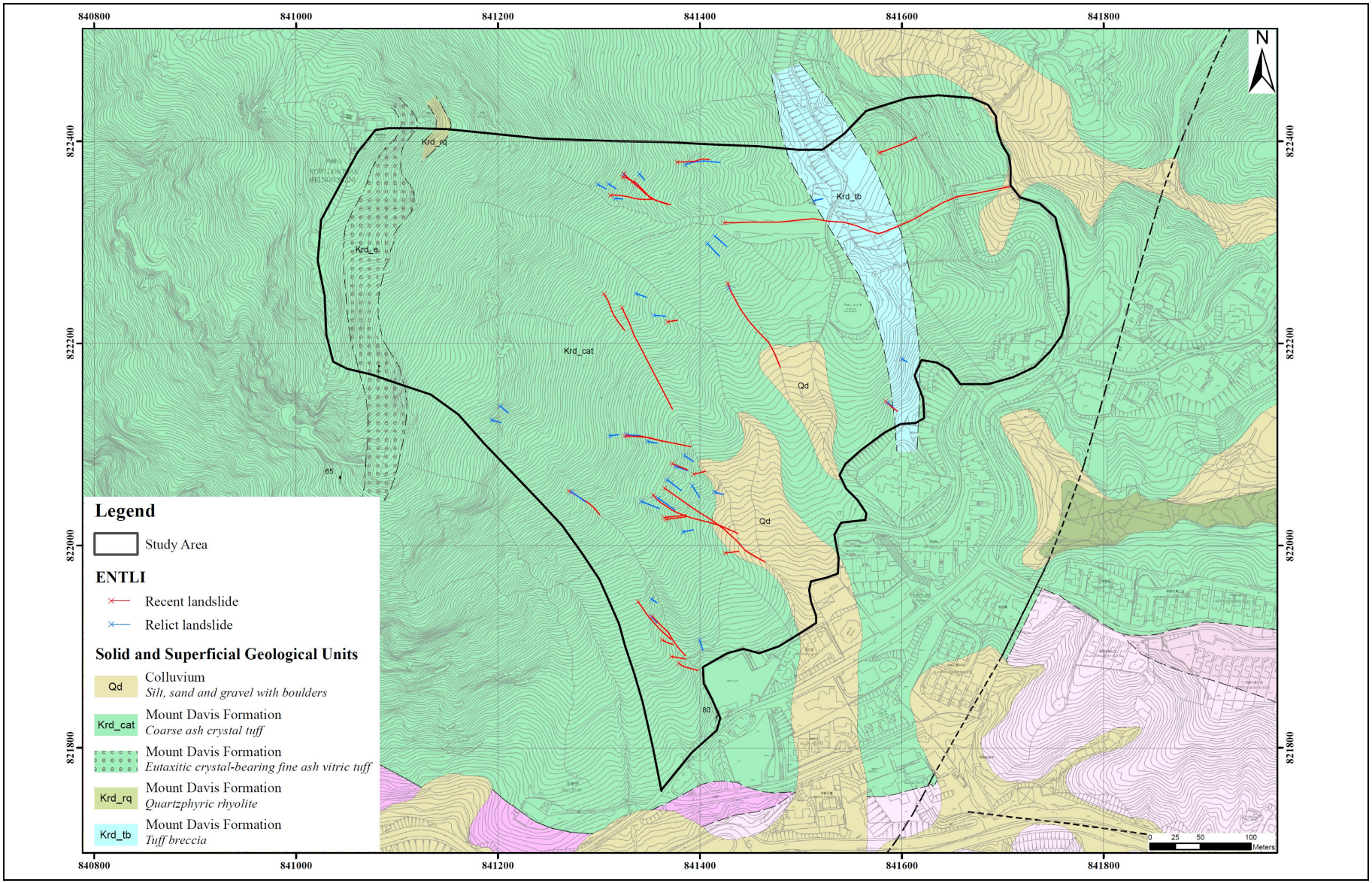

Figure B2.1 Geology of the Study Area

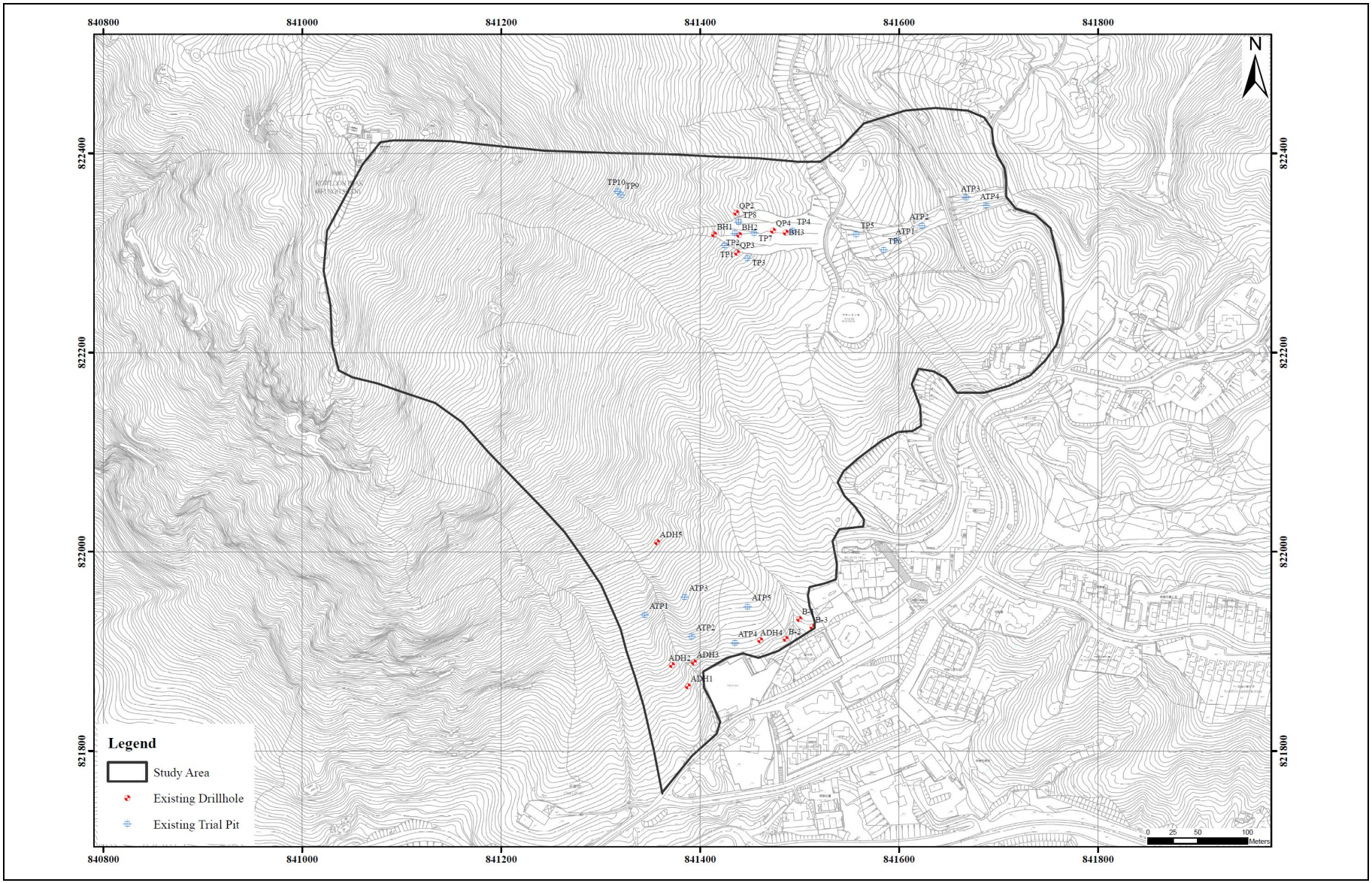

Figure B2.2 Locations of Ground Investigation Stations

B.3 Natural Terrain Landslides

According to the ENTLI (up to 2013), a total of 58 landslide features were recorded within the Study Area, including 27 recent landslides and 31 relict landslides. Study-specific API was carried out to verify these features and confirmed that the Study Area has 27 recent landslides, in which more than one-third (10 nos.) of the landslides were occurred in 2008. Four additional landslides have been identified such that the number of relict landslides was increased from 31 to 35.

The source and trail area of the confirmed recent landslides as well as the scarp of the confirmed relict landslides were delineated (Figure B3.1). A slope angle map of 5-m grid (derived from 2010 airborne LiDAR data; Figure B3.2) was prepared for the Study Area and reviewed with the verified landslides. Table B3.1 shows the distribution of landslides under the eight slope angle classes. No landslide is observed on slope with gradient less than 20°. Over 95% of the landslides were located on slope with a gradient greater than 30°, with a highest percentage for the slope angle class 6 (35 - 40°). Majority of the relict landslides occurred with slope angle classes 5 to 7 and with a few features that were found on slopes with gradient less than 30°.

The verified recent landslides have a source width varying from a few metres to 37 m. The depth of the recent landslides was generally shallow (typically 1 - 1.5 m, up to 4.5 m) and the estimated landslide source volumes were mostly less than or around 100 m^3 with one recent feature (ENTLI No. 11NEB0572E) up to around 280 m^3 and the largest one (ENTLI No. 11NEB0566E) approximately 3,400 m^3.

The largest landslide within the Study Area occurred near Fei Ngo Shan Service Reservoir, at about 6 a.m. on 21 August 2005. The source of the landslide was mainly within a rounded, scoop-shaped depression located slightly beneath a spurline. The landslide scar was up to 40 m long, 25 - 32 m wide and 3.5 - 5 m deep. Material exposed within the main landslide scar comprised residual soil and saprolite overlain by a thin layer of colluvium. The rupture surface of the landslide was largely controlled by persistent, adversely-oriented, undulating, clay-infilled joints. The close correlation between the intense rainfall recorded on 19 and 20 August 2005 and the time of the failure suggests that the landslide was probably rain-induced (MGSL, 2006).

The relict landslides generally had a smaller source width ranging from 6 m to 23 m. The source depth of most of the relict landslides was shallow as well, typically 1 - 2 m. The estimated volume of more than 80% of the relict landslides was less than 200 m^3 with six relict features up to around 340 m^3.

In summary, both the relict and recent landslides within the Study Area were shallow and of relatively small source volume.

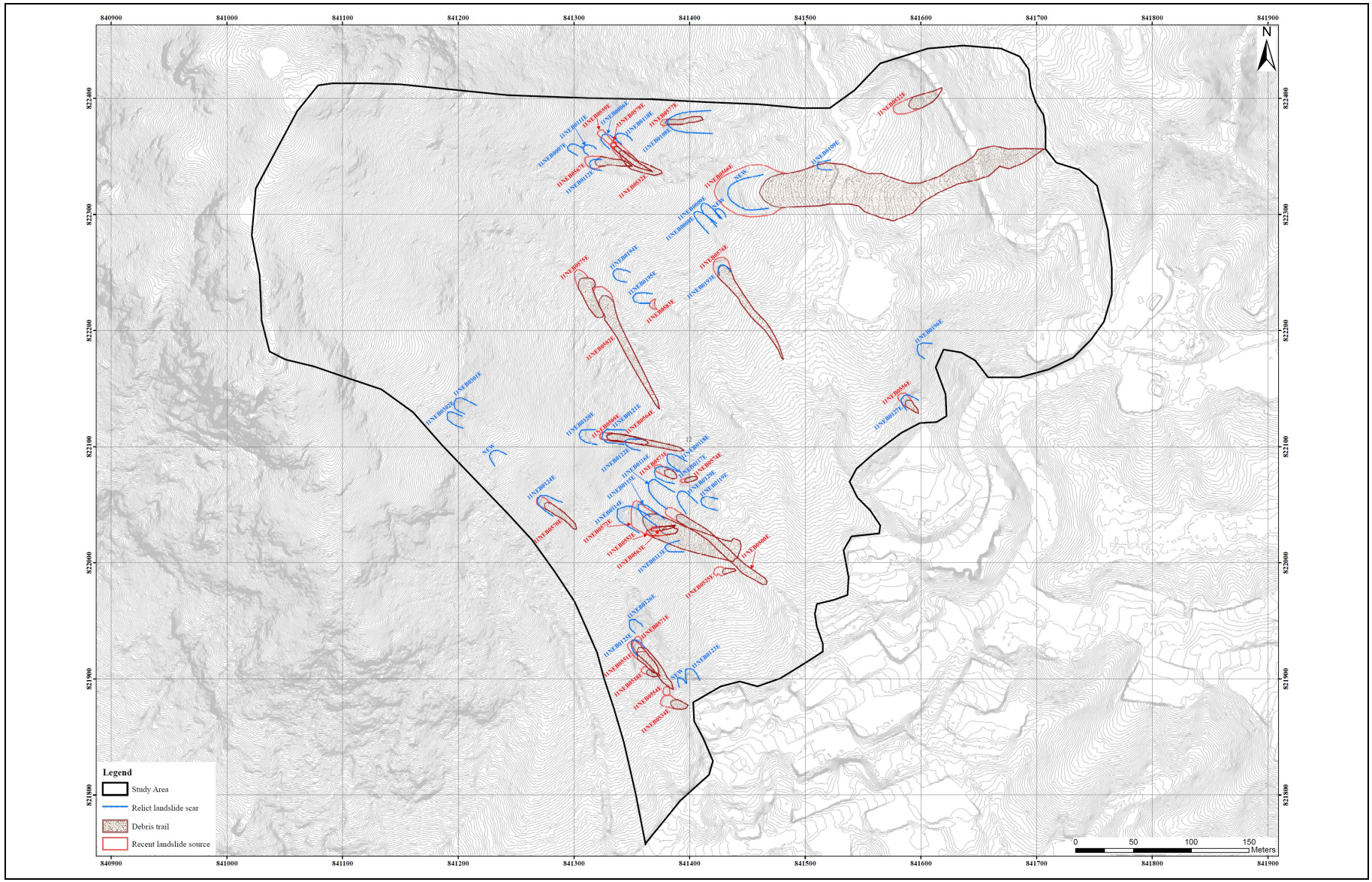

Figure B3.1 Locations of Verified Landslides

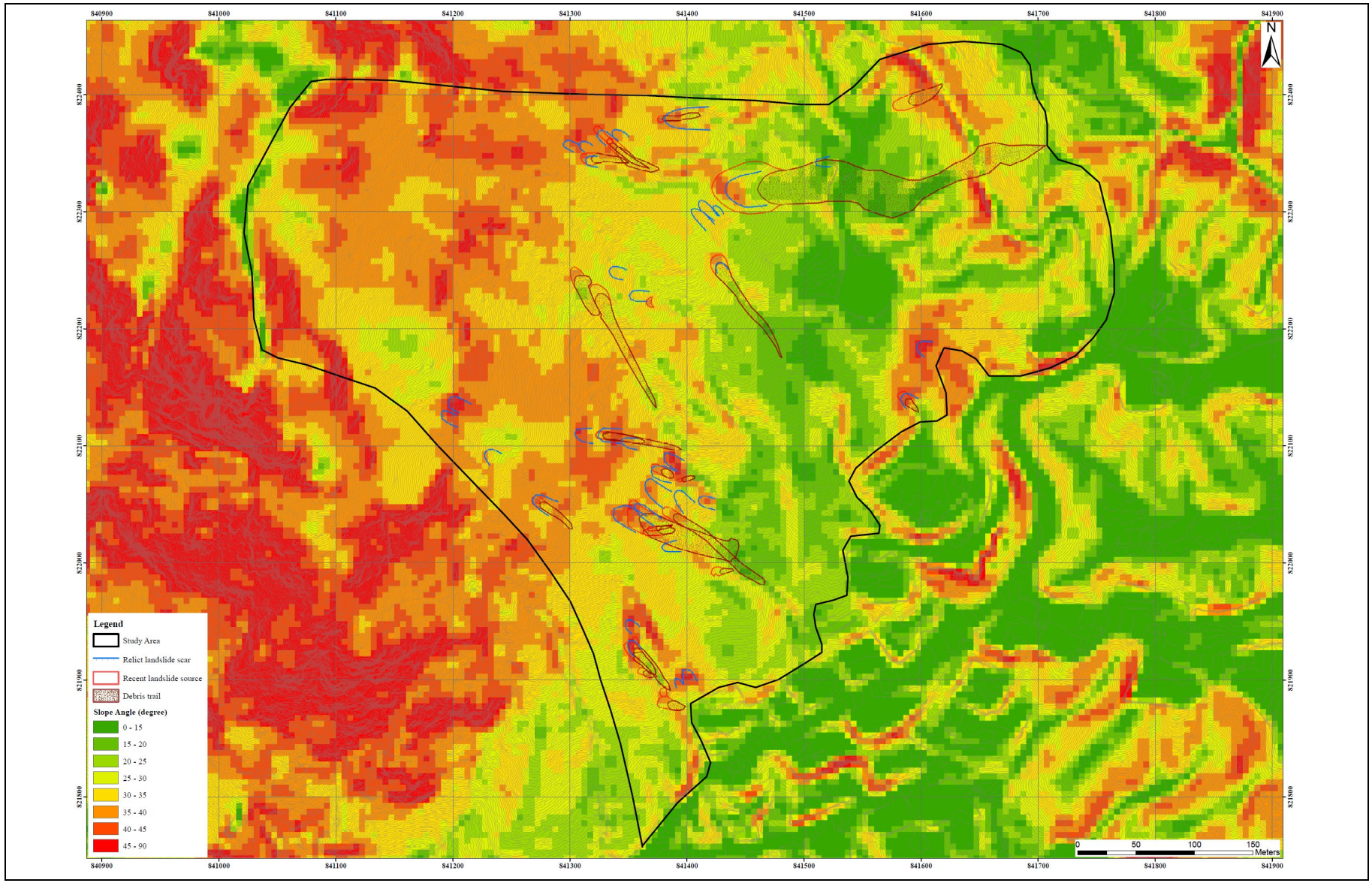

Figure B3.2 Slope Angle Distribution of the Study Area

Table B3.1 Slope Angle of Recent and Relict Landslides

Slope Angle (Degree)		Area (m^2)	Recent Landslides (27 nos.)	Relict Landslides (35 nos.)	All Landslides (62 nos.)
Class 1	0 - 15	5.2	0	0	0
Class 2	15 - 20	8.1	0	0	0
Class 3	20 - 25	13.6	0	1 (3%)	1 (2%)
Class 4	25 - 30	18.1	0	1 (3%)	1 (2%)
Class 5	30 - 35	25.3	8 (30%)	9 (26%)	17 (27%)
Class 6	35 - 40	20.6	13 (48%)	11 (31%)	24 (39%)
Class 7	40 - 45	6.9	6 (22%)	10 (29%)	16 (26%)
Class 8	45 - 90	2.3	0	3 (8%)	3 (4%)

B.4 Regolith

In the site-specific API, four types of regolith were identified and their distributions were mapped for the Study Area (Figure B4.1). Majority of the Study Area is underlain by volcanic saprolite, which accounts for about 80% of the Study Area. Intermittent rock outcrop accounts for about 7% of the Study Area. Colluvial deposits cover about 7% of the Study Area. Talus covers about 6% of the Study Area.

The steeper upper slopes of the Study Area are mainly underlain by rock outcrops while the gentler lower slopes are underlain by saprolite (Figure B4.1). The extent of talus deposits and the boundaries between talus and saprolite are defined by their changes in texture and geomorphology of the Study Area. Saprolitic terrain displays a smooth texture while the areas that are underlain by talus are rough with the presence of angular boulders.

More than 95% of the recent and relict landslides are located on saprolitic slopes as shown in Table B4.1.

Table B4.1 Regolith Type for Recent and Relict Landslides

Regolith Type	Area in Respect of the Entire Study Area (%)	Recent Landslides (27 nos.)	Relict Landslides (35 nos.)	All Landslides (62 nos.)
Intermittent Rock Outcrop	7	0	0	0
Saprolite	80	25 (93%)	35 (100%)	60 (97%)
Talus	7	2 (7%)	0 (0%)	2 (3%)
Colluvium	6	0	0	0

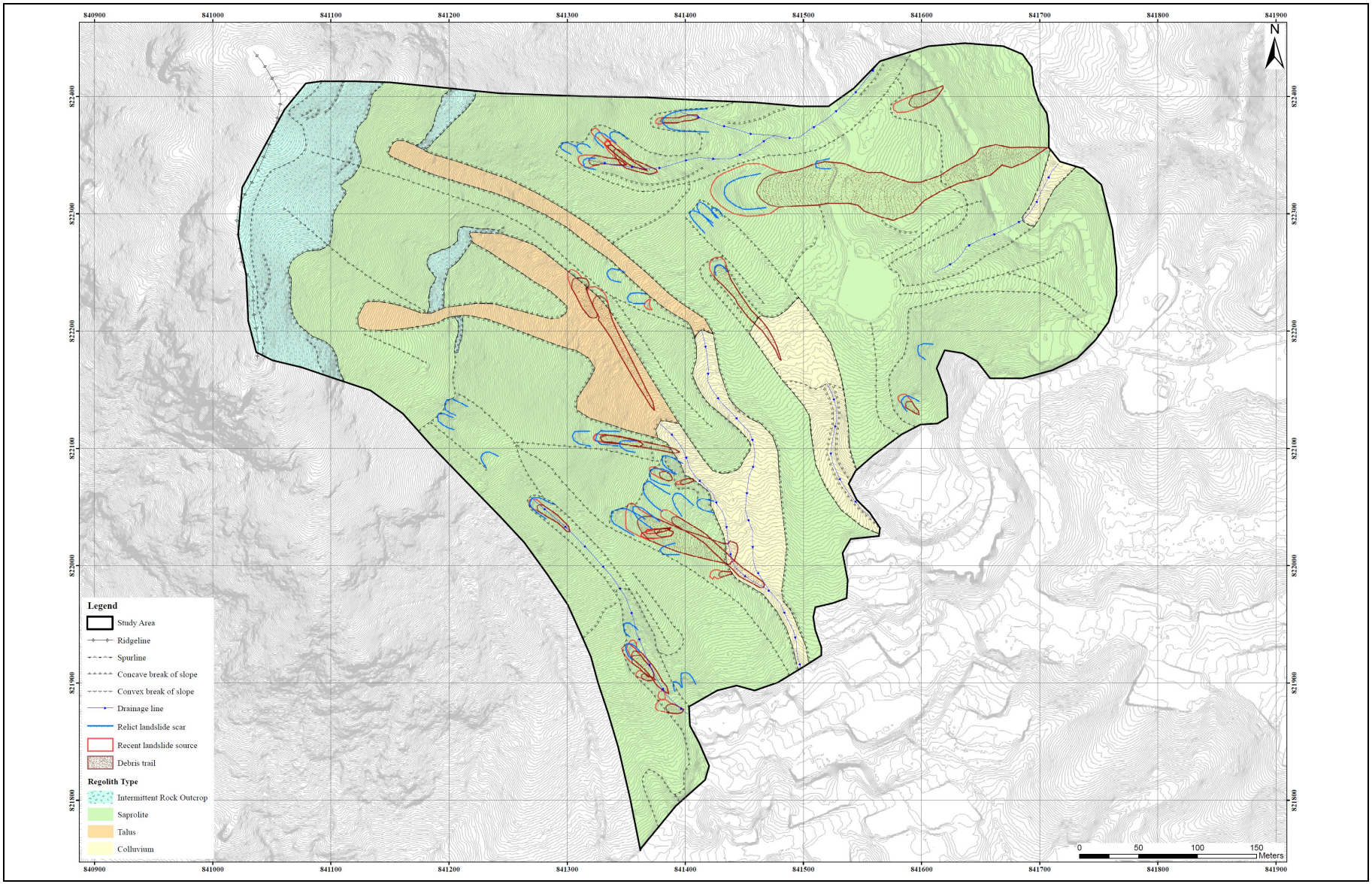

Figure B4.1 Regolith Map of the Study Area

B.5 Terrain Unit

The Study Area was divided into eight terrain units based on geology, geomorphology, geomorphological process, regolith, etc., mainly based on site-specific API (Figure B5.1). The main technique for the production of the geomorphological map was largely based on Anon (1982). Hilllslope evolution models which were proposed by Dalrymple et al (1968) and Hansen (1984) were also considered. The distribution and characteristics of each terrain unit are described below. The distribution of landslides in different geomorphological settings is summarised in Table B5.1.

Table B5.1 Terrain Units for Recent and Relict Landslides

Terrain Unit	Area in Respect of the Entire Study Area (%)	Recent Landslides (27 nos.)	Relict Landslides (35 nos.)	All Landslides (62 nos.)
Ridge Unit	1	0	0	0
Fall Face Unit	6	0	0	0
Transportation Unit (Upslope)	28	3 (11%)	8 (23%)	11 (18%)
Incised Unit (Upslope)	6	2 (7%)	0	2 (3%)
Transportation Unit (Mid-slope)	27	3 (11%)	2 (6%)	5 (8%)
Incised Unit (Mid-slope)	15	17 (63%)	23 (65%)	40 (65%)
Transportation Unit (Downslope)	10	2 (8%)	2 (6%)	4 (6%)
Deposition Unit	7	0	0	0

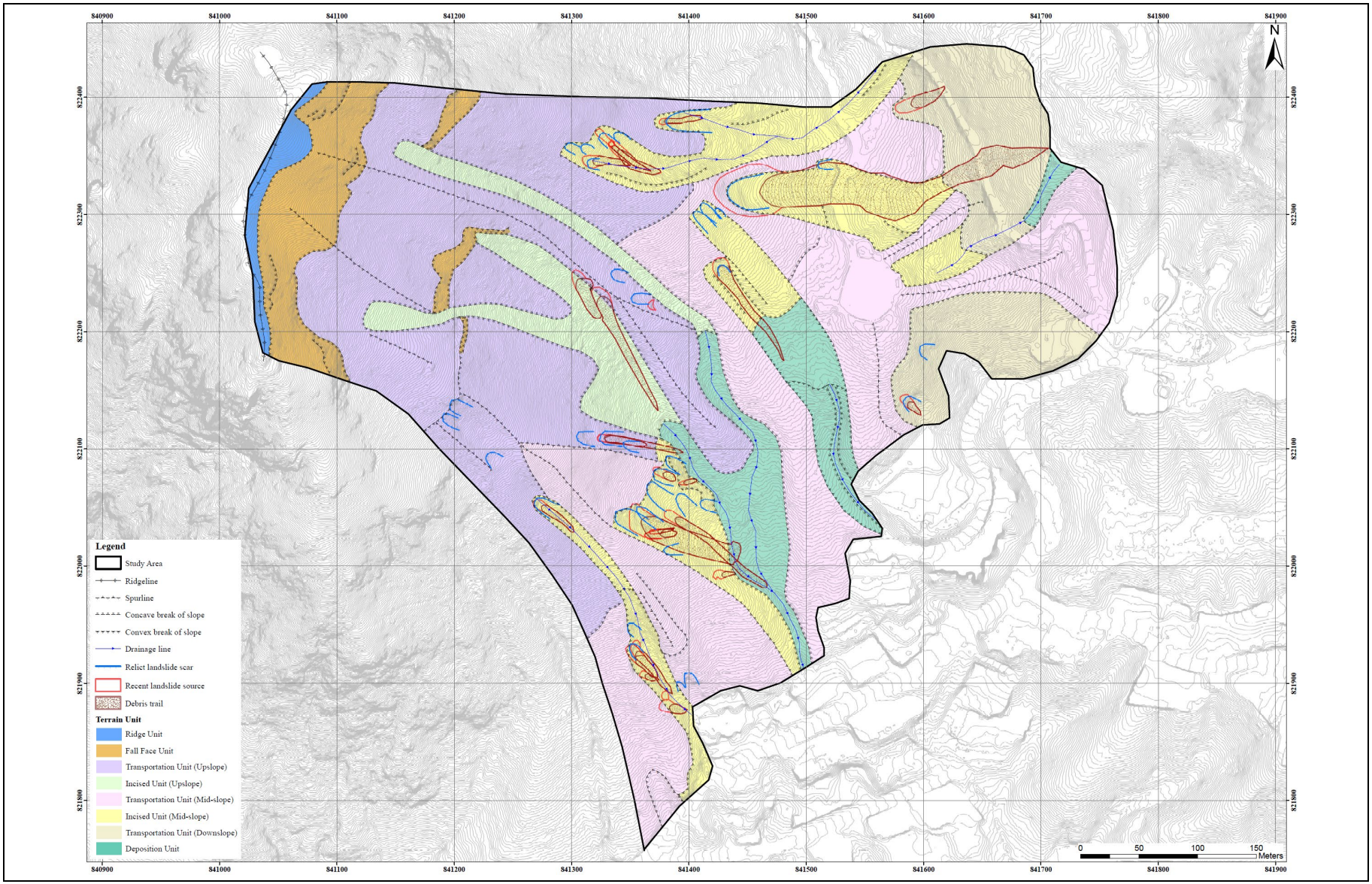

Figure B5.1 Terrain Unit Map

B.5.1 Ridge Unit

The ridge unit includes a narrow strip of hillside along the Fei Ngo Shan ridge at the crest of the Study Area. The gradient of this terrain unit ranges from 0 - 25°. The regolith interpreted for the ridge unit mainly includes saprolite. No landslide is initiated within this unit, which could be due to relatively gentle slope angle and absence of well-defined drainage lines. The ridge unit accounts for about 1% of the Study Area. The dominant process within this unit is mainly in-situ rock weathering.

B.5.2 Fall Face Unit

The fall face unit is characterised by rugged rocky slopes, forming a prominent rock cliff below the upper ridge unit. Three narrow cliff faces are also observed to the east of the prominent rock cliff. This unit has a steep gradient (> 50% with gradient > 40°), mainly underlain by intermittent rock outcrops of volcanic rocks with subordinate saprolite. This unit accounts for about 6% of the Study Area. Rock falls from the steepest portions of the rock cliff are the sources of the talus deposits on the slopes of the Incised Unit (Upslope). No discernible landslide source can be seen in this terrain unit, probable because of the nearly absence of regolith. The major process within this unit is rock fall and rock slide.

B.5.3 Transportation Unit (Upslope)

This unit occupies the largest plan area of the Study Area (approx. 28%). The general gradient of the unit is about 30 - 45°. This unit essentially encompasses planar volcanic saprolitic slopes with exhumed corestones. About 18% of landslides occurred within this unit. The main process within this unit is slope degradation and slope wash.

B.5.4 Incised Unit (Upslope)

The incised unit (upslope) traverses in the downslope of the upper cliff, with a gradient less than 40° in general. This unit is characterised by talus in the form of angular boulders and intermittent rock outcrops. Compared with the incised unit (mid-slope), the incised unit (upslope), which only accounts for about 6% of the Study Area, has slightly incised into the transportation units. Two recent landslides are recorded within this unit. The dominant process within this unit is shallow incision.

B.5.5 Transportation Unit (Mid-Slope)

The transportation unit (mid-slope) occupies a large plan area of the Study Area (approx. 27%). Compared to the transportation unit (upslope), the transportation unit (mid-slope) comprises gentler, planar saprolitic slopes, with a gradient less than 30° in general. Saprolite spurlines are also common in this terrain unit. Two relict landslides and three recent landslide features, including the largest landslide (ENTLI No. 11NEB0566E) of the Study Area occurred within this terrain unit. The major process within this unit is transportation (e.g. slope wash).

B.5.6 Incised Unit (Mid-slope)

The deeply-incised unit comprises valley side slopes and valley floors formed through erosion which extend upslope to the transportation unit (upslope) or transportation unit (mid-slope). The general gradient of this unit falls within a range of 30 - 45°. This unit only accounts for about 15% of the Study Area. However, more than 60% of the recent landslides were located within this unit, which has the highest landslide density (~724 nos. of recent landslides / km^2) in the Study Area. The regolith interpreted for the incised unit (mid-slope) includes volcanic saprolite and subordinate colluvium. The high percentage of landslides is considered related to slope gradient, undercutting processes and over-steepened side slopes. The main process within this unit is mainly incision, landsliding and slope wash.

B.5.7 Transportation Unit (Downslope)

This unit accounts for about 10% of the Study Area and is underlain mainly by saprolite. The general gradient of the unit is about 30 - 45°, which is generally steeper than the transportation unit (mid-slope). Two recent features and two relict landslides are located within this unit. The principal process within this unit is transportation (e.g. slope wash).

B.5.8 Deposition Unit

The deposition unit occupies the gentler lower slopes of the Study Area, with a gradient less than 30° in general. This unit accounts for about 7% of the Study Area and it is covered with colluvium given the gentler gradient would encourage deposition. No landslide is observed within this unit. The major process within this unit is deposition of sediments from mass movement and the unit is generally stable.

B.6 Landslide Clusters

The 27 recent landslides have been examined in a view to establish if the recent landslides are in cluster with older landslides based on the eight-fold classification system proposed in Tang et al (2018). The result is presented in Table B6.1.

Table B6.1 Summary of Characteristics of Landslide (Recent) Cluster at the Study Area

Type of Landslide Cluster	No. of Recent Landslides	Range of Distance to the Closest Related Relict (Older) Landslides (m)
1	1	1
2	1	6
3	3	3 - 14
4	0	N/A
5	9	2 - 13
6	3	2 - 9
7	0	N/A
8	2	5 - 7
Not in Clusters	8	N/A

The cluster type distribution indicates that about 20% of the recent landslides were related to retrogressive failures or over-steepened slopes at previous failure scars (Types 1, 2 and 3). The distance between the recent landslide and the related relict landslide is in a range of 1 to 14 m. About 45% of the recent landslides are classified as cluster Types 5 and 6, related to headward erosion at the head of drainage lines or to undercutting processes along the drainage lines. About 7% of the recent landslides are classified as cluster Type 8, in which they are located immediately below a well-defined break-in-slope. These failures may be controlled by underlying geology (e.g. presence of resistant layers, adverse joint sets, etc.).

Although the eight-fold classification has not been applied to the relict landslides within the Study Area given the relative age of the relict landslides could not be reliably defined, the distribution of the relict landslides was also examined in a view to see if they are in clusters and the possible controls on their distribution. Within the incised unit (mid-slope), there are mainly two groups (i.e. N1 and S1) of relict landslides, one at the northern part and one at the southern part of the Study Area, each with at least five relict landslides (Figure B5.1).

The northern group (N1) is located on steep slopes with drainage line at or below the cluster. These landslides may be related to undercutting processes along the drainage line. The relict landslides of the southern group (S1) in the south of the Study Area mostly occurred at or below a well-defined break-in-slope, which is similar to Type 8 of the eight-fold classification. It is possible the abovementioned failures are controlled by presence of resistant layers, escarpment, adversely-oriented geological structures, etc.

Most of the relict landslides that are located within the three transportation units (upslope, mid-slope and downslope) appear not as closely spaced of the two groups of relict landslides located within the incised unit (mid-slope). These landslides are possibly controlled by steep slope gradient.

The geomorphological factors (landslide cluster Types 1, 2, 3, 5 and 6) mentioned above have played a more prominent role in the occurrence and distribution of recent and relict landslides. However, it is also probable that the presence of adverse geological structures played an important contributory role in causing the largest failure (ENTLI No. 11NEB0566E) within the Study Area.

B.7 Conclusions

A review of the natural terrain landslides near Fei Ngo Shan has been carried out, mainly based on desk study including a detailed site-specific API. All the landslide features recorded in the ENTLI have been verified and a regolith map and terrain unit map have been produced, in order to decipher the possible geological or geomorphological factors that may have played a role in the occurrence and distribution of the recent and relict landslides. The key observations are summarised below:

(a) The ENTLI features have been verified using API and there are 27 nos. of recent landslides and 35 nos. of relict landslides confirmed within the Study Area. All the recent and most of the relict landslides are shallow failures (< 2 m) and are of relatively small landslide volume (mostly < 200 m^3).

(b) A regolith map for the Study Area has been produced using API and four types of regolith have been mapped within the Study Area, including intermittent rock outcrop, saprolite, talus and colluvium. The majority of the recent and relict landslides were located on saprolitic slopes.

(c) The delineation of terrain units showed that over 80% of the natural terrain landslides were concentrated in the transportation unit (upslope) and incised unit (mid-slope), which account for around 40% of the Study Area. Landslides occurred within these terrain units were likely related to the steep slope gradient, undercutting processes and over-steepened side slopes.

(d) Based on the review of the recent landslides using the eight-fold classification system, about 20% of the recent landslides were related to retrogressive failures or over-steepened slopes at previous failure scars (Types 1, 2 and 3). About 45% of the landslides were classified as cluster Types 5 and 6, therefore related to headward erosion at the head of drainage lines or to undercutting processes along the drainage lines. About 7% of the recent landslides are classified as cluster Type 8, in which they are located immediately below a well-defined break-in-slope.

B.8 References

Anon (1982). Land surface evaluation for engineering practice. *Quarterly Journal of Engineering Geology*, vol. 15, pp 265-316.

Dalrymple, J., Long, R. & Conacher, A. (1968). A hypothetical nine-unit land-surface model. *Zeitschrift fur Geomorphologie*, Germany, vol. 12, pp 71-78.

Geotechnical Engineering Office (GEO) (2012). *Hong Kong & Kowloon.* Hong Kong Geological Survey Map Sheet 11, Solid and Superficial Geology, 1:20,000 Series HGM20 (Edition II). Geotechnical Engineering Office, Hong Kong.

Hansen, A. (1984). Engineering morphology: the application of an evolutionary model of Hong Kong's terrain. *Zeitschrift fur Geomorphologie*, Germany, vol. 51, pp 39-50.

MGSL (Maunsell Geotechnical Services Ltd) (2008). *Detailed Study of the 21 August 2005 Debris Flow on the Natural Hillside near Fei Ngo Shan Service Reservoir (GEO Report No. 233)*. Geotechnical Engineering Office, Hong Kong, 123 p.

Tang, D.L.K., Wong, C.C.J., Sin, Y.M. & Mok, S.C. (2018). *Study of Geological Controls on the Occurrence of Natural Terrain Landslide Clusters - A Pilot Study at a Catchment above Keung Shan Road, West Lantau (Geological Report No. GR 1/2018)*. Geotechnical Engineering Office, Hong Kong, 44 p.

Appendix C

Geological and Geomorphological Review of Landslide Clusters in Catchment 50 - Tai O

(Prepared by Y.M.Sin)

Contents

List of Tables

List of Figures

C.1 Location and Catchment Characteristics

The Study Area is a northwest facing hillside, located to the north of the Tai O Cemetery, Lantau. The area of the Study Area is 96,353m^2, with an elevation arise from the sea-level to +256 mPD at the crest (Figure C1.1). The Study Area is essentially natural without significant human disturbance, except a footpath along the toe of the Study Area and some graves at the lower part of the hillside. A few structures are shown at the toe of the Study Area on the 1:1000-scale LIC map but they were either unoccupied or damaged to varying degree as revealed in previous LPMit study. Two Historical Landslide Catchments (HLCs), HLC No. 9SW-D/DF 21 and 9SW-C/DF/1 are located within the Study Area.

C.2 Geology

According to the published 1:20,000- and 1:100,000-scale geological maps and the accompanying geological reports (Figure C2.1). The upper portion of the Study Area is underlain by eutaxite (welded vitric tuff) of the Shing Mun Formation, while the lower portion of the Study Area is underlain by siltstone and sandstone of the Tai O Formation. The volcanic rock was considered overlying conformably on top of the sedimentary rocks. No major fault is located within or in close proximity to the Study Area. The bedding of the sedimentary rocks at the lower portion of the Study Area is dipping moderately towards southeast, into the hillside.

No existing ground investigation information is available within the Study Area. However, information from previous geological studies and some ground investigation data on the hillside at Tai O Cemetery was used to slightly refine the contact boundary of the volcanic and sedimentary rocks within the Study Area (as shown on the regolith map).

C.3 Geomorphology

The Study Area is a northwest facing hillside. The crest and part of the eastern Study Area is a rounded spur of gentle to moderate gradient and the slope steepen significantly in the upper and middle portions of the Study Area. The gradient reduces at the lower part of the Study Area with a step before descending to the very gentle coastal beach area. A number of well-defined drainage lines present within the Study Area.

The Study Area can be broadly divided into three channelised catchments (Figure C3.1). The southern catchment (CD1) has a bowl shaped upper part lined with steep slopes and contains a number of broad drainage tributaries. These tributaries converge and form a major drainage channel with steep side slopes. The middle catchment (CD2) has a steep planar rocky upper portion and a gentler lower portion with three well-defined drainage lines. The northern catchment (CD3) has a broad rounded spur in the upper part of the catchment. The slope gradient steepen in the middle rocky portion and reduces gradually towards the toe of the catchment. Two drainage lines present in the middle and lower parts of the catchment.

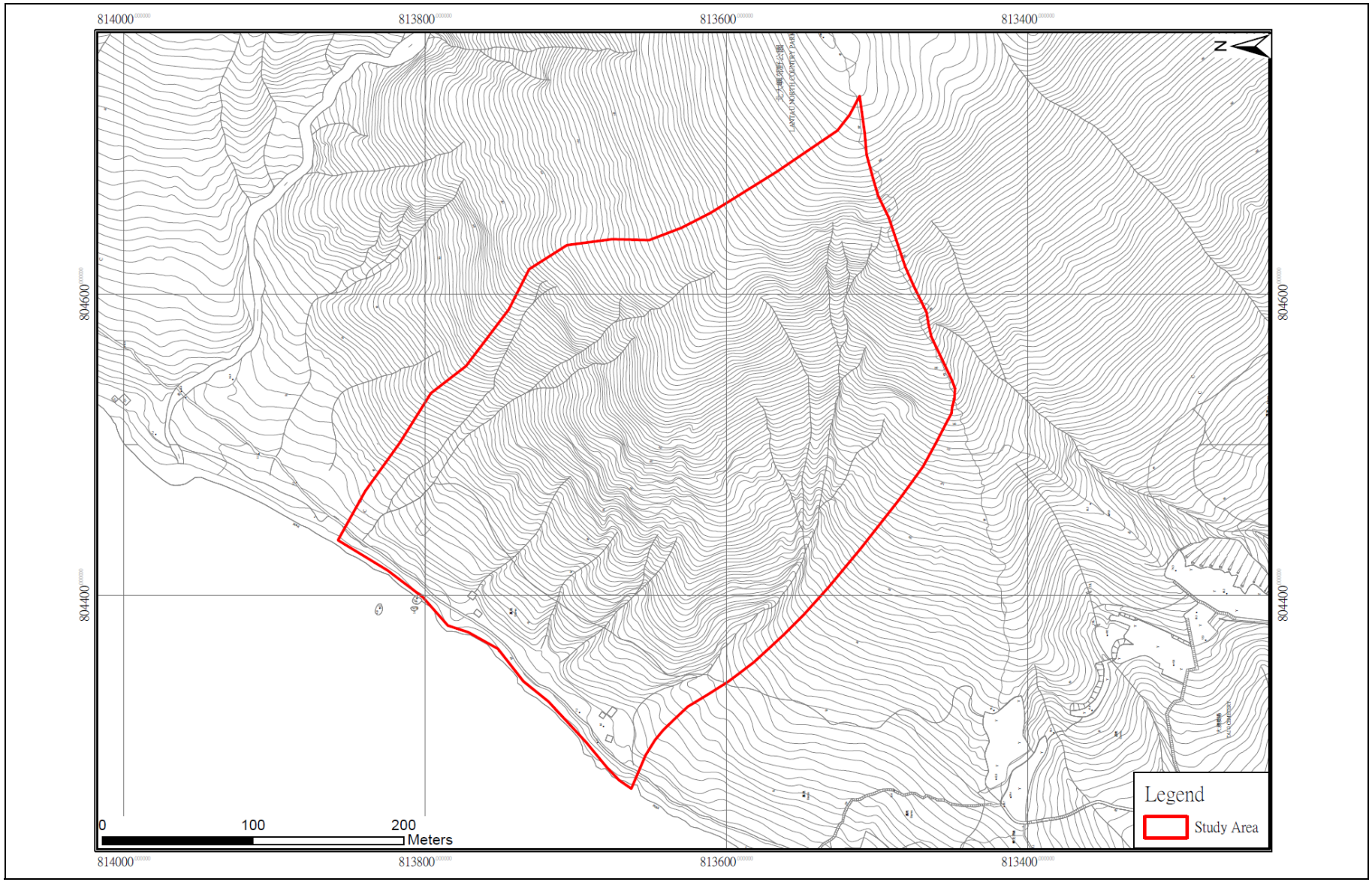

Figure C1.1 Location Plan of the Study Area

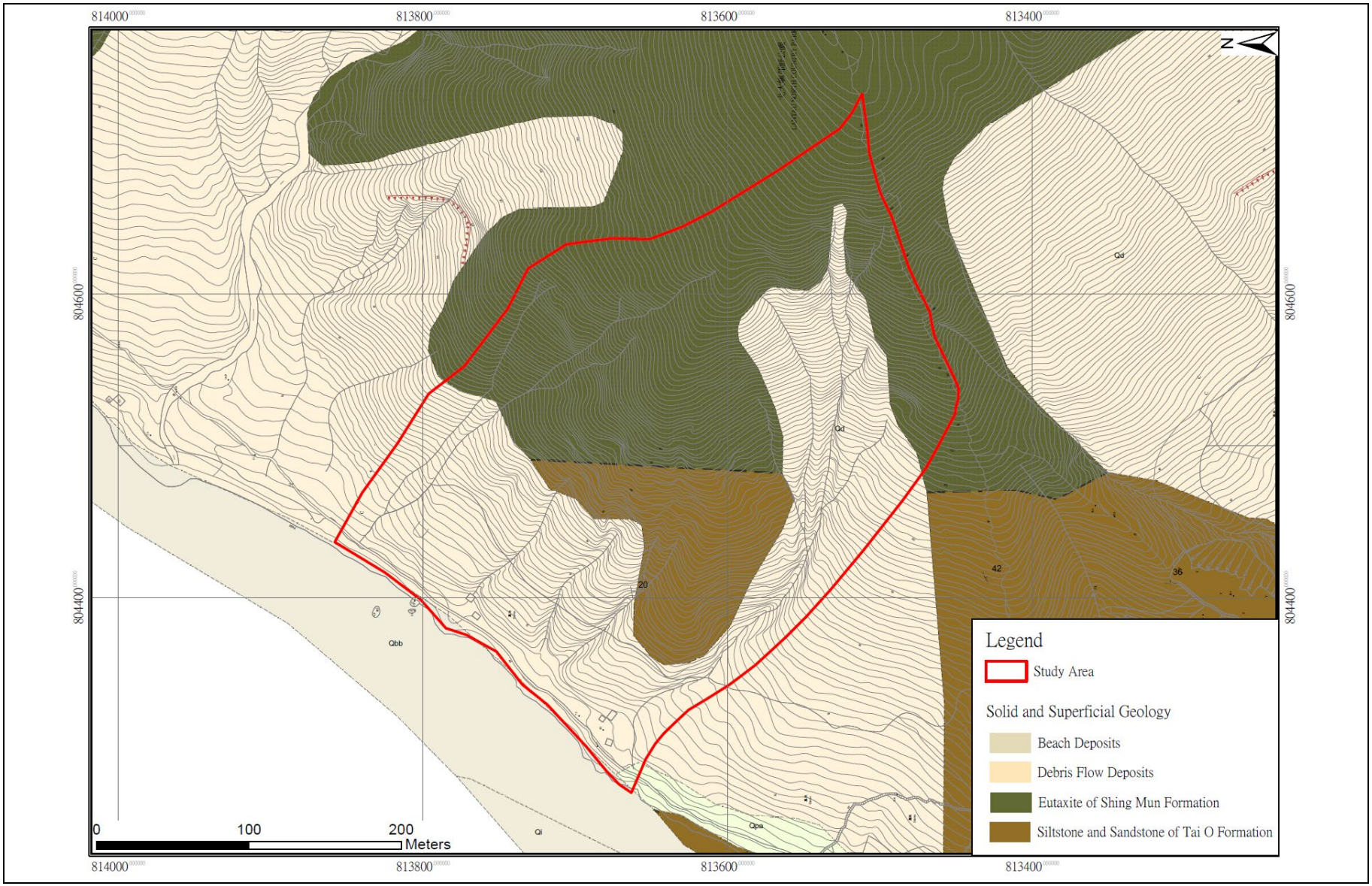

Figure C2.1 Geology of the Study Area

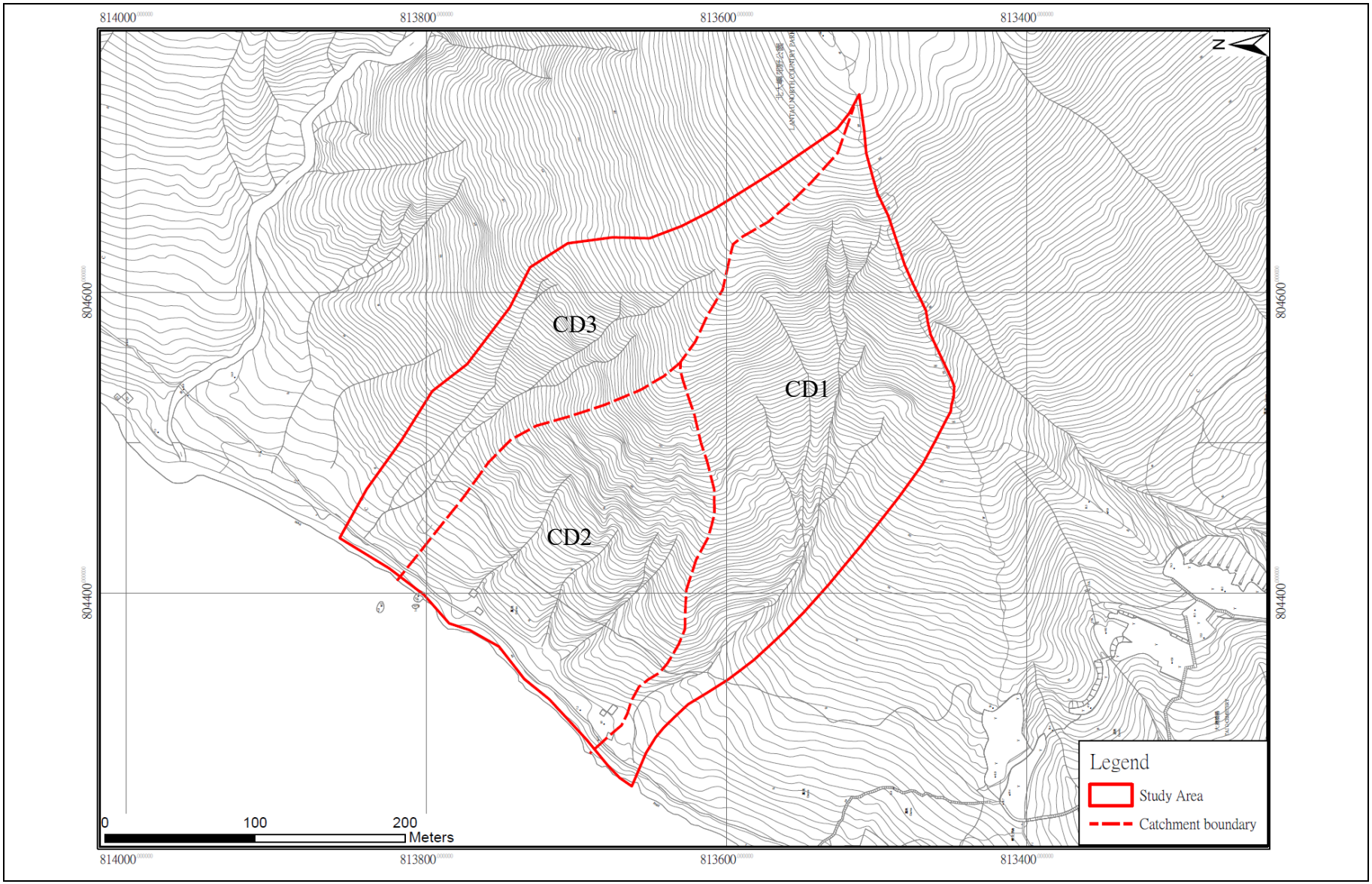

Figure C3.1 Catchments Delineated for the Study Area

C.4 Natural Terrain Landslides

According to the ENTLI, a total of 102 landslide features were recorded within the Study Area, including 17 recent landslides and 85 relict landslides (Figure C4.1). Study specific API was carried out to verify these features and confirmed the Study Area has 18 recent landslides, occurring in 1973, 1977 and mostly in 2008. The number of relict landslides was reduced from 85 to 56.

The source and trail area of the confirmed recent landslides and the scarp of the confirmed relict landslides were delineated (Figure C4.2). A slope angle map (5-m grid) (Figure C4.3) was prepared for the Study Area and reviewed together with the distribution of the verified landslides. Table C4.1 shows the distribution of landslides for the eight slope angle classes defined. No landslide is observed on slope with gradient less than 25°. Over 80% of the landslides are located on slope with a gradient greater than 35°, with the highest percentage for the slope angle class 40 - 45°. Both the recent and relict show a similar trend and pattern in respect of slope angle distribution.

Table C4.1 Slope Angle of Recent and Relict Landslides

Slope Angle (Degree)		Recent Landslides (18 nos.)	Relict Landslides (56 nos.)	All Landslides (74 nos.)
Class 1	0 - 15	0 (0%)	0 (0%)	0 (0%)
Class 2	15 - 20	0 (0%)	0 (0%)	0 (0%)
Class 3	20 - 25	0 (0%)	0 (0%)	0 (0%)
Class 4	25 - 30	1 (6%)	2 (3%)	3 (4%)
Class 5	30 - 35	1 (6%)	7 (13%)	8 (11%)
Class 6	35 - 40	4 (22%)	14 (25%)	18 (24%)
Class 7	40 - 45	8 (44%)	22 (39%)	30 (41%)
Class 8	45 - 90	4 (22%)	11 (20%)	15 (20%)

The verified recent landslides have a source width varying from a few metres to 17 m while the relict landslides have a larger source width ranging from several metres to 33 m. The depth of the recent landslides is shallow (typically 1 - 1.5 m, up to 2 m) in general and the estimated landslide volume is mostly less than or around 100 m^3 with only one recent feature up to around 200 m^3. The source depth of most of the relict landslides is shallow as well, typically 1 - 2 m, except one larger relict with a source depth of 4 m. The estimated volume of more than 90% of the relict landslides is less than 100 m^3 with two relict features up to around 300 m^3 and the largest one approximately 1200 m^3. However, this largest relict landslide is considered to be formed by multiple failures and/or enlarged by continuous erosion. In summary, both the recent and relict landslides within the Study Area are shallow and are of relatively small volume.

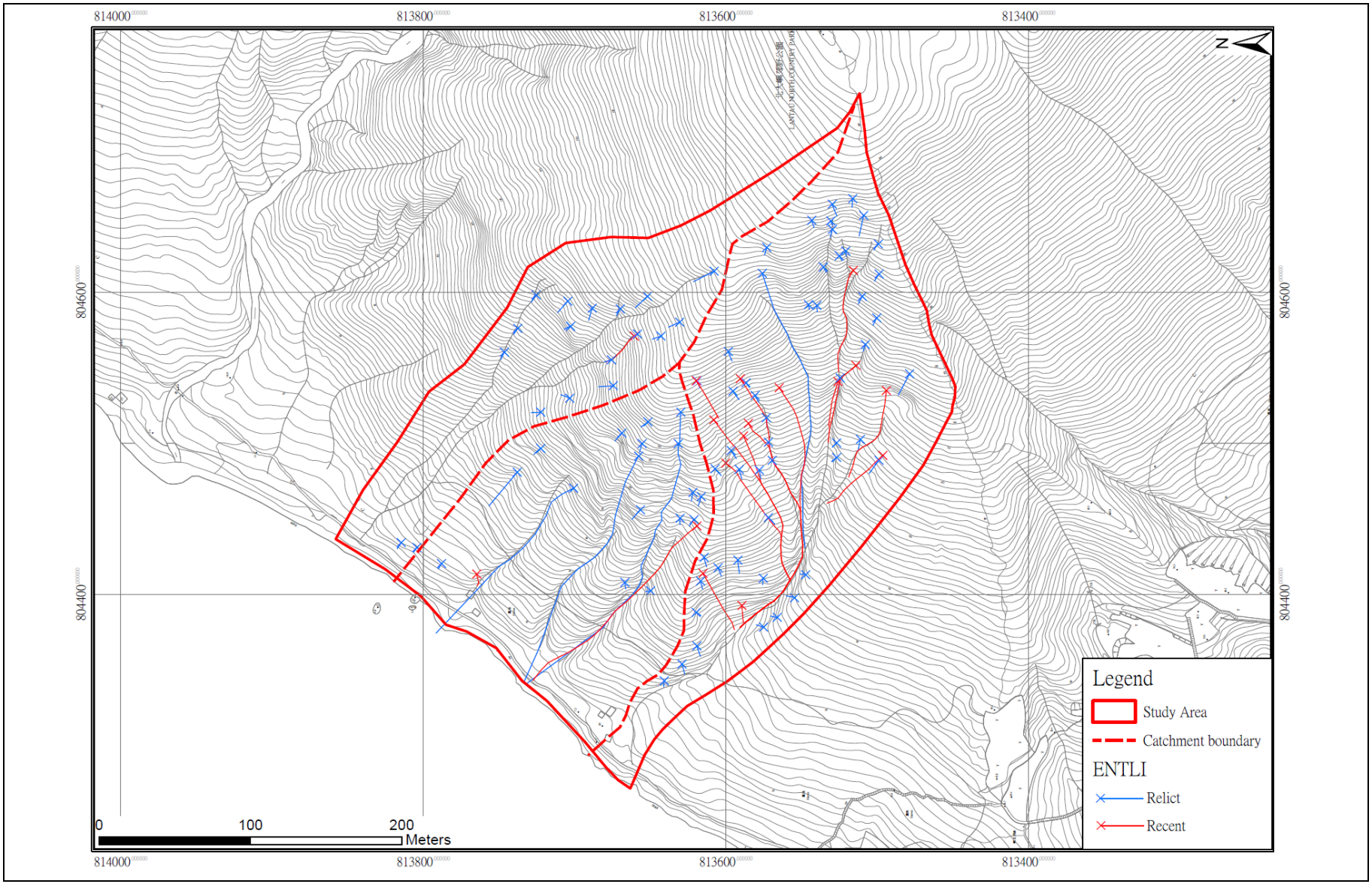

Figure C4.1 ENTLI within the Study Area

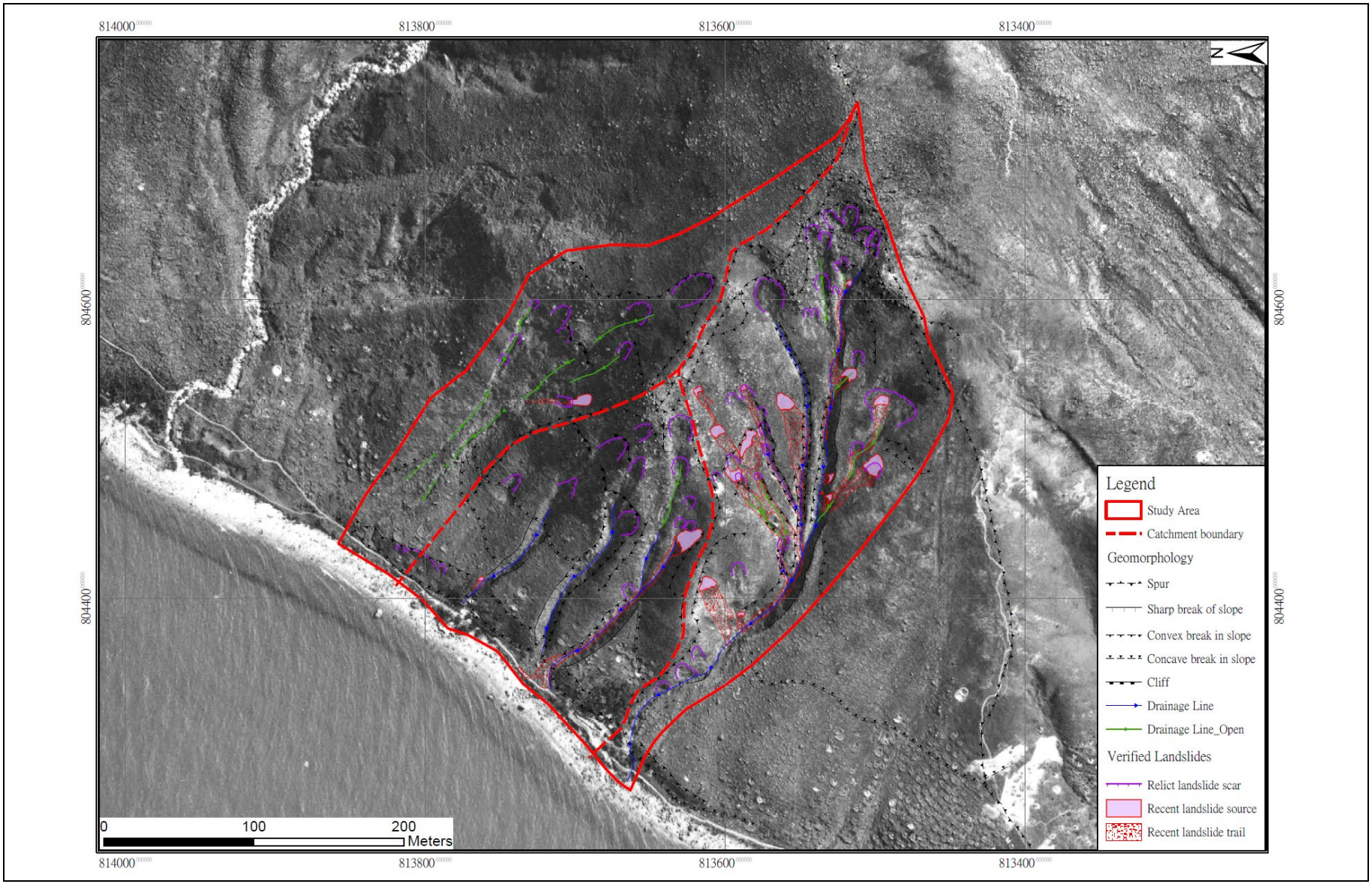

Figure C4.2 Verified Recent and Relict Landslides within the Study Area

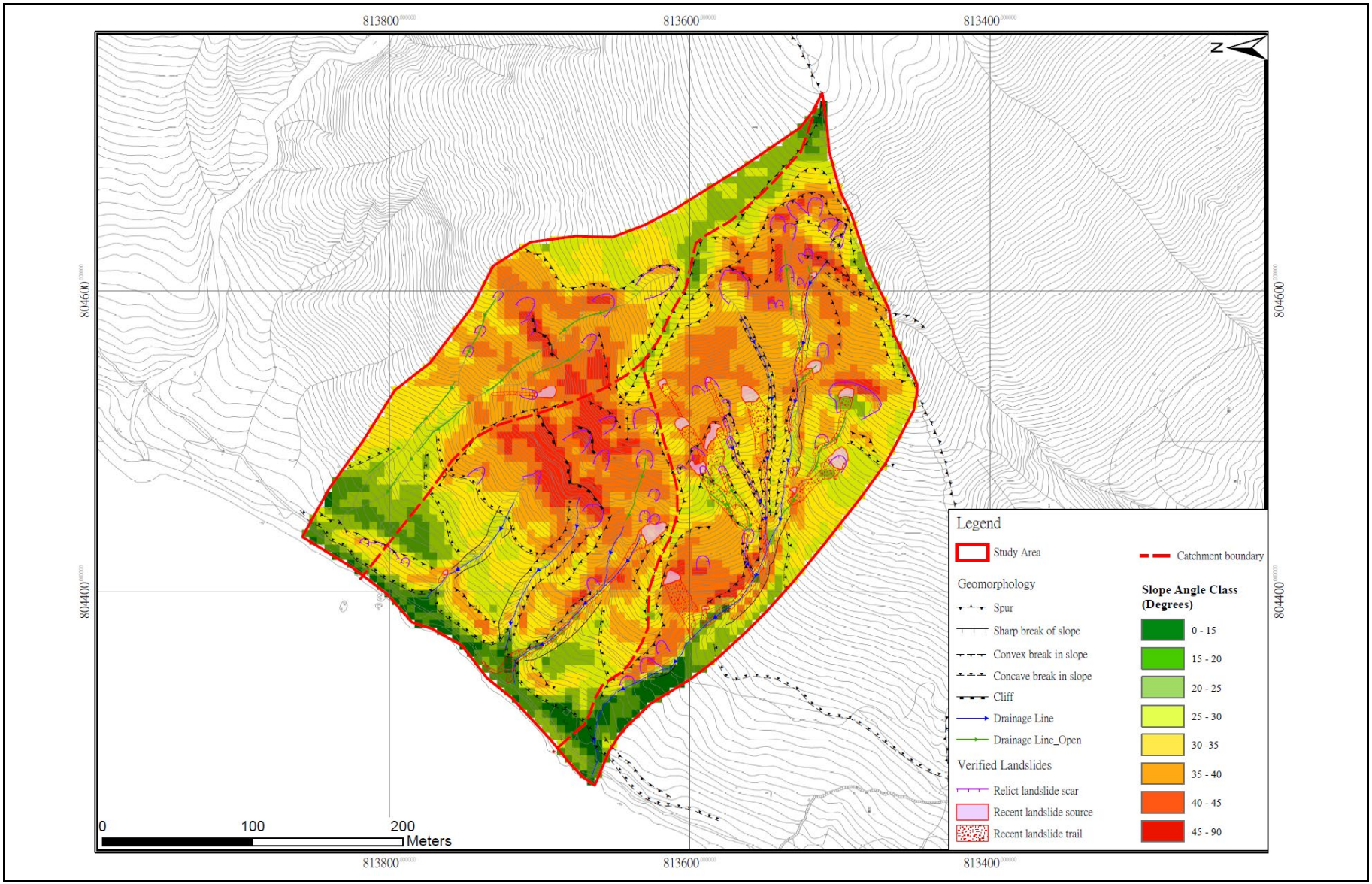

Figure C4.3 Verified Recent and Relict Landslides and Slope Angle Map

C.5 Regolith

In the site-specific API, seven types of regolith were identified and their distribution was mapped for the Study Area (Figure C5.1). Table C5.1 shows the area and number of landslide for each type of regolith mapped. Majority of the Study Area is underlain by volcanic saprolite and sedimentary saprolite (each accounts for about 30% of the Study Area). The intermittent rock outcrop of volcanic rock with the minimal sedimentary intermittent rock outcrop account for about 18% of the plan area of the Study Area. The general colluvial deposits at the lower portion of the Study Area covers about 10% of the Study Area. The remaining minor areas are mapped as beach deposits and landslide debris.

The regolith map also indicates the steeper upper to middle slopes of the Study Area are mainly underlain by volcanic rock outcrop and saprolite while the gentler lower slopes are underlain by sedimentary saprolite. The change in slope gradient and geomorphology of the Study Area may be related to the change of rock type and the contrast in strength of the two rock types. The presence of wide and incised channels mainly in the sedimentary terrain may also be related to the weaker strength of the sedimentary rocks.

More than 50% of the landslides are located on slopes of volcanic saprolite. The rest of the landslides mainly occur in intermittent volcanic rock outcrop and sedimentary saprolite with a minimal portion occurring in colluvium.

Table C5.1 Regolith of Recent and Relict Landslides

Regolith Type	Area in Respect of the Entire Study Area (%)	Recent Landslides (18 nos.)	Relict Landslides (56 nos.)	All Landslides (74 nos.)
Intermittent Rock Outcrop (Volcanic)	17	0 (0%)	18 (32%)	18 (24%)
Intermittent Rock Outcrop (Sedimentary)	1	0 (0%)	0 (0%)	0 (0%)
Saprolite (Volcanic)	36	12 (67%)	27 (48%)	39 (53%)
Saprolite (Sedimentary)	30	5 (28%)	8 (14%)	13 (18%)
Colluvium	10	1 (5%)	3 (6%)	4 (5%)
Landslide Debris	5	0 (0%)	0 (0%)	0 (0%)
Beach Deposits	1	0 (0%)	0 (0%)	0 (0%)

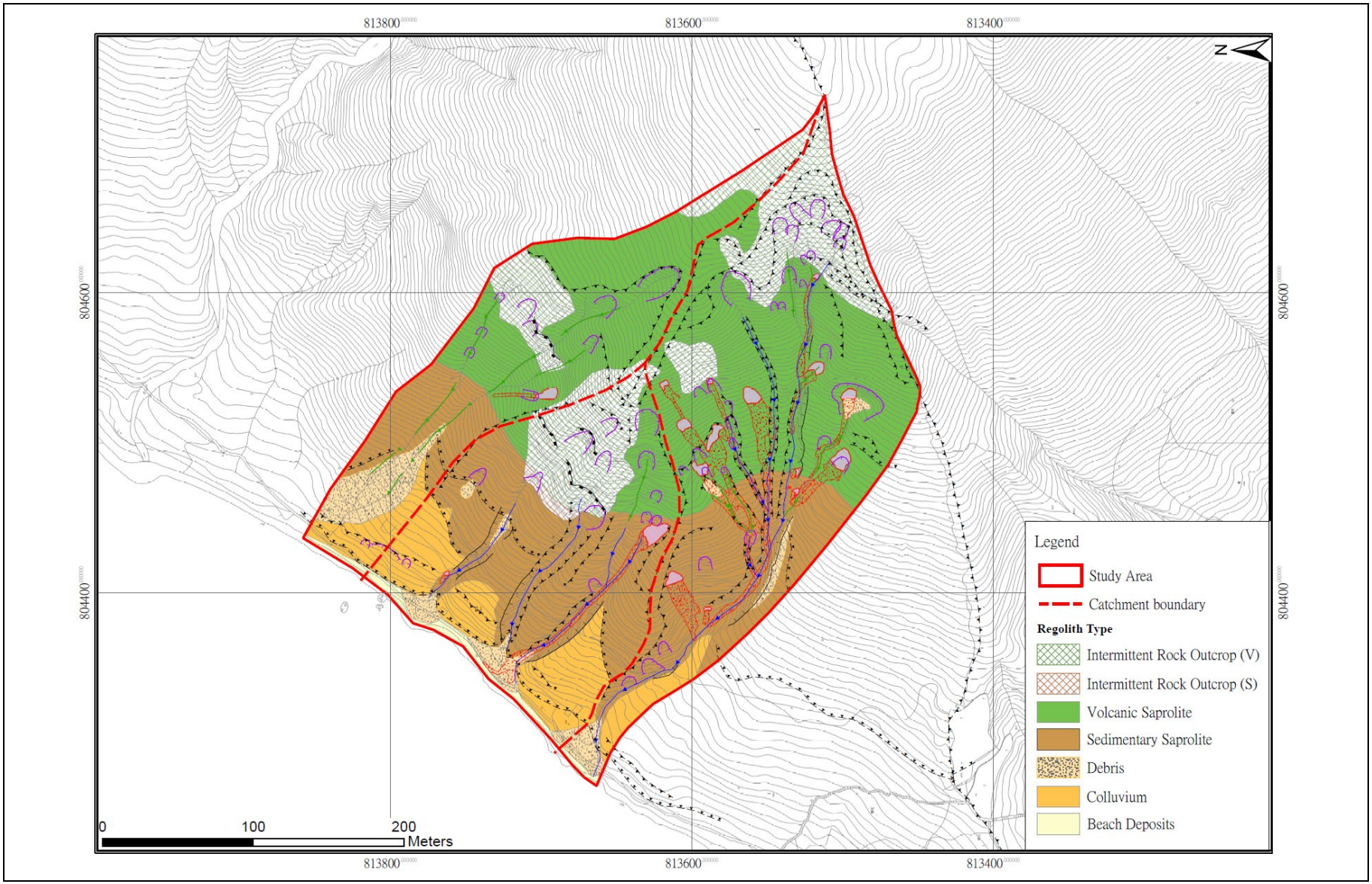

Figure C5.1 Regolith Map for the Study Area

C.6 Terrain Unit

The Study Area was divided into eight terrain units based on geology, geomorphology, geomorphological process, regolith, etc., mainly based on site specific API (Figure C6.1). The distribution and characteristics of each terrain unit are described below.

C.6.1 Upper Spur Unit

This unit include two narrow strips of hillsides along the major spur at the crest of the Study Area and a minor spur separating catchments CD1 and CD2. The gradient of this terrain unit ranges from 20 - 35°. The morphology of this unit is rounded and convex in shape. No landslide is recorded within this unit and this may be related to the relatively gentle slope angle and a convex morphology, which prevented the concentration of surface runoff.

C.6.2 Middle Fall Face Unit

The middle fall face unit present in the upper slopes of catchments CD1 and CD2, and middle slopes of catchment CD3. This unit has a very steep gradient (> 70% area with gradient > 40°), mainly underlain by the intermittent rock outcrops of volcanic rocks with some volcanic saprolite. The morphology varies from rugged rocky planar slopes to planar slopes with broad drainage depressions. This unit accounts for about 15% of the plan area of the Study Area, however, 40% of the landslides are located within this unit and has the highest landslide number among all the terrain units delineated. The high percentage of landslide occurrence within this unit is considered directly related to the steep slope gradient. The geomorphological setting with head of drainage lines and/or well-defined drainage lines just below this unit may also contributed in destabilising the toe of this unit and causing landslides.

C.6.3 Middle Incised Unit

The middle incised unit is mainly delineated as pockets in catchments CD1 and CD2, for the relatively steep slopes with open and well-defined drainage lines. The general gradient of this unit falls within a range of 35 - 45°. This unit only accounts for about 13% of the plan area of the Study Area, however, 36% of the landslides are located within this unit and is the second highest after the middle fall face unit. The regolith interpreted for the middle incised unit mainly includes volcanic and sedimentary saprolite. The high percentage of landslides within this unit is considered related to the slope gradient and also direct influence of drainage lines (e.g. concentration of surface runoff and erosional alluvial processes).

C.6.4 Middle Transportation Unit

The middle transportation unit occupies the largest plan area of the Study Area (approx. 45%). The general gradient of the unit is about 30 - 40°. This unit essentially

encompasses the planar volcanic/sedimentary saprolitic slopes, with minimal influence of drainage lines. About 14% of the landslides occurred within this unit. The main process within this unit is slope degradation and mass wasting by gravitational force.

C.6.5 Lower Deposition Unit

The lower deposition unit occupies the gentler lower slopes of the Study Area, with a gradient less than 30° in general. This unit is expected to be covered with colluvial deposits given the gentler gradient would encourage deposition. The hillside of this unit is planar in general without major depression and drainage line. No landslide is recorded within this unit.

C.6.6 Lower Coastal Erosion Unit

The lower coastal erosion unit appears as a step (about 30 - 35°) along the lower part of the Study Area, bounded at the top and bottom by the gentler lower deposition unit and the lower coastal deposition unit. This unit might be formed by the continuous coastal erosion processes. A few landslides are recorded in this unit, possibly influenced by the moderately steep slope angle and the coastal erosional setting.

C.6.7 Lower Coastal Deposition Unit

The lower coastal deposition unit includes a continuous strip of the very gentle area at the toe of the Study Area, covered with superficial deposits including beach sand and landslide debris lobes. No landslide is recorded within this unit and deposition appears to be the main geomorphological process within this unit.

C.6.8 Incised Drainage Channel Unit

The incised drainage channel unit includes the several wide and incised drainage lines in the middle to lower slopes of catchments CD1 and CD2. These drainage channels incised deeply into the volcanic and mainly sedimentary saprolite with a width of about 15 - 20 m, and bounded by steep side slopes. The sharpness of the edges of the side slope suggests the side slopes are relatively ‘fresh’ and are subject to continuous erosion/undercutting by the alluvial processes along the channels. Debris or loose materials are observed in sections in the channels, probably deposit from previous channelised debris flows. Several small-scale recent landslides are observed on the side slopes within this unit, likely caused by undercutting of the steep side slopes by the drainage lines. It is suspected that the number of landslides that had occurred within this unit may have been underestimated given the erosive and dynamic nature of the drainage banks.

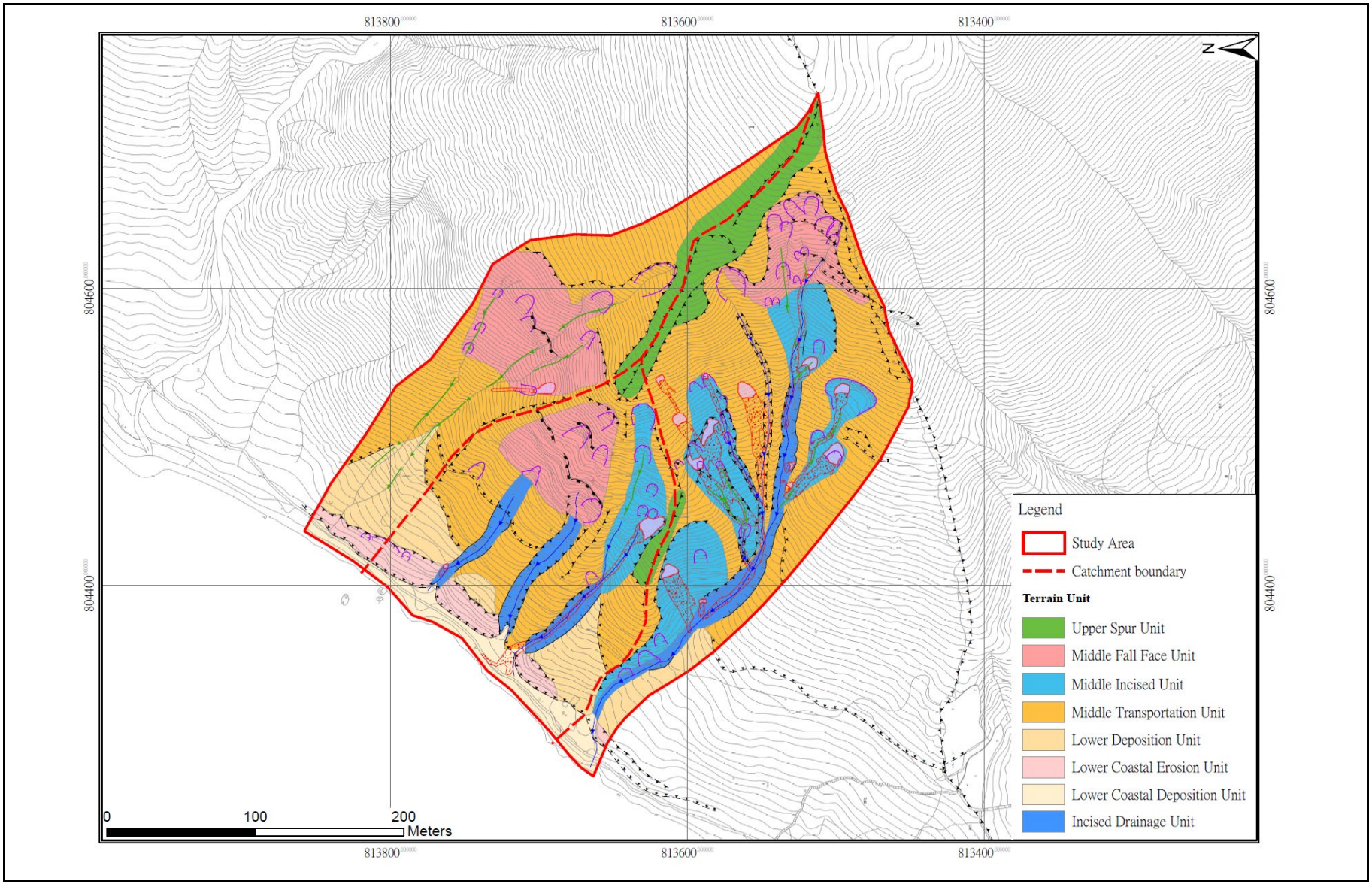

Figure C6.1 Terrain Unit Map for the Study Area

Table C6.1 Terrain Units for Recent and Relict Landslides

Terrain Unit	Area in Respect of the Entire Study Area (%)	Recent Landslides (18 nos.)	Relict Landslides (56 nos.)	All Landslides (74 nos.)
Upper Spur Unit	6	0 (0%)	0 (0%)	0 (0%)
Middle Fall Face Unit	15	2 (11%)	27 (48%)	29 (39%)
Middle Incised Unit	13	6 (33%)	21 (38%)	27 (36%)
Middle Transportation Unit	44	5 (28%)	5 (9%)	10 (14%)
Lower Deposition Unit	9	0 (0%)	0 (0%)	0 (0%)
Lower Coastal Erosion Unit	3	0 (0%)	3 (5%)	3 (4%)
Lower Coastal Deposition Unit	4	0 (0%)	0 (0%)	0 (0%)
Incised Drainage Channel Unit	6	5 (28%)	0 (0%)	5 (7%)

C.7 Landslide Cluster

The eighteen recent landslides were examined in a view to establish if the recent landslides are in cluster with other older landslides based on the eight-fold classification system proposed in GR1/2018. The result is presented in Table C7.1.

Table C7.1 Summary of Characteristics of Landslide (Recent) Cluster at the Study Area

Type of Landslide Cluster	No. of Recent Landslides	Range of Distance to the Closest Related Relict (Older) Landslides (m)
1	5	4 - 22
2	0	-
3	0	-
4	1	4
5	3	2 - 29
6	1	8
7	5	N/A
8	0	-
Not in Clusters	3	N/A

The cluster type distribution indicates about one-third of the recent landslides were related to retrogressive failures or over-steepened slopes at previous failure scars (Types 1 & 4). The distance between the recent landslide and the related relict landslide is in a range of 4 - 22 m.

About half of the landslides were classified as cluster Types 5, 6 and 7, therefore related to headward erosion at the head of drainage lines or to undercutting processes along the drainage lines.

Although the eight-fold classification was not applied to the relict landslides within the Study Area given the relative age of the relict landslides could not be reliably defined, the distribution of the relict landslides was also examined in a view to see if they are in clusters and the possible controls on their distribution. In catchment CD1, there are two groups of relict landslides at the head and northern flank of the catchment. Both groups are located on steep slopes with drainage lines at or below the cluster. These landslides may be related to the over-steepened slopes at previous failure scars and to undercutting process at drainage lines. Three relict landslides in catchment CD1 are located on the steep side slope of the major drainage channel at the toe of the Study Area, this is similar to Type 7 of the eight-fold classification and likely related to the steepening of the toe area by drainage process.

Most of the relict landslides in catchments CD2 and CD3 appear not as closely spaced as the relict landslides in CD1. They were located mainly at the cliff and near/at drainage lines, possibly controlled by the steep slope gradient and influence of drainage lines.

C.8 Conclusions

A review of the landslides within the natural terrain catchments to the north of Tai O Cemetery was carried out, mainly based on a desk study including a detailed site-specific API. All the landslide features recorded in the ENTLI were verified and a regolith map and a terrain unit map were produced, in order to decipher the possible geological or geomorphological factors that may have played a role in the occurrence and distribution of the recent and relict landslides. The key observations are summarised below:

(a) The ENTLI features were verified and there are 18 nos. of recent landslides and 56 nos. of relict landslides confirmed within the Study Area. The type, dimension and estimated volume of the verified landslide were determined. All the recent and most of the relict landslides are shallow failures (< 2 m) and are of relatively small landslide volume (mostly < 100 m^3).

(b) A regolith map for the Study Area was produced using API and seven types of regolith were mapped within the Study Area, including intermittent rock outcrops of volcanic rock and sedimentary rock, volcanic and sedimentary saprolite, landslide debris, colluvium and beach deposits. The regolith map together with the slope angle map indicate the volcanic terrain is generally steeper than the sedimentary

terrain and this may be related to the strength of the two rock types. The lithological change may have controlled the slope morphology and gradient, in turn, affected the distribution of landslides.

(c) The delineation of terrain units showed that the landslides were concentrated in the middle fall face unit and middle incised unit (75% of landslides within less than 30% of the plan area of the Study Area). Landslides occurred within these terrain units were likely related to the steep slope gradient and also erosional processes of the drainage lines.

(d) Based on the review of the recent landslides using the eight-fold classification system, about one-third of the recent landslides were related to retrogressive failures or over-steepened slopes at previous failure scars (Types 1 and 4). The distance between the recent landslide and the related relict landslide is in a range of 4 - 22 m. About half of the landslides were classified as cluster Types 5, 6 and 7, therefore related to headward erosion at the head of drainage lines or to undercutting processes along the drainage lines.

Appendix D

Geological and Geomorphological Review of Landslide Clusters in Catchment KSR56 and KSR56A - Keung Shan Road

(Prepared by S.H.S. Leung)

Contents

List of Tables

List of Figures

List of Plates

D.1 Location and Catchment Characteristics

The Study Area in Keung Shan Road, western Lantau comprises two catchments, namely "Catchment KSR56" and an adjoining catchment (hereafter referred to as "Catchment KSR56A") to the southwest (Figure D1.1).

Both Catchments KSR56 and KSR56A are generally elongated SE-NW-oriented catchments, covering an area of about 0.06 km^2 and 0.02 km^2 respectively. In terms of aspect ratios (width of long axis divided by width of short axis) are about 1.8:1 and 2.9:1 respectively. In terms of elevation difference, Catchment 56 has an elevation difference of about 158 m (from 286 mPD at its highest point to 128 mPD to its lowest point), whereas Catchment KSR56A has an elevation difference of about 139 m (from 271 mPD to 132 mPD). The dimensions and aspect ratios of the Study Area are summarized in Table D1.1 below.

Table D1.1 Dimensions of the Study Area

	Catchment KSR56	Catchment KSR56A
Catchment Area	0.0599 km^2	0.0238 km^2
Aspect Ratio	1.78:1	2.89:1
Elevation Difference	158 m	139 m

Parts of the Study Area have been significantly modified by human activities, including mainly construction of Keung Shan Road and site formation works at the northern part of Catchment KSR56. The areas that have been significantly modified and altered are excluded from analyses and discussion in this Study.

D.2 Geology

According to the published 1:20,000-scale geological map Sheet No. 13, the Study Area is mainly underlain by rhyolite lava and tuff of the Lantau Formation (undifferentiated, JLT, Figure D2.1), which has been renamed as the Lantau Volcanic Group by Sewell et al (2000). Slope debris (Qd, comprising sand, gravel, cobbles and boulders in silt matrix) was also recorded in the lower parts of the Study Area. According to Langford et al (1995), the lavas are typically banded and do not contain lithic fragments, while the tuffs usually contain lithic lapilli, and both are characterised by large white euhedral feldspar crystals. Intermittent rock outcrops were observed as intermittent rock from aerial photographs in the source areas of previous landslides as well as along the bed of drainage lines (AECOM, 2015). On the published geological map, an ESE-trending inferred fault was recorded in Catchment 56 and may have influenced the drainage line orientations.

Ground investigation (GI) fieldwork reports for GI stations within and in the vicinity of the Study Area (Figure D2.1) have been reviewed. Previous GI works within the Study Area include four drillholes and six trial pits.

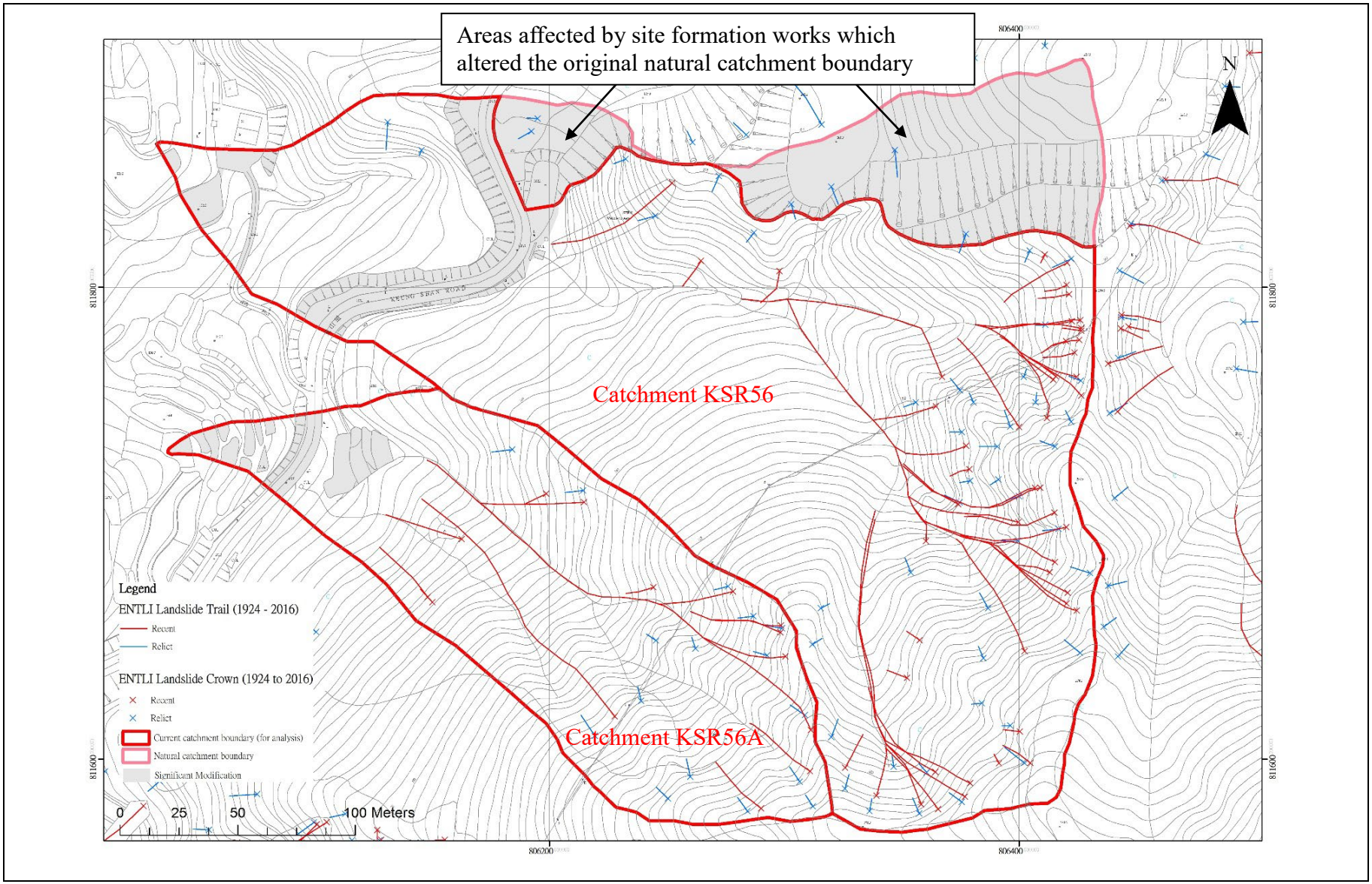

Figure D1.1 Catchment KSR56 and KSR56A (the Study Area) above Keung Shan Road, West Lantau

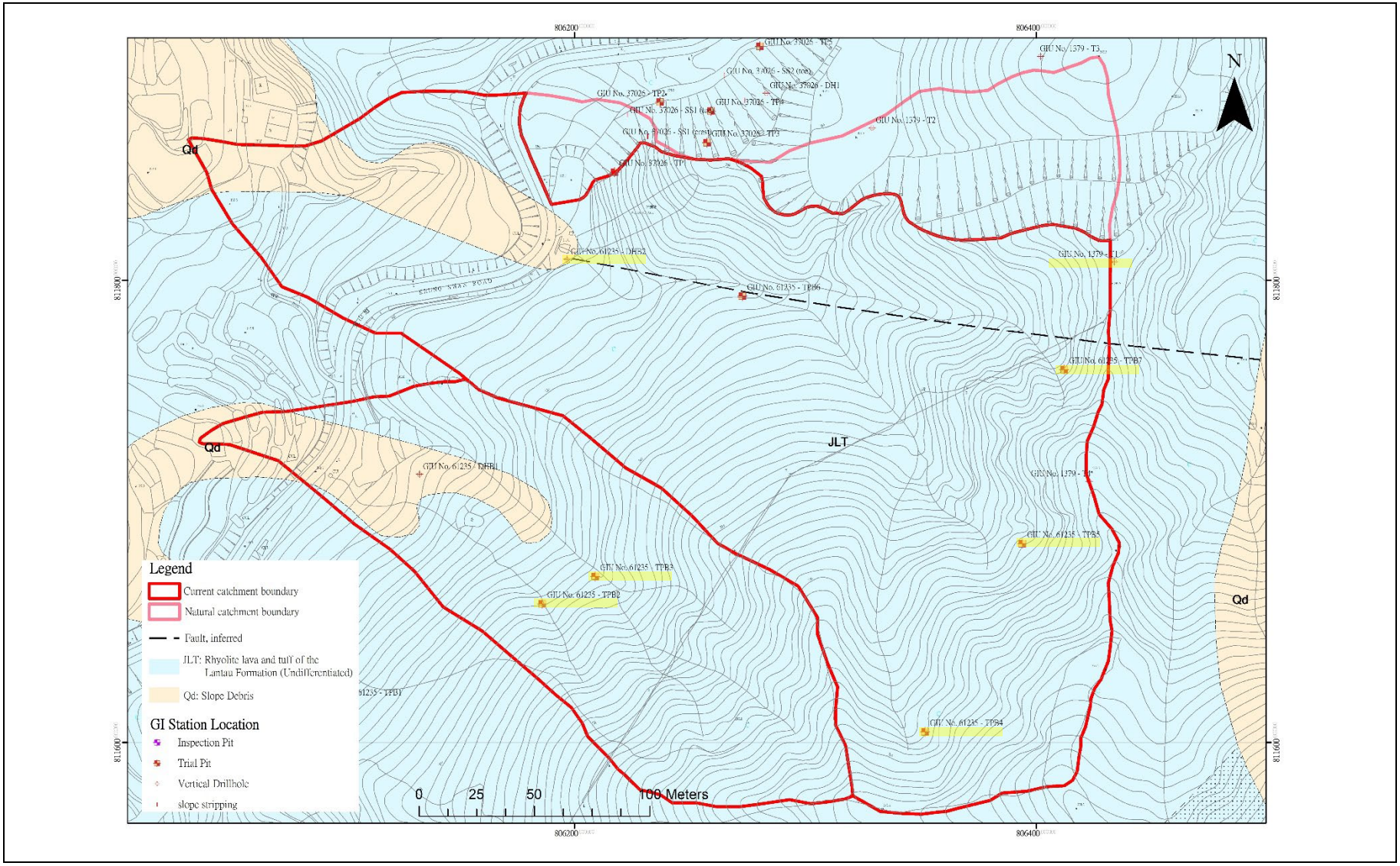

Figure D2.1 Solid and Superficial Geology of the Study Area adopted from the Published 1:20,000-scale Geological Map Sheet No. 13 (GEO, 1995) and Ground Investigation Station Locations

Slightly-decomposed to completely-decomposed coarse ash tuff and fine ash tuff (Grades II to V) and their residual soil (Grade VI) were reported in the drillholes and trial pits. A total of 15 nos. measurements on relict joints were recorded in four trial pits (TPB2, TPB4, TPB5 and TPB7, all in GIU Report No. 61235), the dip angles and dip directions of which are presented as poles on a stereoplot in Figure D2.2. Among these four trial pits, kaolin-infilling in the relict joints were reported in TPB5, and quartz veins were reported in TPB5 and TPB7 dipping at 62°/284°, 80°/142° and 75°/070°.

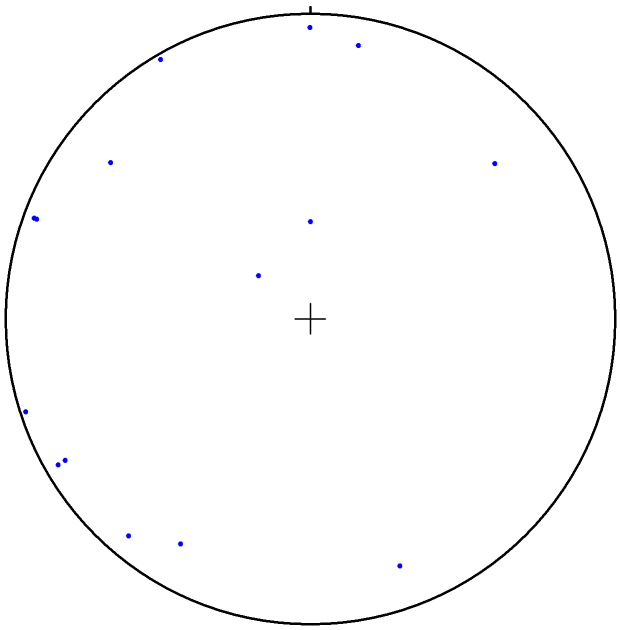

Total number of poles: 15

Note: Rock joint data are plotted on equal area stereonet, lower hemispheric projection.

Figure D2.2 Equal Area Stereonet of Measurements on Relict Joints in the GI Stations in the Study Area.

Colluvium was the only type of superficial deposit reported in the GI stations within the Study Area. Where the thickness of colluvium could be determined, it varies from 0.5 m to 4 m thick (drillhole T1 in GIU Report No. 01379), but the base of colluvium was not reached at the termination depths of trial pit nos. TPB3 and TPB6 of GIU Report 61235. The colluvium is generally described as comprising silt or sand with varying amounts of rock fragments ranging in size from gravels to boulders. In trial pit TPB3 (GIU Report No. 61235), two layers of colluvium beneath a 0.3 m thick layer of top soil/slope wash were reported, the upper layer (0.2 m thick) was described as clayey silty sand with occasional gravel and cobbles of tuffs and some roots, whereas the lower layer (at least 2 m thick) was described as sandy clayey silt with some gravel and cobbles and much boulders (< 800 mm) of tuff and occasional roots. A 0.5-m thick layer of fill was recorded in drillhole DHB2 (GIU Report No. 61235) in Catchment KSR56, and was described as comprising sandy clayey silt with some gravel of tuff fragments.

D.3 Site Geomorphology

The Study Area have been subdivided into five geomorphological units, namely Ridge, Drainage Depressions, Valley Side Slopes, Planar Side Slopes and Deposition Lower Slopes (Figure D3.1). The characteristics of these geomorphological units are described below.

D.3.1 Ridge

This geomorphological unit comprises generally rounded, gentle terrain at the uppermost part of the two catchments, gradients are typically < 25° but locally up to over 30° at where intermittent rock outcrops occur. In terms of percentage of catchment area, this unit is the lowest among the geomorphological units (about 6% of Catchment 56 and 0.4% of Catchment 56A). This unit is spatially separated from other geomorphological units below by a convex break-in-slope. In terms of regolith, this unit generally comprises saprolite, locally with intermittent outcrop/corestones (only in Catchment KSR56).

D.3.2 Drainage Depressions

This unit comprises topographic depressions at the upper reaches (below the Ridges) with gradients up to about 45°. These drainage depressions are located at heads of drainage lines and are mainly affected by headward fluvial undercutting. This unit comprises saprolite, locally with intermittent outcrops/corestones (only in Catchment KSR56).

D.3.3 Valley Side Slopes

This unit comprises incised slopes at the lower reaches of the two catchments along drainage lines, with gradients up to about 45°. Compared with Drainage Depressions, this unit is not located at heads of drainages, and are located along the sides of the drainages. In terms of percentage of catchment area, this unit is the highest among the geomorphological units (about 30% of Catchment KSR56 and 64% of Catchment KSR56A). In terms of surficial processes, this unit is more affected by sideward fluvial undercutting. Similar to Drainage Depression, this unit comprises saprolite with a thin veneer of colluvium, and intermittent outcrops/corestones are locally observed (in both Catchments KSR56 and KSR56A).

D.3.4 Planar Side-Slopes

This unit is present only in Catchment KSR56 but not in Catchment KSR56A. This geomorphological unit is characterized by planar saprolitic hillslopes facing NW with gradients up to about 35°. Spatially, this unit is located between the Ridge terrain above and the Valley Side Slope and Deposition Lower Slope along the valleys below. In terms of superficial process, this unit is mainly affected by gravity-driven erosion with little influence of drainage lines.

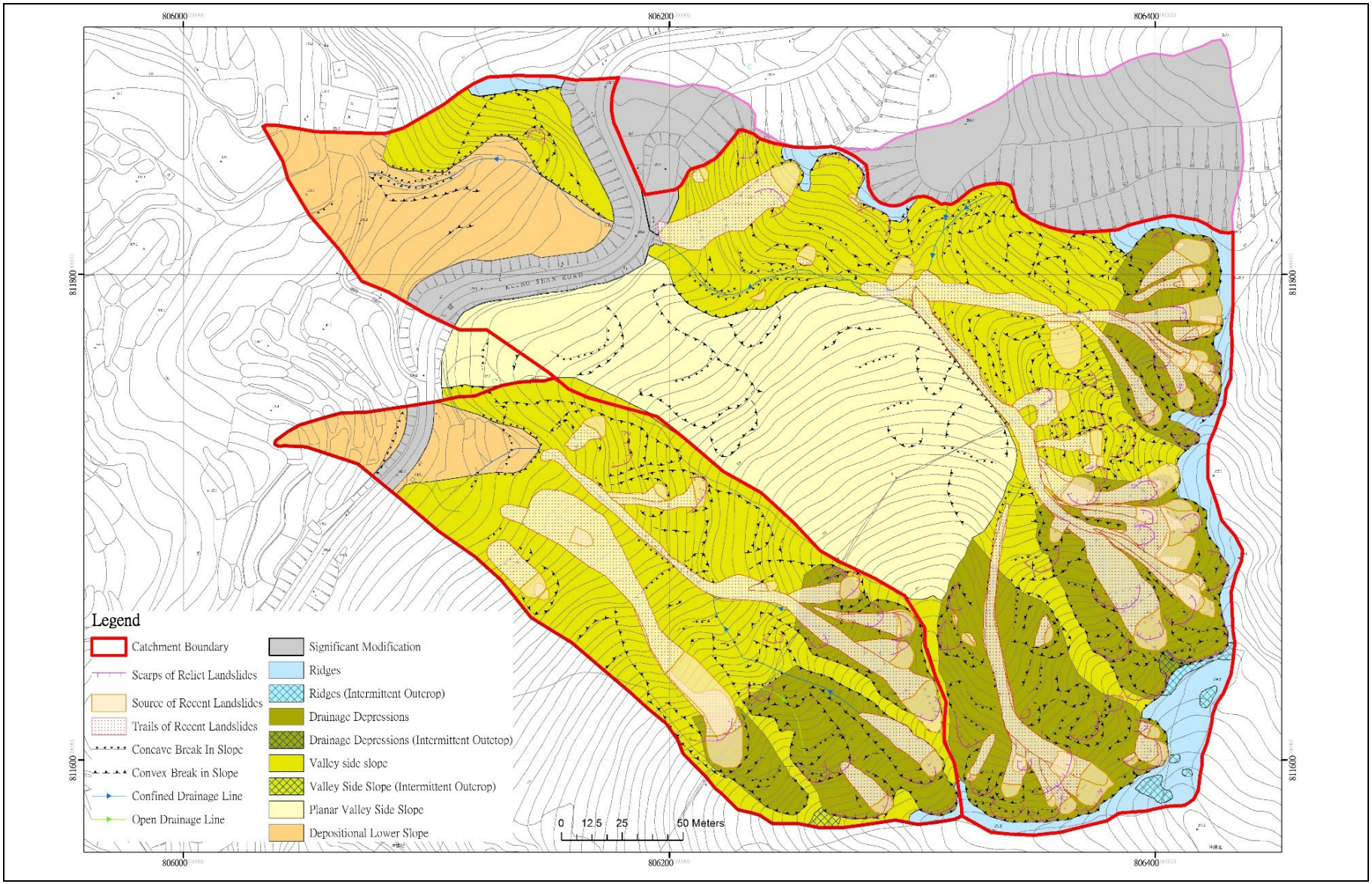

Figure D3.1 Distribution of Landslides in Geomorphological Units

D.3.5 Deposition Lower Slopes

This unit is characterized by gentle (0 - 30°) terrains which are zones of colluvial deposition near the toe of the two catchments. Part of this unit overlaps with areas marked as "Qd" (slope debris) on the 1:20,000-scale geological map.

D.4 Review of Past Instabilities

D.4.1 Overview

According to the Enhanced Natural Terrain Landslide Inventory (ENTLI) database, there are a total of 92 nos. and 30 nos. of natural terrain landslides that occurred in Catchments KSR56 and KSR56A respectively (Table D4.1 and Figure D4.1). Among the recent ENTLI landslides, the number of channelized debris flows are slightly higher than that of open hillslope landslide for both Catchments KSR56 and KSR56A. Six relict landslides which were located in the northern portion of Catchment KSR56 had been subsequently modified by site formation works that were mentioned in Section D.1. Therefore, these relict landslides were not considered in the analysis under this Study.

Table D4.1 Number of ENTLI Landslides in the Study Area

	Catchment KSR56	Catchment KSR56A
Relict Landslides	43*	16
Recent Landslides	49 (25 channelised debris flows, 24 open hillslope landslide)	14 (8 channelised debris flows, 6 open hillslope landslide)
Total	92	30

Note: Asterisk denotes excluding six nos. of relict landslides that occurred in areas of significant modification mentioned in Section D.1.1.

A project-specific aerial photograph interpretation (API) has been carried out under this review to verify the number of natural terrain landslides, including the ENTLI landslides and also landslides that were identified by AECOM (2015) and FSWJV (2014). An inventory of natural terrain landslides has been compiled and is summarised in Table D4.2.

Compared with the ENTLI landslides, for Catchment KSR56, eight additional relict landslides and six additional recent landslides have been identified (including one recent landslide (site-specific landslide ID No. 98) which was identified during field reconnaissance by AECOM (2015) and was not identifiable on API), whereas two relict landslides (ENTLI Nos. 13NWB1343E and 13NWB1861E) and one recent landslide (ENTLI No. 13NWB2180E) could not be identified in the site-specific API. For Catchment KSR56A, two additional relict landslides and two additional recent landslides have been identified, whereas one relict landslide (ENTLI No. 13NWB1837E) could not be identified in the site-specific API.

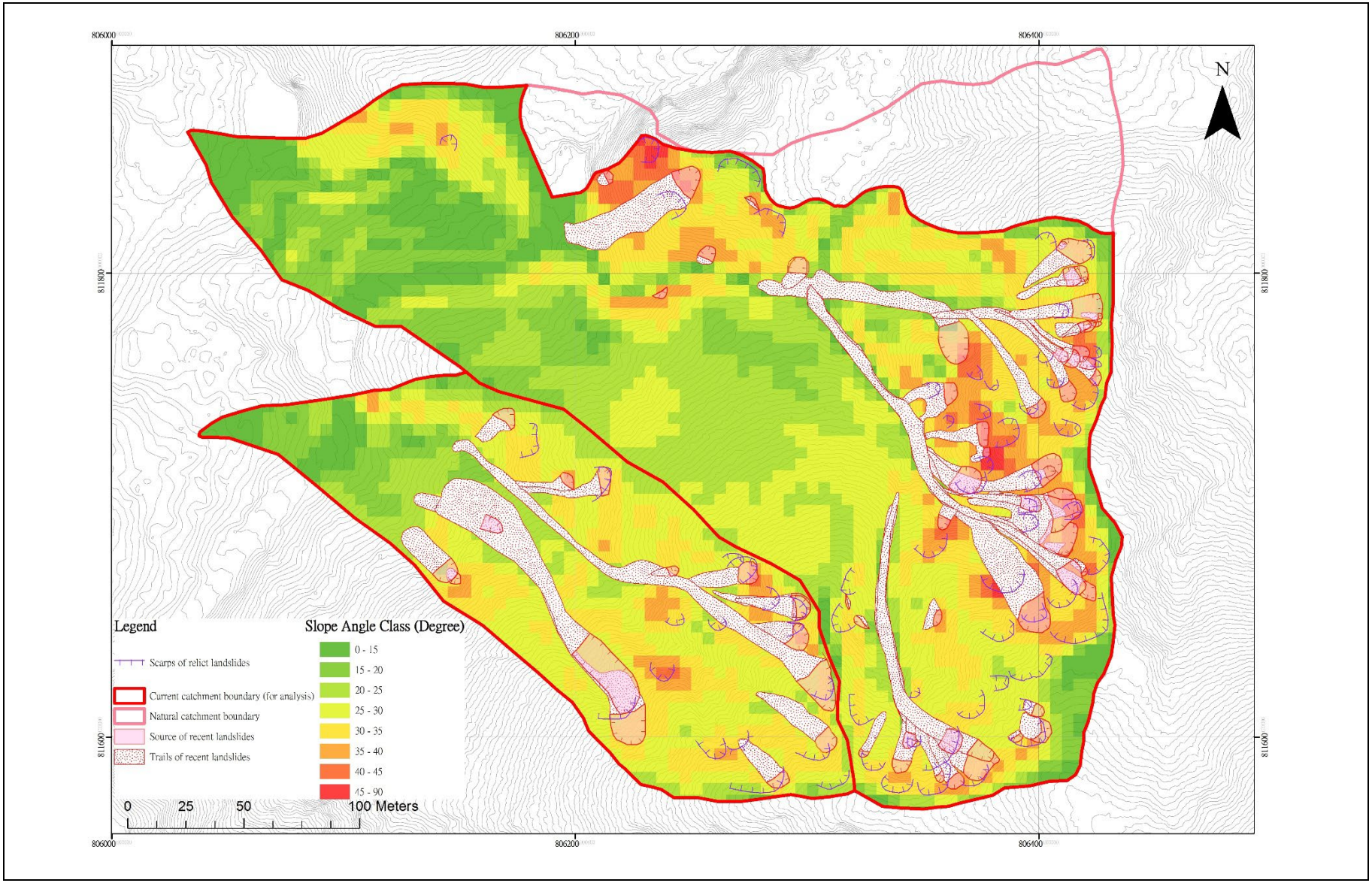

Figure D4.1 Slope Angle Classes of the Study Area based on the DEM Generated from the 2010 Airborne LiDAR Data

Table D4.2 Number of Landslides in the Study Area

	Catchment KSR56	Catchment KSR56A
Relict Landslides	49	17
Recent Landslides	54#	16
Total	103*	33

Notes: (1) Hashtag denotes a recent landslide (site-specific landslide ID No. 98) included was identified during field reconnaissance by AECOM(2015) and was not identifiable on API, therefore the year of occurrence is uncertain.
(2) Asterisk denotes excluding six relict landslides that fall outside the current catchment boundary.

Among the recent landslides, for Catchment 56, 33 (61%) of the landslides were debris open hillslope landslides and 21 (39%) were debris flows, whereas for Catchment 56A, seven (44%) of landslides were open hillslope landslides and nine (56%) were debris flows. For both catchments, the recent landslides were temporally concentrated in 1982, 1992, 1993 and 2008. The highest number of landslides occurred during the June 2008 rainstorm, during which 28 and nine recent landslides occurred in Catchments 56 and 56A, respectively.

D.4.2 Landslide Characteristics

Summary of landslide dimensions of the two catchments are presented in Table D4.3. In general, the landslides are relatively shallow in depth (0.5 - 2.0 m in Catchment KSR56, 1 - 1.5 m in Catchment KSR56A). The estimated source volumes of the recent landslides (by using the formula 1/6 x π x width x length x depth) are up to about 250 m^3 (recent ENTLI No. 13NWB2213E in Catchment KSR56A). Debris runout distance of the recent landslides were also estimated based on API in this Study, and the longest runout distance in Catchments 56 and 56A are about 200 m (recent ENTLI No. 13NWB2704E) and 187 m (recent ENTLI No. 13NWB2722E) respectively.

In terms of landslide locations, most of the landslides initiated at upper valley/head of slopes, probably as a result of headward fluvial undercutting and over-steepened slopes.

Table D4.3 Summary of Dimensions of Landslides in the Study Area

	Catchment KSR56		Catchment KSR56A	
	Relict	Recent	Relict	Recent
Source Width (m)	4.5 - 30.0	2.0 - 17.0	5.0 - 25.0	4.5 - 17.0
Source Length (m)	2.6 - 10.7	0.9 - 17.3	5.2 - 13.0	3.4 - 37.0
Source Depth (m)	0.5 - 2.0	0.5 - 2.0	1 - 1.5	0.5 - 1.5
Source Volume (m^3)	6 - 178	1 - 152	17 - 180	5 - 252

D.4.3 Density of Landslides by Slope Angle Class

Based on slope angle class map from LiDAR elevation data (5-m grid, Figure D4.1), slope angles in Catchment KSR56 range in 0 - 47°, while those in Catchment KSR56A range from about 6 - 42°. In general, slope angles become steeper along channel sides and also in the middle and upper parts of both catchments.

The density of relict and recent landslides in the Study Area are summarised in Tables D4.4 and D4.5. For Catchment KSR56, the slope angle classes with the highest density of relict and recent landslides are 30 - 35° and 35 - 40° respectively. For Catchment KSR56A, the slope angle classes with highest density of relict and recent landslides are both in the 35 - 40° slope angle class.

D.4.4 Distribution of Landslides in Geomorphological Units

The distribution of both relict and recent landslides in the above-mentioned geomorphological units are presented in the Table D4.6 and Figure D3.1. The recent landslides were most concentrated in the Drainage Depressions geomorphological unit (about 80% in Catchment KSR56 and 65% in Catchment KSR56A), followed by the Valley Side Slopes (about 25% in Catchment 56 and 35% in Catchment KSR56A). Given the geomorphological settings of these two units, the recent landslides are likely related to fluvial undercutting and over-steepened slopes.

D.4.5 Relevant Field Observations as Reported in S2(H)R 11/2015 (AECOM, 2015)

Although site-specific field reconnaissance has not been carried out in this Study, field observations in the Study Area were recorded in AECOM (2015). Selected field photos and observations as extracted from AECOM (2015) are shown in Plates D4.1 to D4.6, and the location plans of the field photos are shown in Figure D4.2.

AECOM (2015)'s field observations regarding the recent landslides within the Study Area are summarised as follows. Highly-decomposed tuff (HDT) and moderately-decomposed tuff (MDT) have been found in the source areas of several landslides. Structurally-controlled rupture surface along joint surface was also recorded (Plates D4.1 to D4.6). Where mapping was carried out, AECOM (2015) recorded at least two types of rupture surfaces, namely the interface between colluvium and CDT/HDT (e.g. recent ENTLI No. 13NWB2178E, Plate D4.7) and within colluvium (e.g. Landslide ID No. 135). In addition, tension crack (about 5 m long, 0.2 m wide and with a vertical displacement of 0.7 m) and soil pipes were also reported. Regarding debris, intact displaced debris rafts have been reported at Landslide ID No. 135 (Plate D4.8) and below recent ENTLI No. 13NWB2704E.

Table D4.4 Landslide Density by Slope Angle Class - Catchment KSR56

Slope Angle Class (Degree)	Total Area (km^2)	% of Catchment Area	No. of Landslides				Landslide Density (no. of Landslide/km^2)	
			Recent	%	Relict	%	Recent	Relict
0-15	0.0062578	10.5	0	0	1	2.0	0	160
15-20	0.0084743	14.2	0	0	2	4.1	0	236
20-25	0.0122548	20.5	2	3.7	2	4.1	163	163
25-30	0.0152347	25.5	12	22.2	11	22.5	788	722
30-35	0.0104694	17.5	11	20.4	17	34.7	1051	1624
35-40	0.0055888	9.3	21	38.9	10	20.4	3758	1789
40-45	0.0012894	2.2	7	13.0	4	8.2	5429	3102
45-90	0.0002890	0.5	1	1.9	2	4.1	3461	6921

Table D4.5 Landslide Density by Slope Angle Class - Catchment KSR56A

Slope Angle Class (Degree)	Total Area (km^2)	% of Catchment Area	No. of Landslides				Landslide Density (no. of Landslide/km^2)	
			Recent	%	Relict	%	Recent	Relict
0-15	0.0009972	4.2	0	0	0	0	0	0
15-20	0.0017997	7.6	0	0	0	0	0	0
20-25	0.0049285	20.7	4	25.0	1	5.9	812	203
25-30	0.0088456	37.2	2	12.5	4	23.5	226	452
30-35	0.0062458	26.3	7	43.8	9	52.9	1121	1441
35-40	0.0008718	3.7	3	18.8	3	17.7	3441	3441
40-45	0.0000750	0.3	0	0	0	0	0	0
45-90	0	0	0	0	0	0	0	0

Plate D4.1 Tension Crack Extending towards the East Flank of Landslide ID No. 135 in Catchment 56A in this Study

Plate D4.2 Deeply Incised Gullies on the Landslide Floor of Recent ENTLI Nos. 13NWB2723E and 13NWB2724E (Landslide ID Nos. 130 and 131 in Catchment KSR56A in this Study)

Plate D4.3 Soil Pipe (0.2 m in dia. And 0.5 m deep) observed on the Scarp of Landslide Recent ENTLI No. 13NWB2013E (Landslide ID No. 51 in Catchment KSR56)

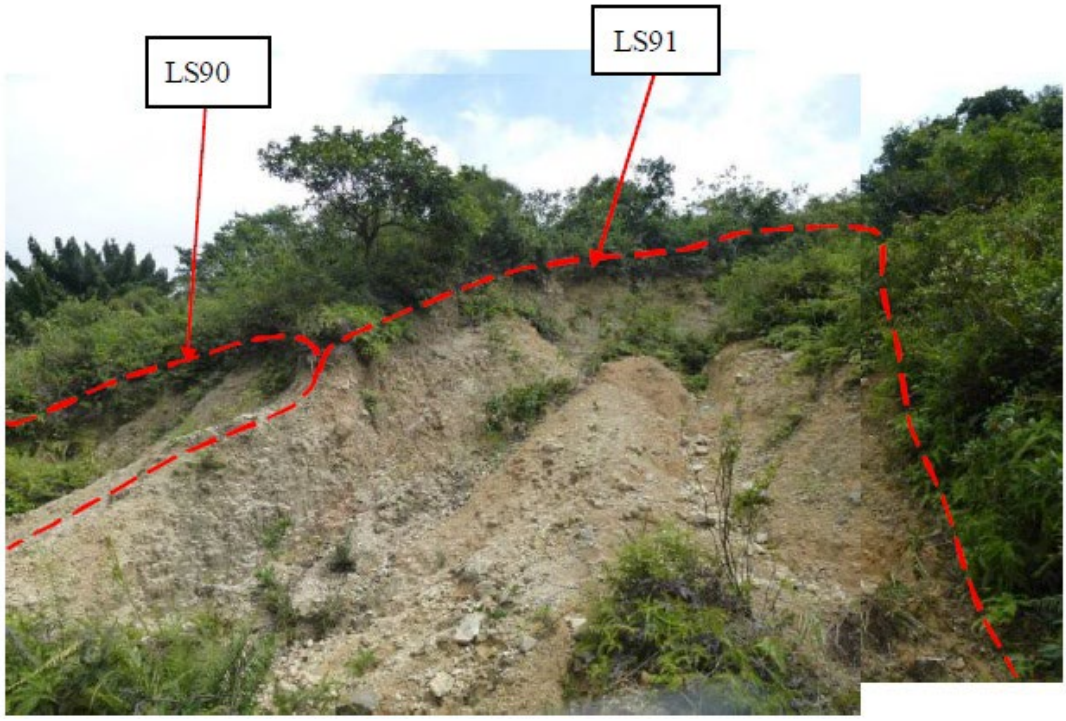

Plate D4.4 General View of Recent ENTLI Nos. 13NWB2704 ("LS91") and 13NWB2705E ("LS90") (i.e. Landslide ID Nos. 82 and 81 respectively in Catchment KSR56 in this Study)

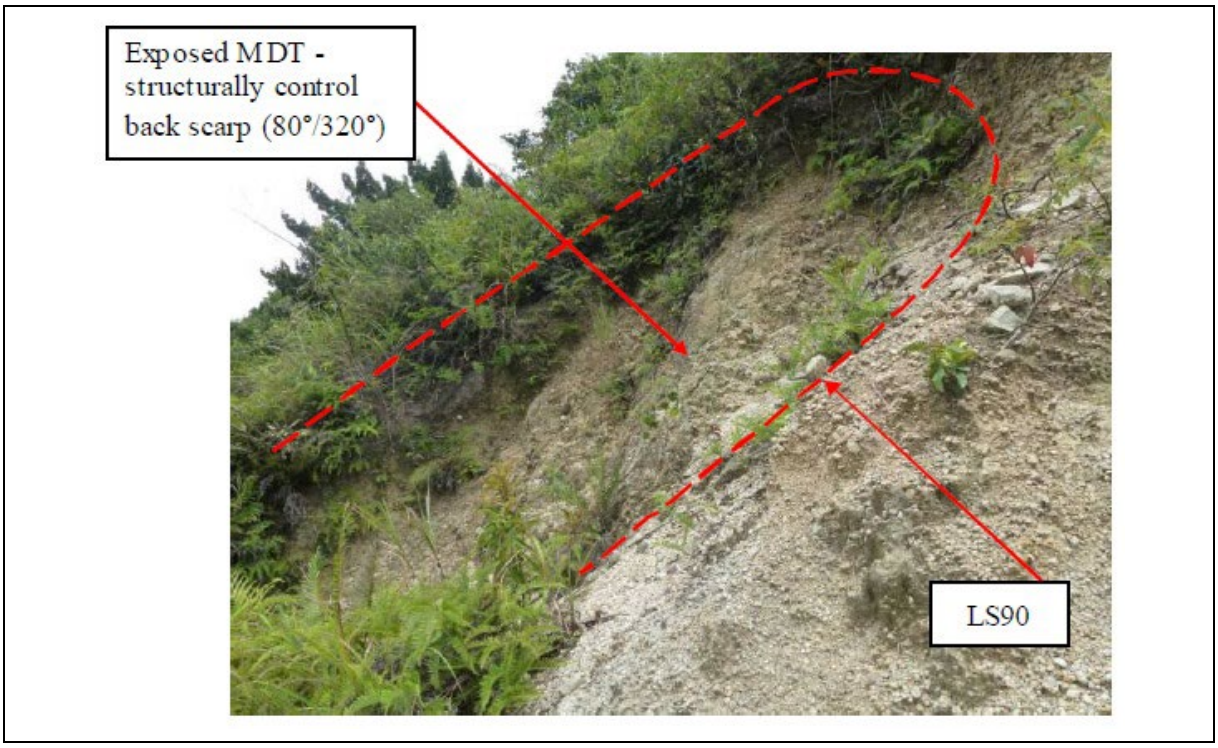

Plate D4.5 Exposed Moderately Decomposed Tuff (MDT) at the Floor of Recent Landslide "LS90" (recent ENTLI No. 13NWB2705E, Landslide ID No. 82 in Catchment KSR56)

Plate D4.6 Exposed MDT at the Floor of Recent ENTLI No. 13NWB2703E (Landslide ID No. 80 in Catchment KSR56)

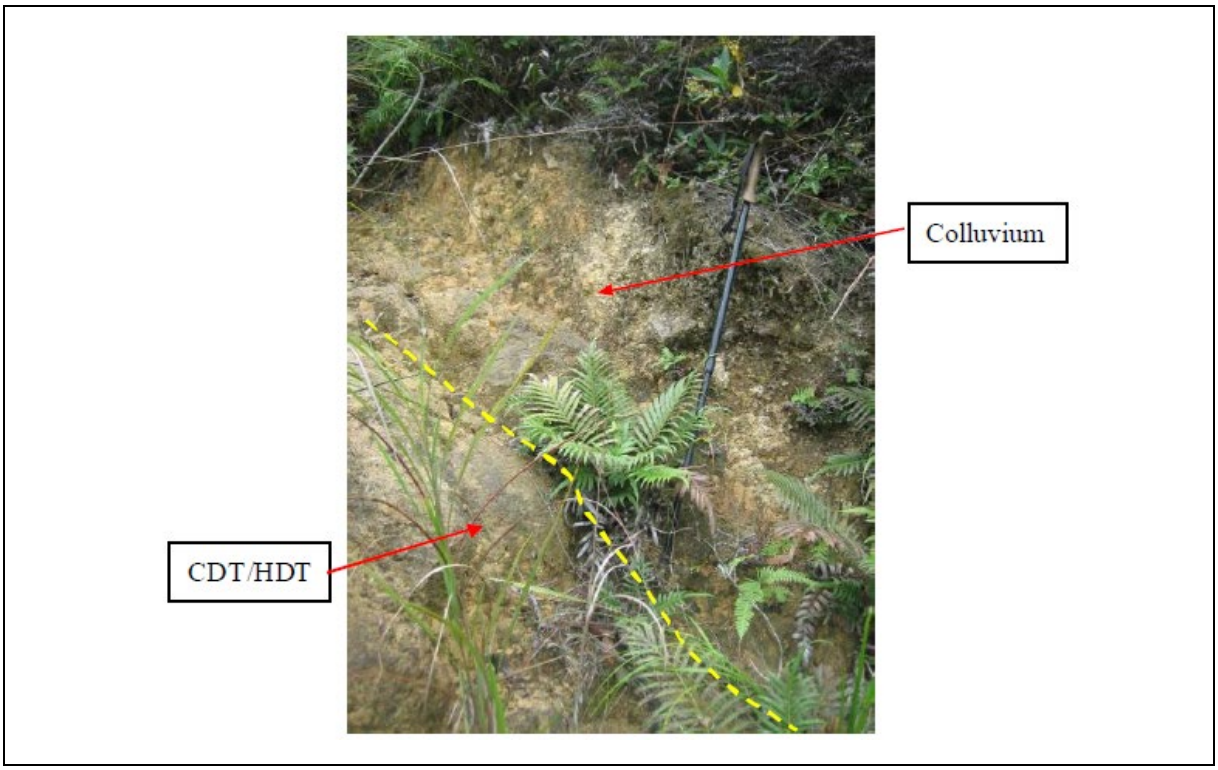

Plate D4.7 Rupture Surface along the Interface between Colluvium and CDT/HDT at Recent ENTLI No. 13NWB2178E in Catchment KSR56

Plate D4.8 Displaced Intact Debris Raft on Recent Landslide ID No. 135 in Catchment KSR56A

Table D4.6 Distribution of Landslides in Different Geomorphological Units within the Study Area

Terrain Units	Area in Catchment 56 (km^2)	% of Area	Number of Landslides in Catchment KSR56				Density		Area in Catchment 56A (km^2)	% of Area	Number of Landslides in Catchment KSR56A				Density	
			Relict	%	Recent	%	Relict	Recent			Relict	%	Recent	%	Relict	Recent
Ridge	0.004	6.4	1	2.0	1	1.9	260.9	260.9	0.0001	0.4	0	0.0	0	0.0	0.0	0.0
Drainage Depressions	0.015	24.6	36	73.5	43	79.6	2444.3	2919.6	0.0060	25.3	11	64.7	7	43.8	1830.6	1164.9
Valley Side Slopes	0.018	29.6	12	24.5	10	18.5	678.2	565.1	0.0153	64.4	6	35.3	9	56.3	392.1	588.2
Planar Side Slopes	0.015	25.5	0	0.0	0	0.0	0.0	0.0	0.0000	0.0	0	0.0	0	0.0	-	-
Deposition Lower Slopes	0.006	9.2	0	0.0	0	0.0	0.0	0.0	0.0019	8.2	0	0.0	0	0.0	0.0	0.0
Area Modified by Human Activities	0.003	4.7	-	-	-	-	-	-	0.0004	1.7	-	-	-	-	-	-

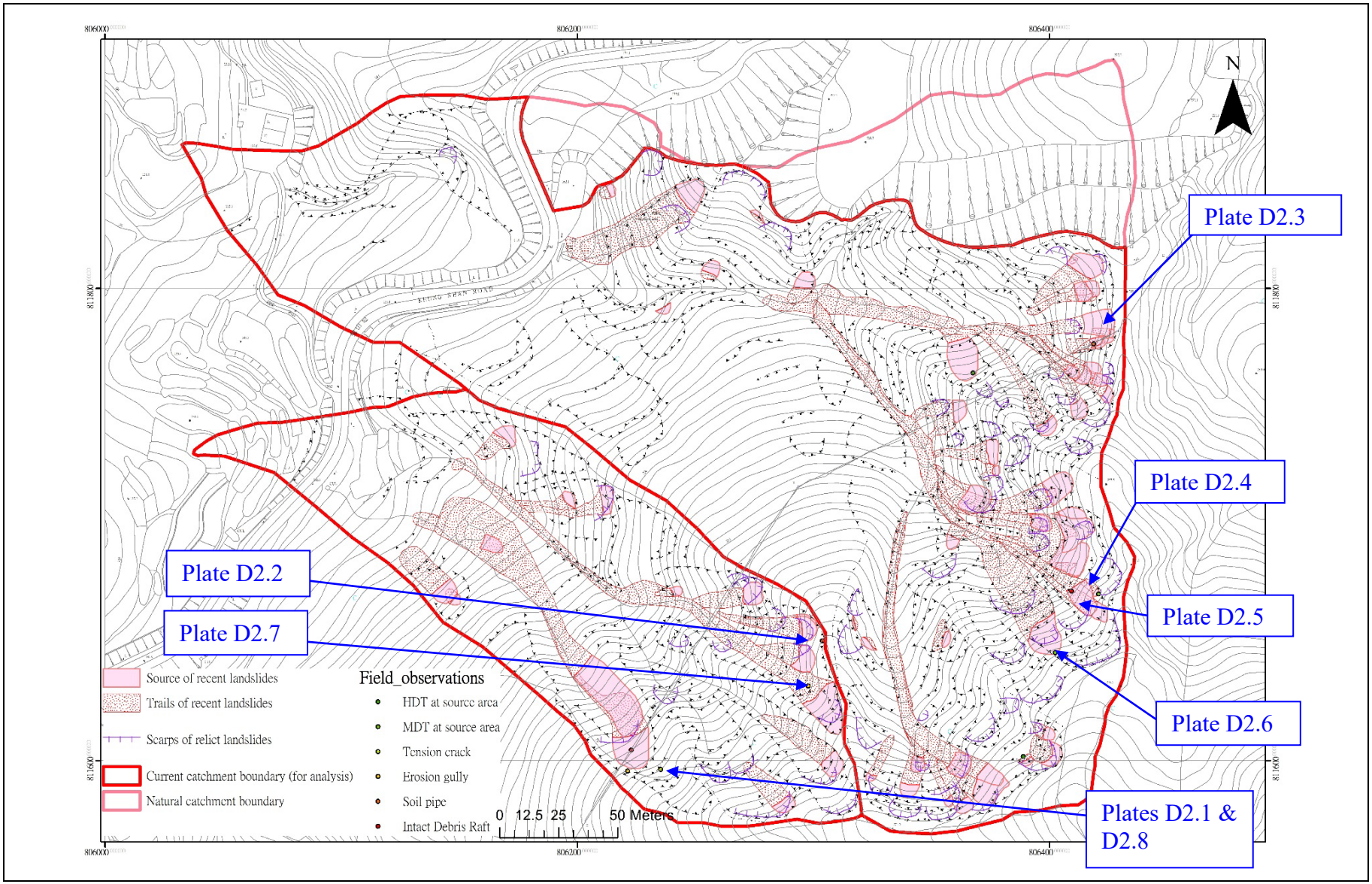

Figure D4.2 Location Plan of Field Photos (Plates D2.1 - D2.8) Taken by AECOM (2015)

D.5 Classification of Cluster of Recent and Relict Landslide

Based on the 8-fold classification scheme proposed by Tang et al (2018), most of the landslides in both Catchments KSR56 and KSR56A fall within Type 6 which were multiple failures that occurred at the head of a drainage or a topographic depression formed at the head of a drainage line and Type 7 which were multiple failures that occurred at the side slopes of an incised drainage channel. Details are summarized in Table D5.1.

Table D5.1 Classification of Landslide Clusters in the Study Area

Type of Landslide Cluster	Catchment KSR56			Catchment KSR56A		
	No. of Recent Landslides	%	Range of Distance to the Closest Related Relict Landslide (m)	No. of Recent Landslides	%	Range of Distance to the Closest Related Relict Landslide (m)
1	1	1.85	15.5	0	0.00	-
2	0	0.00	-	0	0.00	-
3	1	1.85	13.5	0	0.00	-
4	0	0.00	-	0	0.00	-
5	0	0.00	-	0	0.00	-
6	38	70.37	1.3 - 17.4	9	56.25	2.1 - 12.9
7	8	14.81	2.0 - 12.1	2	12.50	5.4 - 16.8
8	1	1.85	1.8	0	0.00	-
Not in Cluster	5	9.26	-	5	31.25	-
Total	54	100		16	100	-

D.6 Summary

A review of the landslides within two natural terrain catchments (Catchments KSR56 and KSR56A) above Keung Shan Road was carried out, mainly based on desk study of available information and also a site-specific API, with an aim to identify possible geological or geomorphological controls on the occurrence and distribution of relict and recent landslides. The key observations are summarised below:

(a) The ENTLI landslides were verified. In Catchment KSR56, and there are 49 nos. of relict landslides and 54 nos. recent landslides. In Catchment KSR56A, there are 17 nos. relict landslides and 16 nos. recent landslides. Characteristics of the landslides, e.g. dimensions and estimated volumes were determined. All the recent landslides are relatively shallow ($\leq$ 2 m) with volume mostly < 250 m^3.

(b) A geomorphological unit map for the two catchments were produced using API and five geomorphological units were identified, namely Ridge, Drainage Depression, Valley Side Slopes, Planar Side Slopes and Deposition Lower Slopes.

(c) The landslides were concentrated in the Drainage Depressions geomorphological unit (about 80% in Catchment KSR56 and 65% in Catchment KSR56A) likely related to fluvial undercutting and over-steepened slopes.

(d) Based on the eight-fold classification system of landslide clusters proposed by Tang et al (2018), most of the landslides in the Study Area fall within Type 6 which were multiple failures that occurred at the head of a drainage or a topographic depression formed at the head of a drainage line and Type 7 which were multiple failures that occurred at the side slopes of an incised drainage channel.

D.7 References

AECOM Asia Company Limited (2015). *Stage 2(H) Study Report - Study Area 13NW-B/SA6 Keung Shan Road Near Sham Wat Road, Lantau Island (LPMitP Agreement No. CE 27/2012 (GE) Landslip Prevention and Mitigation Programme, 2012, Package D, Landslip Prevention and Mitigation Works - Investigation, Design and Construction)*. Geotechnical Engineering Office, Hong Kong, 440 p.

Arup Fugro Joint Venture (AFJV) (2010). *Natural Terrain Hazard Review Report (LPMitP Agreement No. CE62/2008(GE) Landslip Prevention and Mitigation Programme, 2008, Package N, Natural Terrain Mitigation Works, West Lantau - Investigation, Design and Construction).* Geotechnical Engineering Office, Hong Kong, 405 p.

Fugro Scott Wilson Joint Venture (FSWJV) (2014). *Summary Report on the Identification of June 2008 Natural Terrain Landslides on Lantau Island (Agreement No. CE 40/2007 (GE) Study of Landslides Occurring in Hong Kong Island and Outlying Islands in 2008 and 2009 - Feasibility Study*. Geotechnical Engineering Office, Hong Kong, 35 p.

Geotechnical Engineering Office (GEO) (1995). *Shek Pik.* Hong Kong Geological Survey Sheet 13, Solid and Superficial Geology, 1:20,000 Series HGM20. Geotechnical Engineering Office, Hong Kong.

Ho, H.Y. & Roberts, K.J. (2016). G*uidelines for Natural Terrain Hazard Studies (GEO Report No. 138 (Second Edition))*. Geotechnical Engineering Office, Hong Kong, 176 p.

Langford, R.L., James, J.W.C., Shaw, R., Campbell, S.D.G., Kirk, P.A. & Sewell, R.J. (1995). *Geology of Lantau District. Hong Kong Geological Survey Memoir No. 6.* Geotechnical Engineering Office, Hong Kong, 173 p.

Lo, F.L.C., Law, R.P.H. & Ko, F.W.Y. (2015). *Territory-wide Rainfall-based Landslide Susceptibility Analysis (Special Project Report No. SPR 1/2015)*. Geotechnical Engineering Office, Hong Kong, 27 p.

Lo, F.L.C. & Ko, F.W.Y. (2017). *Rainfall-based Correlation of Recent Landslides with Clusters of Relict Landslides (Discussion Note No. DN 2/2017).* Geotechnical Engineering Office, Hong Kong, 10 p.

Sewell, R.J., Campbell, S.D.G., Fletcher, C.J.N., Lai, K.W. & Kirk, P.A. (2000). *The Pre-Quaternary Geology of Hong Kong*. Geotechnical Engineering Office, Hong Kong, 181 p.

Tang, D.L.K., Wong, C.C.J., Sin, Y.M. & Mok, S.C. (2018). S*tudy of Geological Controls on the Occurrence of Natural Terrain Landslide Clusters - A Pilot Study at a Catchment above Keung Shan Road, West Lantau (Geological Report No. GR 1/2018)*. Geotechnical Engineering Office, Hong Kong, 45 p.

Appendix E

Geological and Geomorphological Review of Landslide Clusters in Catchment in Fan Kam Road

(Prepared by C.C.J. Wong and D.L.K. Tang)

Contents

List of Tables

List of Figures

E.1 General Characteristics of the Study Catchment

The subject catchment (828800E 836000N) is located to the west of Fan Kam Road and opposite to Ta Shek Wu Tsuen, in the central New Territories (Figure E1.1). It covers an area of 0.046 km^2, with an elevation difference of 102 m from 157 mPD at its highest point to 55 mPD at its lowest point. The semi-oval-shaped catchment has an aspect ratio (i.e. width of long axis to width of short axis) of about 3 to 2, with relatively short, not well-developed drainage line, which is a minor tributary of Sheung Yue River. The catchment is transected by Fan Kam Road at the base at around 55 mPD. Two man-made terraces with several abandoned temporary structures (squatter huts) are present at the lower catchment.

E.2 Site Geology

According to the published 1:20,000-scale geological maps (GCO, 1988; 1989), the catchment is underlain by coarse ash crystal tuff of the Tai Mo Shan Formation (Figure E2.1). Langford et al (1989) reported that the volcanic unit is affected by dynamic and hydrothermal metamorphisms that form a series of ENE-trending metamorphic belts (with foliations) up to several hundred meters wide in the region. There were also abundant quartz veining and "resistant ribs of metatuffs" in the area (Langford et al, 1989). Numerous hydrothermal quartz veins were found at the source area of some 2018 landslides (see Section E.4.1 below), corroborating the geological descriptions in the published memoir. A ribbon of (late?) Pleistocene debris flow deposit (Qpd) was mapped along the drainage line of the catchment (GCO, 1988; 1989).

No previous ground investigation station is present within the study catchment. However, one drillhole, four trial pits and two slope strippings, with various in-situ field tests and instrumentations, were carried out on the nearby man-made slope feature no. 6NE-B/C12 under an LPM project (GIU report no. 32750; Figure E2.1). Both the existing drillhole and the trial pits had recorded the presence of relatively thin (generally < 2.5 m thick) topsoil/colluvium overlying in-situ weathered volcanic rocks. The colluvium encountered comprised surrounded to subangular, cobbles and gravels, with occasional boulders, in silty matrix.

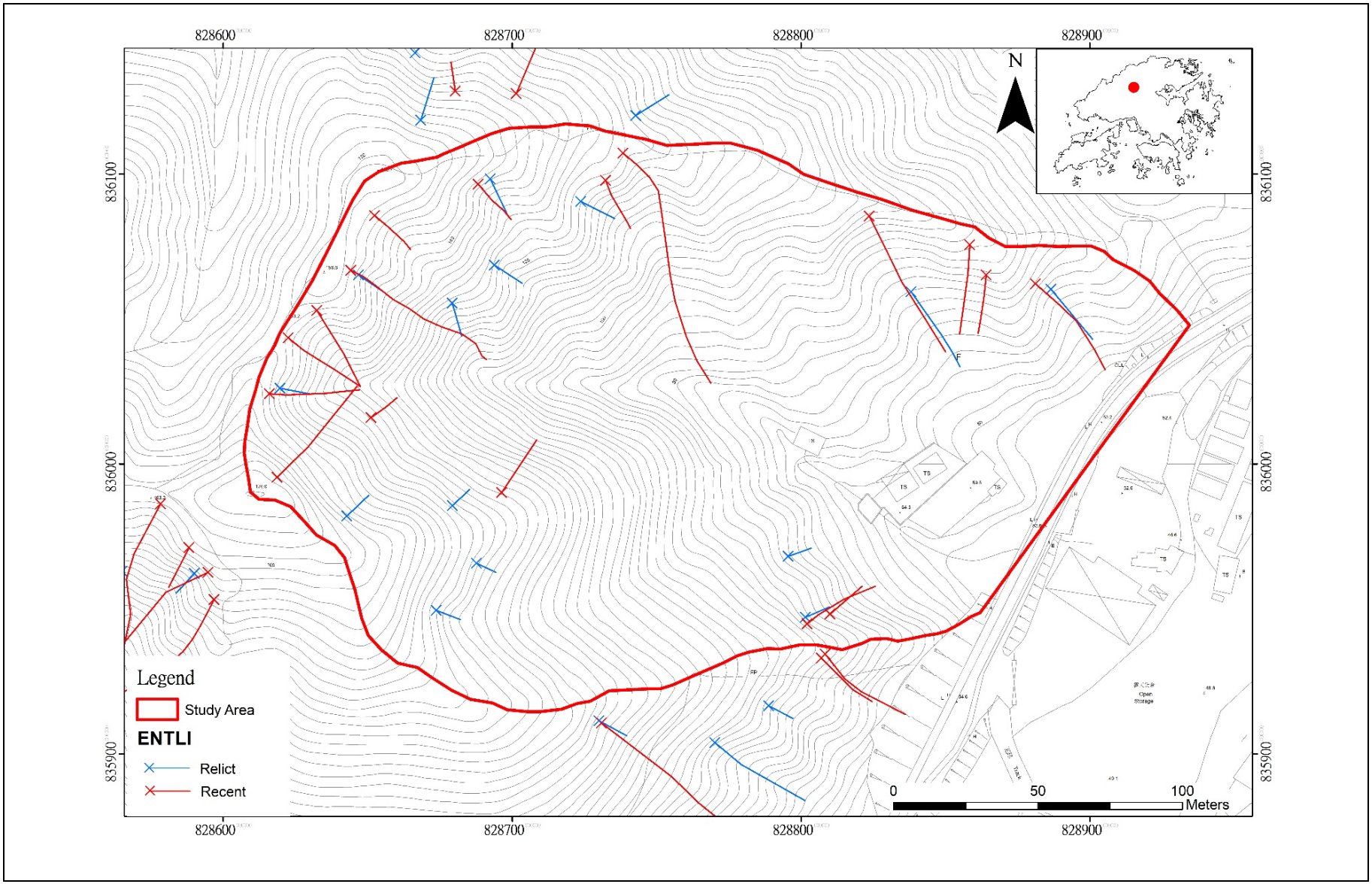

Figure E1.1 Location Plan of the Study Catchment at Fan Kam Road (with ENTLI features)

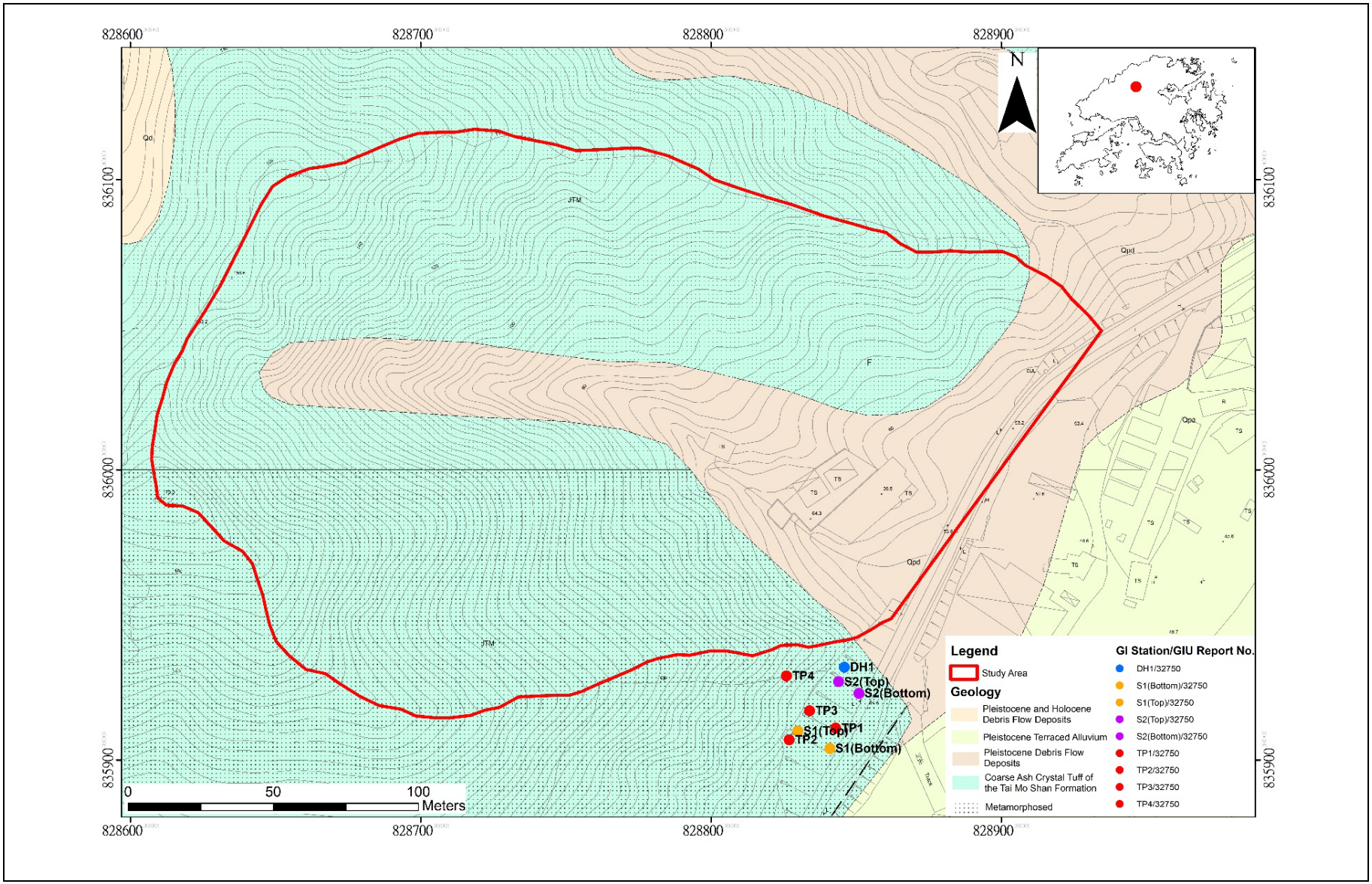

Figure E2.1 Geology of the Study Catchment (after GCO, 1988; 1989), with Locations of Existing GI stations

E.3 Site Geomorphology

E.3.1 Slope Angle Class Distribution

Slope angle of the catchment is derived from 5-m grid digital terrain model (DTM) generated from the 2010 airborne LiDAR data (Figure E3.1). The slope angle class (8-fold classification) distribution, is outlined in Table E3.1.

Table E3.1 Distribution of Slope Angle Class of Catchment FKR

Slope Angle Class (Degrees)	Area (km^2) (Total Catchment Area = 0.046 km^2)	Area (%)
0-15	0.0039	8.4
15-20	0.0038	8.4
20-25	0.0062	13.6
25-30	0.0105	22.9
30-35	0.0100	21.8
35-40	0.0079	17.3
40-45	0.0033	7.2
45-90	0.0002	0.5

E.3.2 Drainage Pattern

The study catchment is a small sub-catchment at the upper reach of Sheung Yue River that forms one of the tributaries of Ng Tung River. The total length of drainage line, including those epithermal streams, is 0.55 km, which gives a drainage / catchment area ratio of 12. Within the study catchment, the drainage lines display a dendritic pattern, but is not well developed nor particularly incised. The upper part of the catchment is dominated by epithermal streams are dominated within open drainage / topographic depressions; whilst relatively more incised and better-defined river channel is present at the middle and lower portion. Given the small size of the catchment, the head of drainage lines from the ridgeline are very close, within 10 - 20 m in plan distance.

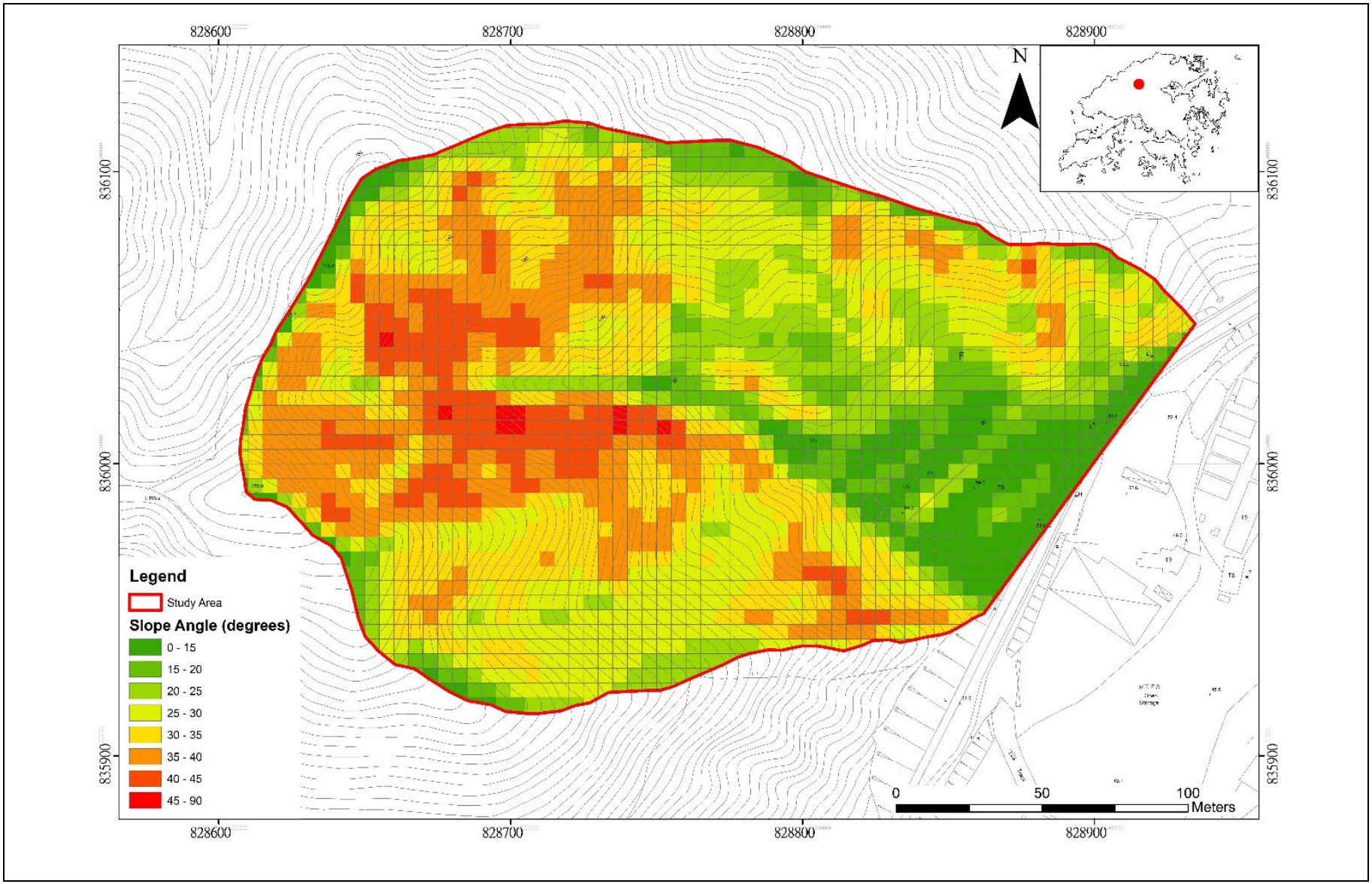

Figure E3.1 Slope Angle Distribution Map for the Study Catchment

E.3.3 Regolith Mapping

The types of regolith in the study catchment were mapped based on site-specific API. The majority of the study catchment is mantled by relatively thin volcanic saprolite, with local intermittent rock outcrops in the upper portion of the catchment. The middle portion of the valley side slopes are covered by recent landslide debris, whereas the colluvial (reworked) and fluvial deposits accumulated along the drainage course. According to field observations, the volcanic saprolite contains significant portion of sub-angular gravel to cobble-sized quartz fragments. These quartz fragments reflects the presence of mineral veins in the underlying altered tuff.

E.3.4 Terrain Units

The study catchment is sub-divided into seven terrain units (Figure E3.2) based on interpretation of landforms, regolith types, slope gradient and dominant geomorphological processes from aerial photograph observations and the 3D terrain model generated from LiDAR data (see Section E.3.1).

E.3.4.1 Ridge/Spur

The unit comprises the ridge and spurs at the uppermost portion of the catchment around the catchment boundary, and makes up > 9% of the catchment area. The unit is characterized by very gentle (0 - 15°, locally up to 20°), narrow strip of area at the upper boundary of the catchment. The ridge surrounding the catchment is generally rounded, and is inferred to be underlain by thin weathered volcanic saprolite. Based on observation from 1963 aerial photographs, a number of trenches and pits, and strips of low-vegetated disturbed areas were evident along the ridgeline. These features are interpreted to be abandoned foxholes and previous alignments of barbed wire fences, respectively, which were probably related to the military (training) activities in the area.

E.3.4.2 Drainage Depression

Drainage depressions are deep, bowl-shaped valleys separated by interfluves. The steepest, upper portions of the depression have slope gradients of most > 30°, where frequent instabilities due to headward erosion of drainages are evident. This terrain unit makes up about 18% of the catchment area. The upper limit of this unit is a well-defined convex break-in-slope below the Ridge/Spur unit. The unit is interpreted to be generally underlain by thin volcanic saprolite, with local intermittent outcrops (possibly of more resistant quartz-rich altered tuff). At the middle section of this unit, some parts of the terrain have gentler gradient (20 - 30°), and appears to show rough, hummocky surfaces, with highly irregular, wavy break-in-slopes. It is interpreted that landslide debris from recent landslides may have temporarily accumulated at this part of the depressions. Given the moderate gradient and influence of drainage incision, these colluvial deposits are susceptible to future failures or remobilization (entrainment).

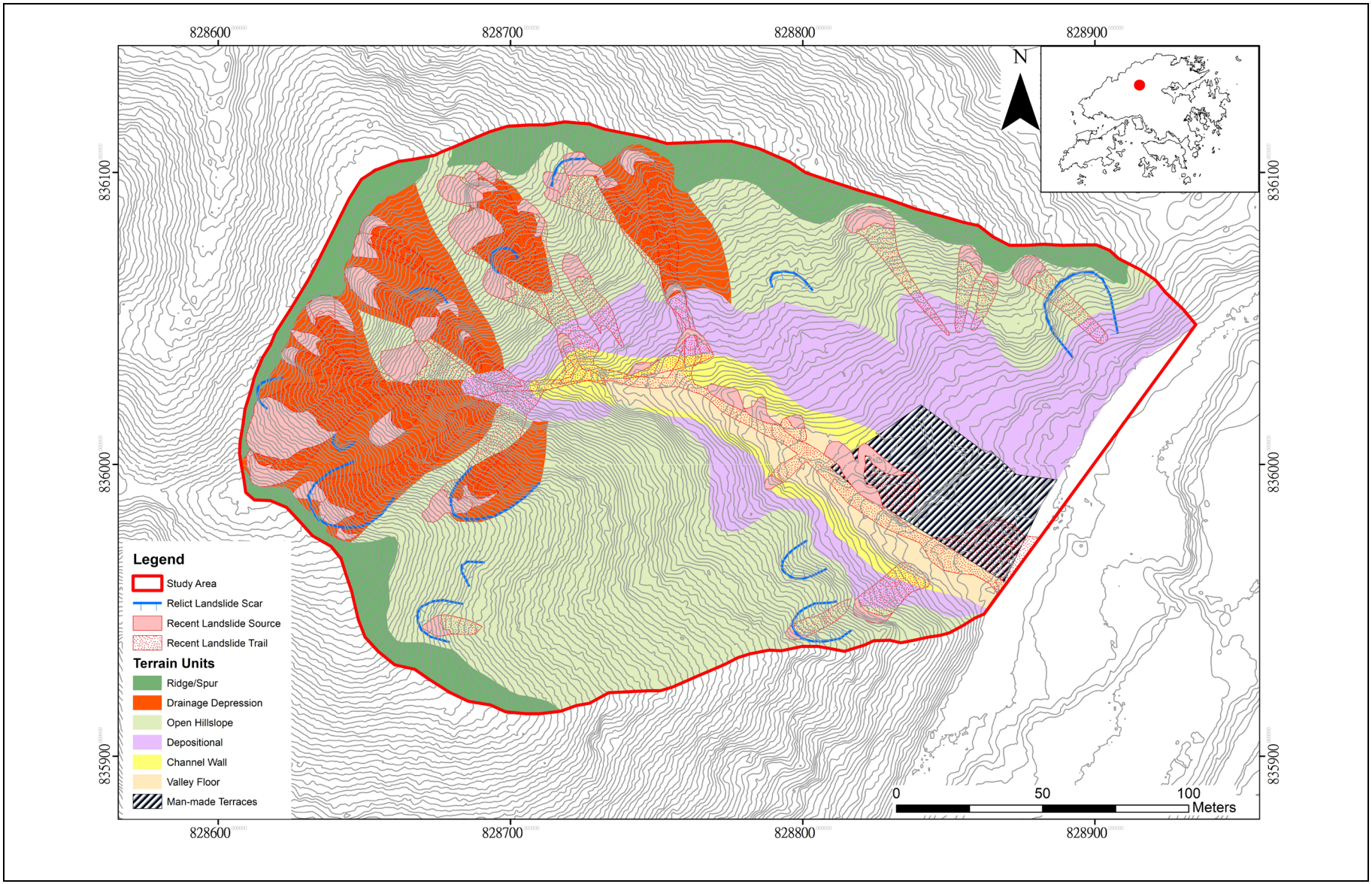

Figure E3.2 Terrain Unit Map of the Study Catchment (with Confirmed Relict and Recent Landslides)

E.3.4.3 Open Hillslope

The terrain unit includes those generally planar to slight divergent slopes along the side of the river valley. The slope gradient is generally 30 - 40°. The unit makes up about 41% of the catchment area. The major drainage flows across, and thereby undercut, the toe of the slope. The regolith is inferred to be mainly volcanic saprolite covered by thin colluvial deposits. The dominant geomorphological processes of this unit are soil development and mass wasting. The influence of river is minor, where initial incision of the drainage has just begun to widen into small, broad valley.

E.3.4.4 Depositional

This unit is located is gently inclined slope, with gradient generally < 25° at the lower part of the catchment and make up about 18% of the catchment area. The regolith is predominantly colluvial deposits, part of which might have been reworked and eroded by the incision of stream course. Based on API observations, a number of trenches and pits, inferred to be military fox-holes, were evident on the depositional slope to the northeastern side of the stream course. Although these features have subsequently covered by dense vegetation, they are still “visible” from the DEM generated from the airborne LiDAR data and give the unit a hummocky appearance.

E.3.4.5 Channel Wall

This unit comprises the steeply-inclined channel walls immediately adjacent to the river channels. This terrain unit is being actively undercut and eroded by fluvial actions. The regolith of this unit is either in-situ weathered rocks overlain by recent colluvium from the overlooking hillslopes and/or reworked colluvial (mapped as debris flow deposits). The gradient of channel walls is generally 30 - 45°, rendering the unit susceptible to landsliding and other mass wasting processes.

E.3.4.6 Valley Floor

This unit comprises the valley floor, with a gentle gradient of 0 - 15°. This unit covers about 4.5% of the catchment area, and is mantled by fluvial and reworked colluival deposits. Locally, in-situ weathered volcanic rocks are exposed on the valley floor, where the erosional process predominates especially at the confluence of tributaries. No landslide has been recorded in this terrain unit due to the gentle gradient.

E.3.4.7 Man-made Terraces

This unit, contributing to > 6% of the catchment area, comprises a series of man-made (cut and fill) terraces located at the lower reach of the drainage catchment. Based on observation of the 1963 aerial photographs, the area was originally part of the depositional slopes at the lower reach of the catchment before human disturbance. The formation of the terraces had significant modified the landform and might have caused a slight diversion of the

natural streamline. Field observations after the 2018 landslide events have confirmed the presence of several abandoned temporary structures (squatter huts) on these terraces.

E.4 Landslide Characteristics

E.4.1 Landslide Records

The ENTLI (updated to 2016) records 31 landslide features within the study catchment, including 14 relict and 17 recent landslides (Figure E1.1). Only one of the relict landslides was classified as Type A, nine were Type B and eight were Type C. For the recent landslides, eleven were classified as open hillside failures and the remaining ten reached the drainage line and were interpreted as channelized debris flows. Four of these landslides were also recorded as confirmed landslide incidents (no. MW89/5/98 and MW99/8/86A, 86B & 86C).

Site-specific API has been conducted under this review to verify the relict and recent landslides. The API confirmed that 13 relict landslides and 25 recent landslides (i.e. 8 addition recent landslides identified in this review) occurred up to year 2016. The natural terrain landslides occurred during the August 2018 rainstorm have also been mapped by LIC, and with the help of ortho-rectified photographs taken using an unmanned aerial vehicle (UAV) (Figure E3.2). A total of 26 failures occurred in 2018, some of which with source area occurred side-by-side with the adjacent failures or with debris trails spatially overlapped, such that the actual dimensions of these overlapping failures could only be estimated at best.

E.4.2 Overall Characteristics

The source and trials areas of the verified recent landslides and the scarp of the verified relict landslides were delineated (Figure E4.1). The distribution of the verified landslides were reviewed with respected to the 8-fold slope angle class (5-m grid) and summarized in Table E4.1 below. Over 80% of both relict and recent landslides were located on slope with a gradient greater than 30°. Only a few relict and recent landslides were found on gentler terrains of 15 - 30°. It is important to note that since the slope angle class of the terrain is derived from the DEM generated from the 2010 LiDAR data, the slope angle for those landslides occurred prior to year 2010 would represent the post-failure slope angle.

Table E4.1 Distribution of Landslides with respect to Slope Angle Class

Slope Angle Class (Degrees)	Relict Landslides		Recent Landslides	
	Number (%)	Number/km^2	Number(%)	Number/km^2
0-15	0	0	0	0
15-20	1 (8%)	261	3 (6%)	783
20-25	1 (8%)	160	1 (2%)	160
25-30	0	0	4 (8%)	381
30-35	2 (15%)	200	19 (37%)	1903
35-40	6 (46%)	757	14 (27%)	1767
40-45	3 (23%)	902	10 (20%)	3008
45-90	0	0	0	0

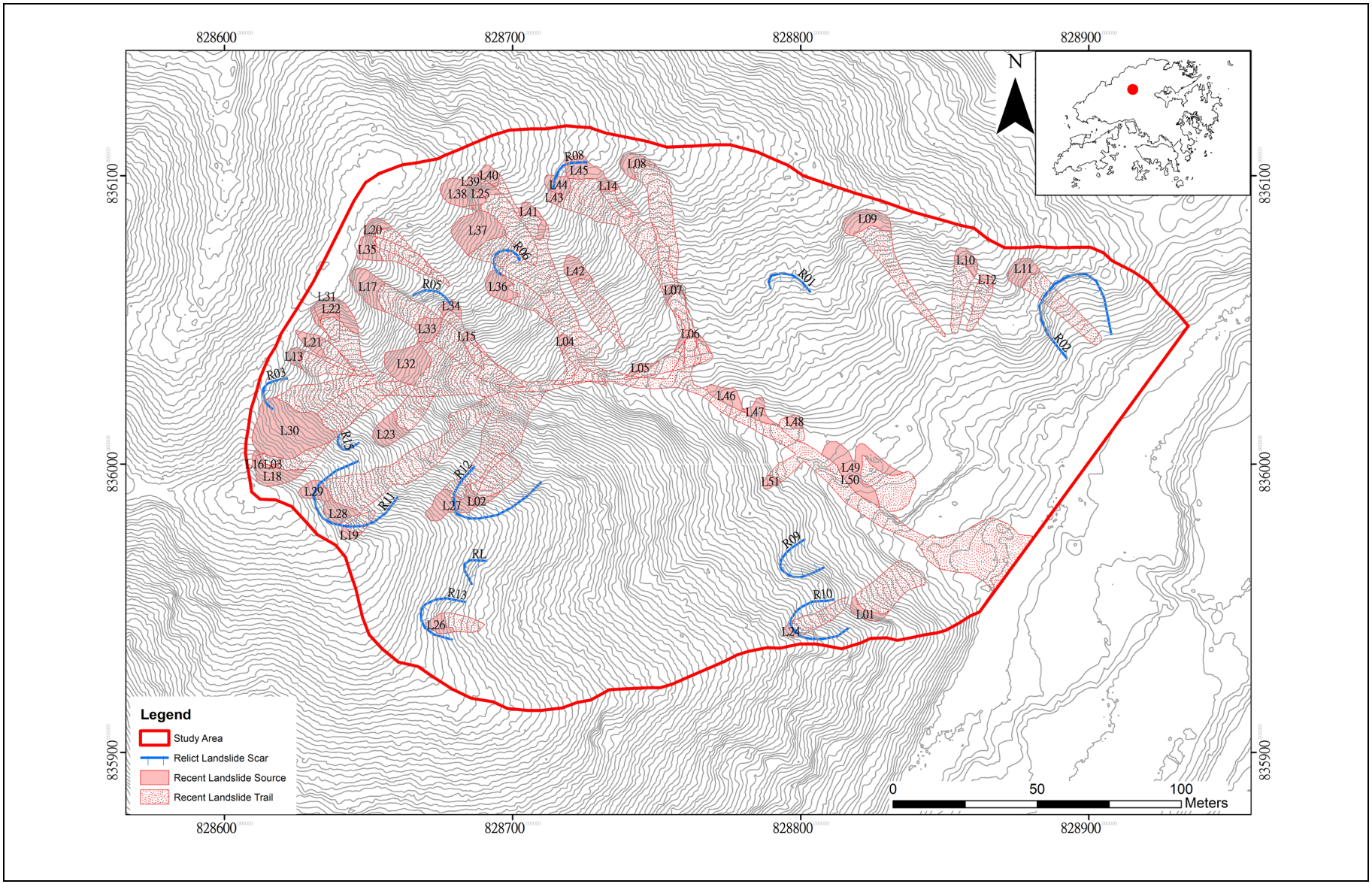

Figure E4.1 Location Plan of Verified Recent and Relict Landslides

The verified relict and recent landslides had a similar source width varying from a few metres to 22 m. The depth of the recent landslides were shallow, typically less than 1 m to up to 2 m. The source volume of the recent landslides ranges from several to ~230 m^3. Based on observations from the field reconnaissance, highly- to moderately decomposed rocks were usually exposed on the landslide scars. Thus, the failure surfaces were probably within the thin mantle of topsoil, colluvium and/or completely decomposed volcanic rocks, or at the interface of these strata. The recent landslides were probably initiated as debris avalanches from open hillslopes or topographic depressions, and 20 (out of 51) of which reached the drainage lines and became channelized.

E.4.3 Temporal Distribution

The temporal distribution of recent landslides in the study catchment is presented in Figure E4.2. The occurrence of landslides was distributed unevenly, as clusters, probably reflecting the time of intense rainstorms hitting the region. Over 50% (26 out of 51 numbers) of the recent landslides happened during / after the August 2018 rainstorm.

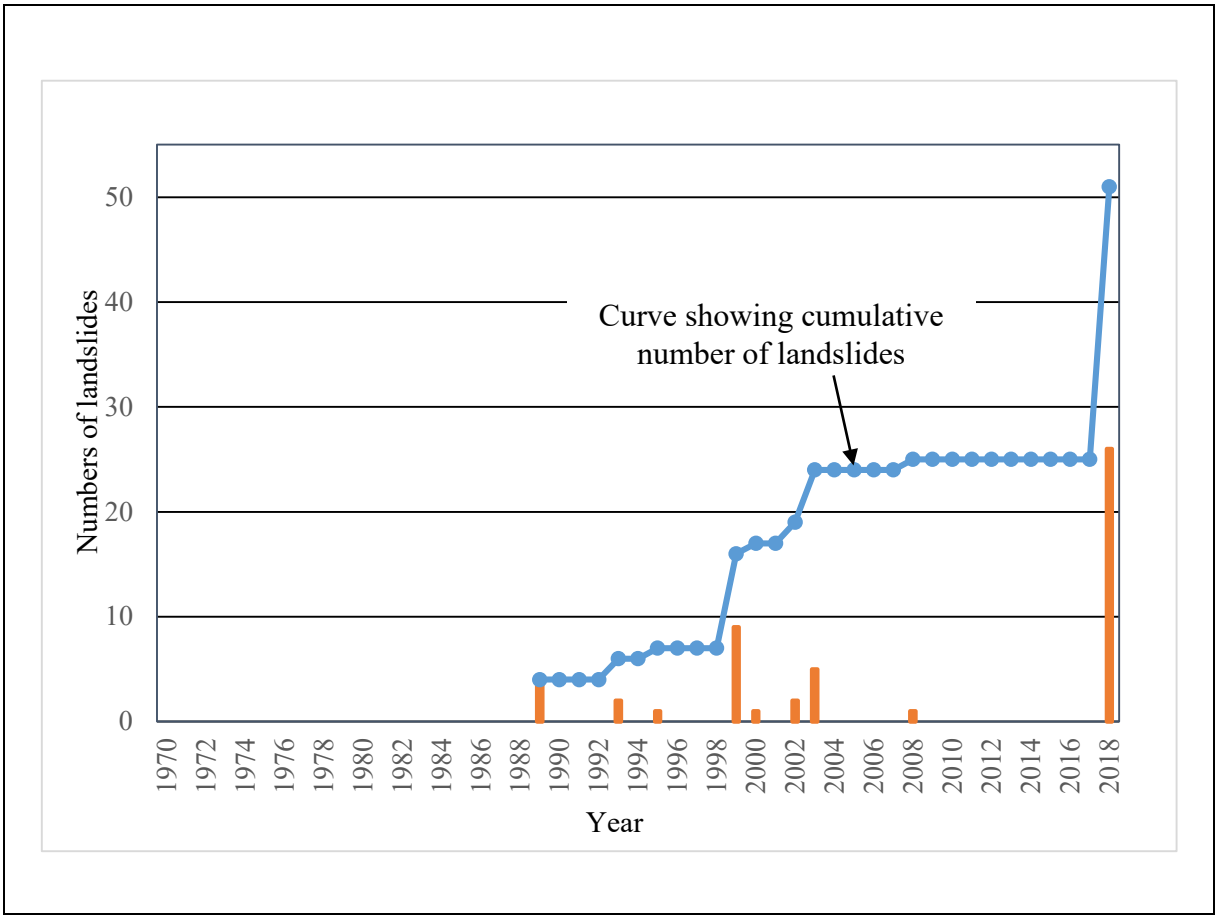

Figure E4.2 Numbers of Recent Landslides in Catchment FKR between years 1970 and 2018

E.4.4 Landslides Occurred During August 2018 Rainstorm

A total of 26 failures[1] occurred within the study catchment during the August 2018 rainstorm. Shortly after the event, Survey Division of CEDD was tasked to conduct UAV photography of in the vicinity of Fan Kam Road, for establishing a 3D terrain model for the landslide locations. In addition, the Landslip Investigation Consultants (LIC, AECOM) was tasked to investigation the natural terrain landslides of the study catchment and its surrounding natural hillsides.

Based on the mapping conducted by AECOM, the 2018 landslides were small-scale, shallow failures. Apart from one landslide (no. L30 in Figure E4.1) with an estimated source volume of > 200 m^3, the estimated source volumes of all other failures ranged between ~10 and 70 m^3. The depth of the source area of all landslides ranged from 0.6 - 0.8 m. The estimated total volume of landslide debris, including the entrained materials along the debris trials was 630 m^3 (AECOM, 2019). AECOM reported that the materials exposed within the main scarps of the landslide clusters were mainly gravelly, sandy silt colluvium with significant exposures of highly- to moderately-decomposed volcanic rocks at the source floor of some failures. Although quartz veins and jointing were observed at the source regions, these features were considered unlikely to have controlled the occurrence of landslides in the catchment.

E.4.5 Human Disturbance

It is evident from the 1963 aerial photographs that some military-related trenches and foxholes were present along the ridgeline, as well as scattered at the middle and lower portions of the study catchment. These features are probably abandoned now, but could potentially affect surface runoff and infiltration (c.f. AECOM, 2019). In addition, a series of man-made terraces were formed at the lower reach of the catchment, and had significantly modified the landform.

E.4.6 Spatial Distribution and Cluster Analysis

The spatial distribution of the 51 verified recent landslides have been reviewed to establish if they formed clusters with other older landslides based on the eight-fold classification system proposed by Tang et al (2018). Nine of the 51 recent landslides (17%) are considered not in a landslide cluster (Table E4.2). About 10% of the recent landslides are classified as Type 1 to 3, which were related to retrogressive failures or over-steepened slopes closed to previous landslide scars. Over 16% of the recent landslides occurred within topographic depressions (Type 4), and over 45% occurred in drainage depressions (Types 5 and 6). That is, over 60% of the recent landslides occurred within topographic depressions either with or without the influence of drainage processes. Another 12% of the failures occurred along over-steepened channel side slopes that are actively undercut by the stream.

---

[1] Some failures had overlapping source areas, such that the number of failures depends on how the overlapping sources were counted.

Table E4.2 Summary of Characteristics of Landslide (Recent) Cluster at the Study Area

Type of Landslide Cluster	No. of Recent Landslides	Range of Distance to the Closest Related Relict (Older) Landslides (m)
1	3 (6%)	5 - 10
2	1 (2%)	20
3	1 (2%)	15
4	8 (16%)	5 - 15
5	19 (37%)	2 - 55
6	4 (8%)	< 1 - 5
7	6 (12%)	N/A
8	0	N/A
Not in Clusters	9 (17%)	N/A

The distribution of both recent and relict landslides with respect to various terrain units (described in Section E.3.4) are analysed (Table E4.3). The 'Drainage Depression' unit, which only accounts for 18% of the catchment area, has over 50% of the total numbers of relict and recent landslides. The occurrence of landslide clusters appears to be most obvious in this terrain unit. The second highest number of relic and recent landslides combined is found in the 'Open Hillslope' unit, which has over one-third of total number of landsides.

Table E4.3 Distribution of Relict and Recent Landslides with Respect to Terrain Units

Terrain Unit	Percentage of Study Area	No. of Relict Landslides (13 nos.)	No. of Recent Landslides (51 nos.)	Total no. of Relict and Recent Landslides
Ridge/Spur	9%	0	0	0
Drainage Depression	18%	6 (46%)	27 (53%)	33 (52%)
Open Hillslope	41%	7 (54%)	16 (31%)	23 (36%)
Depositional	18%	0	2 (4%)	2 (3%)
Channel Wall	3%	0	6 (12%)	6 (9%)
Valley Floor	4%	0	0	0
Man-made Terraces	6%	0	0	0

E.5 Conclusions

The characteristics of the natural terrain landslides within catchment FKR was carried out, mainly based on a desk study, including a detailed site-specific API, with field reconnaissance carried out in after the occurrence of landslide clusters in August 2018. All the landslide features recorded in the ENTLI were verified and a regolith map and a terrain unit map were produced, in order to decipher the possible geological or geomorphological factors that may have played a role in the occurrence and distribution of the recent and relict landslides. The key observations are summarised below:

(a) The ENTLI features (updated to year 2016) and the landslides occurred in August 2018 were reviewed and verified. In total, there are 13 nos. of recent landslides and 51 nos. of relict landslides confirmed within the Study Area. Twenty-six recent landslides occurred during the rainstorm in August 2018. The type, dimension and estimated volume of the verified landslide were determined, mostly based on observations from the API and the field reconnaissance carried out after the August 2018 rainstorm. All the recent and most of the relict landslides were shallow failures (typically < 1 m to up to 2 m) and were of relatively small landslide volume (mostly 10 - 70 m^3; largest volume 230 m^3). The failure surfaces were probably within the thin mantle of topsoil, colluvium and/or completely decomposed volcanic rocks, or at the interface of these strata.

(b) The regolith covering the majority of the catchment is relatively thin volcanic saprolite, with local intermittent rock outcrops in the upper portion of the catchment. The middle and lower portion of the catchment are covered by recent landslide debris, whereas the reworked colluvial and fluvial deposits accumulated along the drainage course. According to the regolith type, slope gradient, morphological features and inferred slope processes, seven terrain units, including ‘Ridge/Spur’, ‘Drainage Depression’, ‘Open Hillslope’, ‘Depositional’, ‘Channel Wall’, ‘Valley Floor’ and ‘Man-made Terraces’, were classified.

(c) Over half of all landslides (relict and recent) occurred within the ‘Drainage Depression’ unit, which accounts for only 18% of the catchment plan area. The concentration of landslides within this terrain unit is likely to be related to active erosion along the drainage lines, presence of over-steepened slopes adjacent to heads of drainage, as well as concentrated runoff in the bowl-shaped drainage depressions. Another 36% of all landslides occurred within the ‘Open Hillslope’ unit, which takes up 41% of

catchment plan area and includes generally steep terrain (30 - 40°).

(d) Based on the review of the recent landslides using the eight-fold classification system, about 57% the recent landslides were classified as cluster Types 5, 6 and 7, therefore related to headward erosion at the head of drainage lines or to undercutting processes along the drainage lines. About 26% of the recent landslides were related to retrogressive failures or over-steepened slopes at previous failure scars (Types 1 and 4).

E.6 References

AECOM Asia Company Limited (AECOM) (2019). *Detailed Study of the 29 August 2018 Landslides on the Natural Hillside above Fan Kam Road, Pat Heung (Landslide Study Report No. LSR 2/2019).* Geotechnical Engineering Office, 84 p.

Geotechnical Control Office (GCO) (1988). *Yuen Long.* Hong Kong Geological Survey Sheet 6, Solid and Superficial Geology, 1:20,000 Series HGM20. Geotechnical Control Office, Hong Kong.

Geotechnical Control Office (GCO) (1989). *San Tin.* Hong Kong Geological Survey Sheet 2, Solid and Superficial Geology, 1:20,000 Series HGM20. Geotechnical Control Office, Hong Kong.

Langford, R.L., Lai, K.W., Arthurton, R.S. & Shaw, R. (1989). *Geology of the Western New Territories. Hong Kong Geological Survey Memoir No. 3.* Geotechnical Engineering Office, Hong Kong, 140 p.

Tang, D.L.K., Wong, C.C.J., Sin, Y.M. & Mok, S.C. (2018). *Study of Geological Controls on the Occurrence of Natural Terrain Landslide Clusters - A Pilot Study at a Catchment above Keung Shan Road, West Lantau (Geological Report No. GR 1/2018).* Geotechnical Engineering Office, Hong Kong, 45 p.

Appendix F

Supplementary Information on Landslide Verification for Catchment 58 - Keung Shan Road

(Prepared by A.H.Y. Wong)

Contents

List of Tables

List of Figures

F.1 Introduction

The Planning Division has been investigating a number of natural terrain catchments with notable landslide clusters in order to review whether there is any physical geological and geomorphological factors that may potentially control the occurrence of these landslide clusters. The background and methodology adopted on catchment selection for review, together with the findings of a pilot review at a selected catchment above Keung Shan Road, West Lantau are documented in Tang et al (2018).

In the pilot study, the geological and geomorphological settings of the catchment above Keung Shan Road (the Study Area) have been reviewed with respect to the distribution of relict and recent landslides recorded in the ENTLI database. Site-specific aerial photograph interpretation (API) to examine the past instability in the Study Area had not been carried out. Further work on verification of the ENTLI data in the Study Area was therefore considered necessary.

This report supplements the information presented in Tang et al (2018), and includes a review of the characteristics of landslides within the Study Area based on a desk study including a detailed site-specific API and the June 2008 landslides mapped by Lee et al (2010). Based on the review findings, the geological and geomorphological model of the Study Area, and spatial cluster analysis using the verified the ENTLI data, have been updated.

F.2 Location and Catchment Characteristics

The Study Area is an elongated, generally ESE-WNW-oriented V-shaped side valley located immediate to the north of Kwun Yam Temple, Keung Shan, Lantau (Figure F2.1). The Study Area covers plan area of about 0.125 km^2, with an elevation difference of about 320 m from +413 mPD at its highest point to +90 mPD to its lowest point. The aspect ratio of the catchment (i.e. width of long axis to width of short axis) is about 3 to 1. The catchment is transacted by Keung Shan Road at about 123 mPD. A Historical Landslide Catchment (HLC), HLC No. 13NW-B/DF 13 is located within the Study Area.

After the June 2008 landslide events, a check dam (Feature No. 13NW-B/ND3) was constructed across the drainage line at the uphill side of Keung Shan Road, to retain future landslide debris.

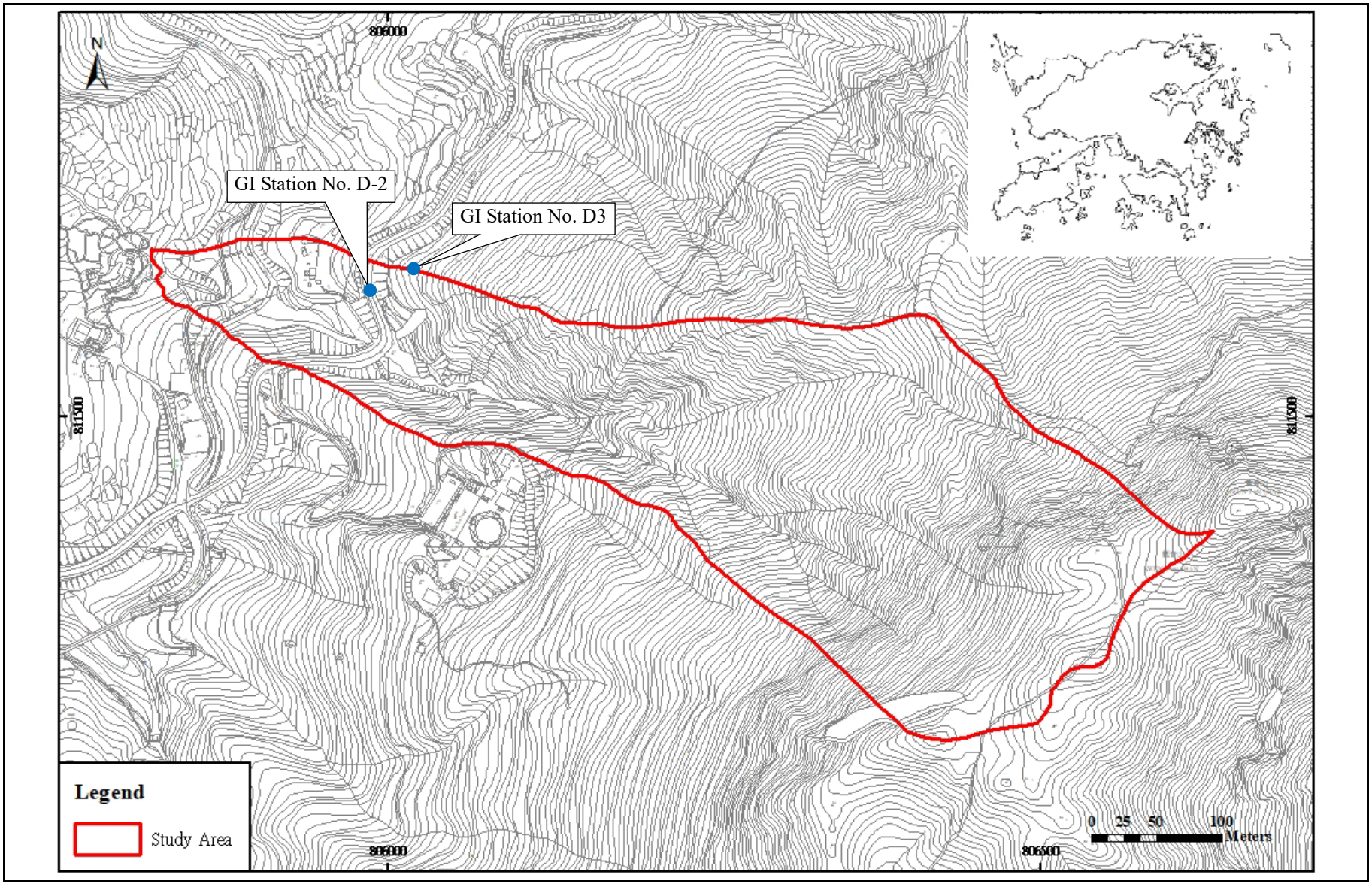

Figure F2.1 The Study Area above Keung Shan Road, West Lantau

F.3 Geology

According to the published 1:20,000-scale geological maps (GEO, 1995), the catchment is underlain largely by rhyolite lava and crystal tuff of the undifferentiated Lantau Volcanic Group, with some subordinate tuffaceous siltstone, tuffite and tuff layers (i.e. the Pak Kok Member; Langford et al, 1995) at the upper part of the catchment (Figure F3.1). Langford et al (1995) reported that the sequences dip variably and form prominent topographic features near Kwun Yam Shan. On the published geological map, the rock layers were mapped to be dipping at 40° out of the hillside near the study catchment, and the rocks in the upper half of the catchment were affected by metamorphism (GEO, 1995). A SE-trending inferred fault, appear to have controlled the main drainage line orientation. However, according to the 1:5,000-scale mapping report by So (2010), there was no field evidence of any faulting or shearing along the drainage valley. Debris flow deposits (Qd) were mapped in the middle part of the catchment (GEO, 1995).

Existing ground investigation information is only available near the toe of the Study Area. The GI data comprised two drillholes (No. D-2 and D3; Figure F2.1) that carried out in 1985 and 1986. The result of GI indicates that the ground profile at the end of the northern spur is underlain by a thick layer (up to 18 m) of completely decomposed tuff.

F.4 Geomorphology

The Study Area lies on a NW-facing hillside below a NE-SW trending ridge of Kwun Yam Shan. The boundary of the Study Area is defined by two ESE-WNW trending spurs in the NE and SW respectively. The crest of the Study Area comprises relatively gently inclined rounded ridge (< 15°) and a moderately steeply inclined concave hillslope (30 - 45°) at the central portion. Immediately below the ridge and the concave hillslope, the hillside comprises steeply inclined upper slopes (> 45°) with widespread of rock faces.

The hillside then becomes less steeply inclined (25 - 35°), relatively open valley side slopes in the upper portion of the mid-slope, except where the hillslopes are incised by the drainage lines. At the lower portion of the mid-slope, the hillslopes are characterized by deeply-incised valley side slopes, which are commonly steepest (> 40° in gradient) near the well-defined drainage line. This portion of the catchment is rather narrow, with a width of about 120 - 150 m. The valley side slopes in this portion consist of a serious of topographic depressions, interpreted to be associated with recent and relict landslides (see Section F.5). Near the toe of the Study Area, the hillside comprises less steeply inclined colluvial footslopes.

The drainage system, which runs in a southeast to northwest direction, is well defined and characterised by shallowly-incised ephemeral streams at the head of drainage, becoming to a deeply-incised, stepped stream course at the lower reaches.

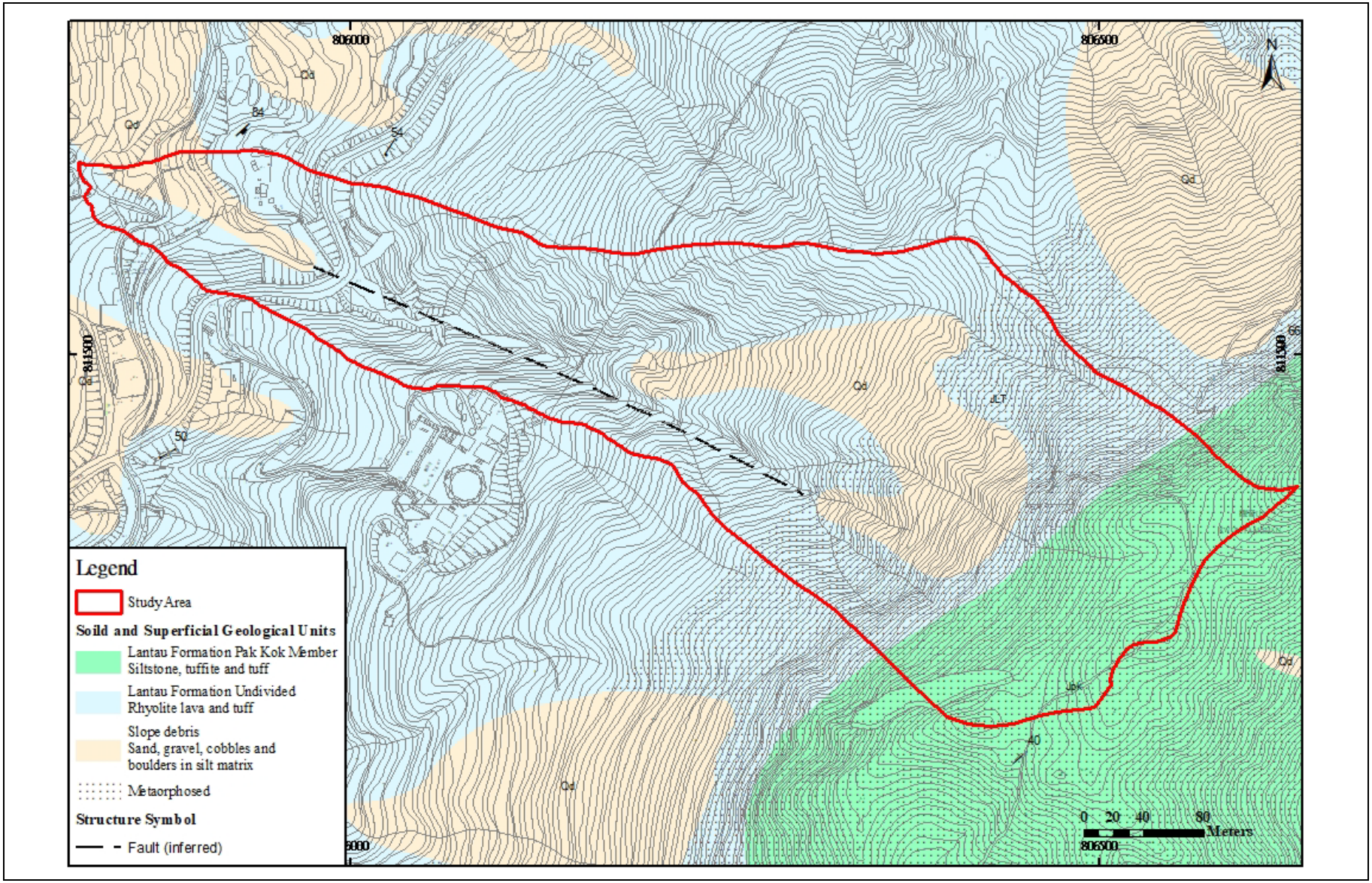

Figure F3.1 Geology of the Study Area

F.5 Site-specific Landslide Inventory

According to the ENTLI (up to 2016), a total of 122 landslide features were recorded within the Study Area, including 72 relict landslides and 50 recent landslides. Of the 72 relict landslides, 50 (69.4%) of which are classified as Class A relict, 21 (29.2%) as Class B relict and one (1.4%) as Class C relict. For the recent landslides, 24 (48%) of those are open hillside failures (OHL) and 26 (52%) are channelised debris flows (CDF).

Past instabilities of the Study Area have been reviewed based on the available aerial photographs taken between 1963 and 2018. A total of 49 recent landslides were confirmed. The landsides occurred in pulse and were concentrated temporally in 1982, 1993 and 2008, corresponding to the occurrence of intense rainstorms in these years. Of those recent landslides, are classified as 17 (35%) OHL and 32 (65%) are CDF. The number of relict landslides reduced from 72 to 54.

The source and trail area of the confirmed recent landslides and the scarp of the confirmed relict landslides were delineated (Figure F5.1). A slope angle map (5-m grid) (Figure F5.2) was prepared for the Study Area and reviewed together with the distribution of the verified landslides. Table F5.1 shows the distribution of landslides for the eight slope angle classes defined. No landslide is observed on slope with gradient less than 15°. Over 88% of the landslides are located on slope with a gradient greater than 30°, with the highest percentage for the slope angle class 30 - 35°. Both the recent and relict show a similar trend and pattern in respect of slope angle distribution.

Table F5.1 Slope Angle of Recent and Relict Landslides

Slope Angle (Degree)		Recent Landslides (49 nos.)	Relict Landslides (54 nos.)	All Landslides (103 nos.)
Class 1	0 - 15	0 (0%)	0 (0%)	0 (0%)
Class 2	15 - 20	2 (4%)	0 (0%)	2 (2%)
Class 3	20 - 25	1 (2%)	0 (0%)	1 (1%)
Class 4	25 - 30	6 (12%)	4 (7%)	10 (10%)
Class 5	30 - 35	18 (37%)	22 (41%)	40 (39%)
Class 6	35 - 40	7 (14%)	11 (20%)	18 (17%)
Class 7	40 - 45	9 (18%)	8 (15%)	17 (17%)
Class 8	45 - 90	6 (12%)	9 (17%)	15 (15%)

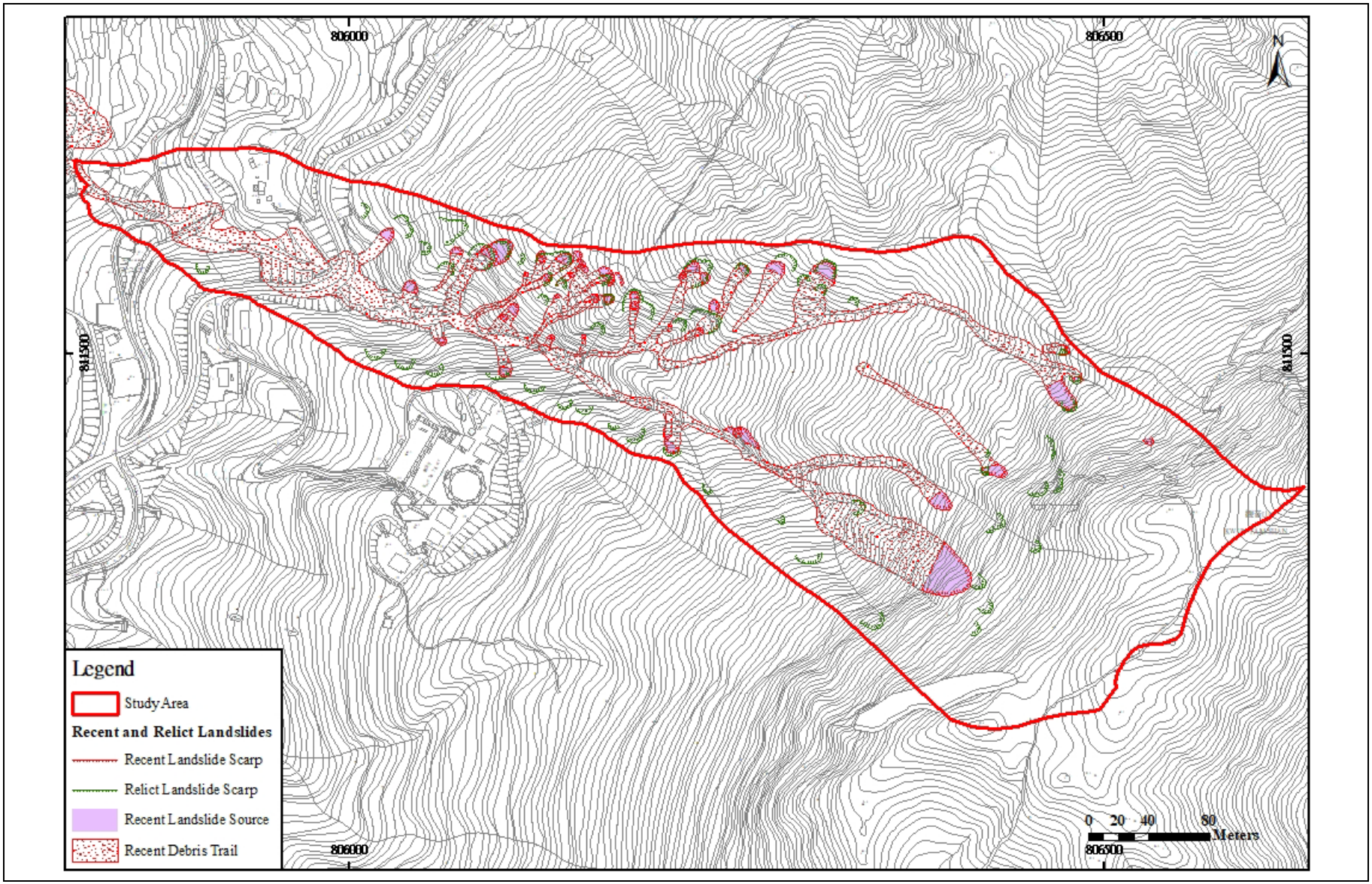

Figure F5.1 Verified Recent and Relict Landslides within the Study Area

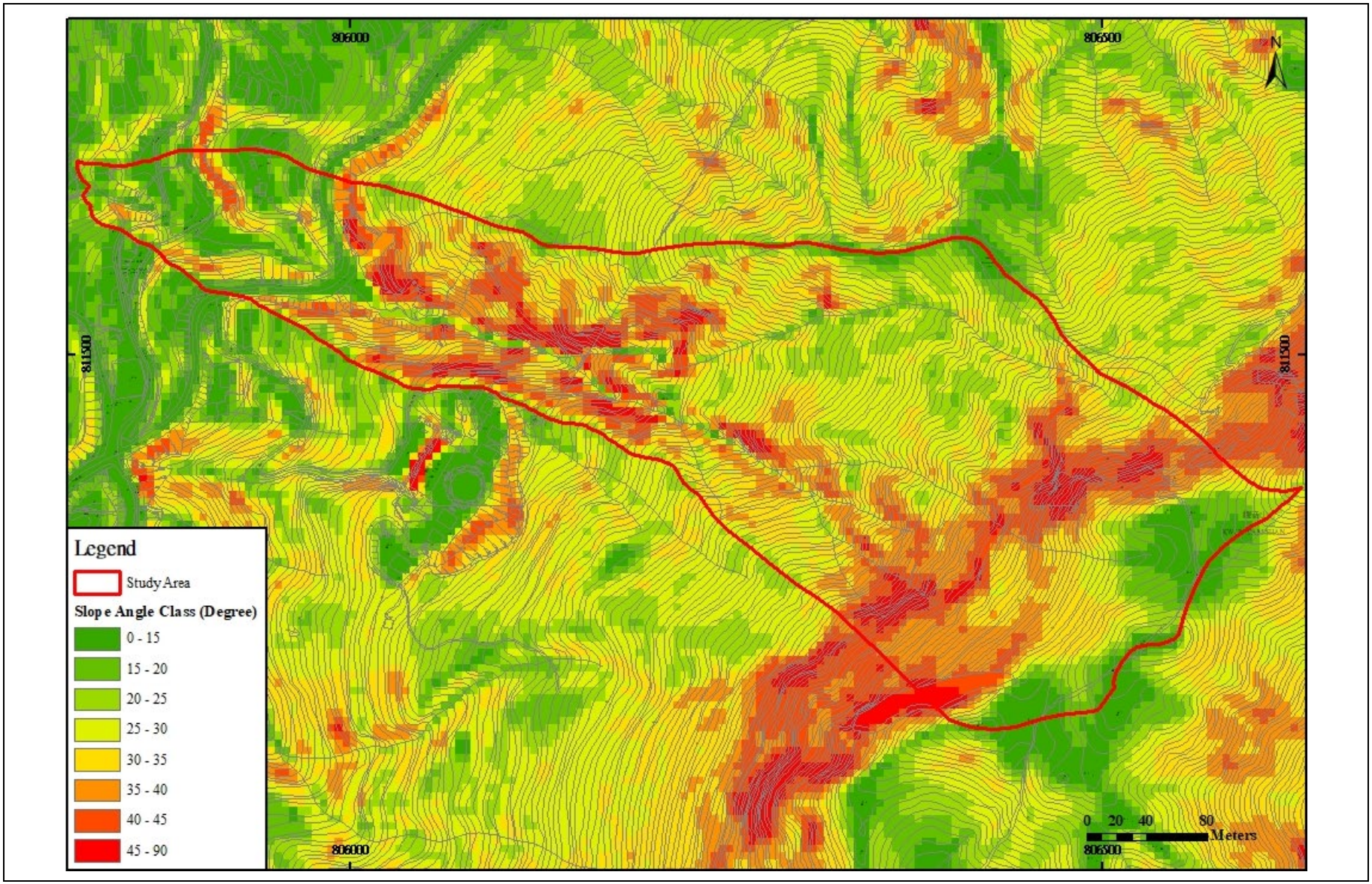

Figure F5.2 Slope Angle Map of the Study Area

The verified recent landslides have a source width varying from a few metres to 33 m while the relict landslides have a larger source width ranging from several metres to 22 m. The depth of the recent landslides is shallow (typically 0.5 - 1.5 m, locally up to 2 m) in general. About 94% of the landsides with estimated landslide volumes less than 150 m^3 (of which about 76% of them are less than 50 m^3), with two recent features up to around 350 m^3 and the largest one approximately 730 m^3.

The source depth of most of the relict landslides is shallow as well, typically 1 – 2 m. About 85% and 96% of the landslides with estimated landslide volumes less than 100 m^3 and 250 m^3 respectively. The two largest relict features have an estimated landslide volumes up to 360 m^3 and 390 m^3 respectively.

The largest landslide with the Study Area was occurred in 2008, with a source volume of about 730 m^3. The failed material was composed mainly of detached rock blocks, and minor portion of colluvium of sand, gravels and cobbles. It was reported that the surface of rupture was along adversely oriented, daylighting sheeting joints in bedrock (Lee et al, 2010). Although the mapping report did not contain detailed descriptions on any variation in lithology at the source area, it is noteworthy that the landslide initiated close to the contact between tuffaceous layers and the underlying metamorphosed volcanic rocks (Figure F3.1), which might also have influenced the occurrence of failure.

F.6 Regolith

In the site-specific aerial photograph interpretation (API), nine types of regolith were identified and their distribution was mapped for the Study Area (Figure F6.1). Table F6.1 shows the area and number of landslide for each type of regolith mapped. Majority of the Study Area is underlain by volcanic saprolite and volcanic saprolite with intermittent rock outcrop, which account for a total of 63% of the Study Area. The volcanic and sedimentary rock outcrops account for about 14% of the plan area of the Study Area. The sedimentary saprolite at the upper slopes covers about 11% of the Study Area. Taluvium was mapped below rock cliffs and encounters about 5% of the Study Area. The remaining areas are mapped as rocky channel bed filled with valley colluvium along the middle and lower portion of the drainage lines and colluvium footslope near the toe of the Study Area.

More than 85% of the landslides are located on slopes of volcanic saprolite and volcanic saprolite with intermittent rock outcrop. The rest of the landslides mainly occur in intermittent volcanic rock outcrop with a minimal portion occurring in sedimentary rock outcrop and taluvium.

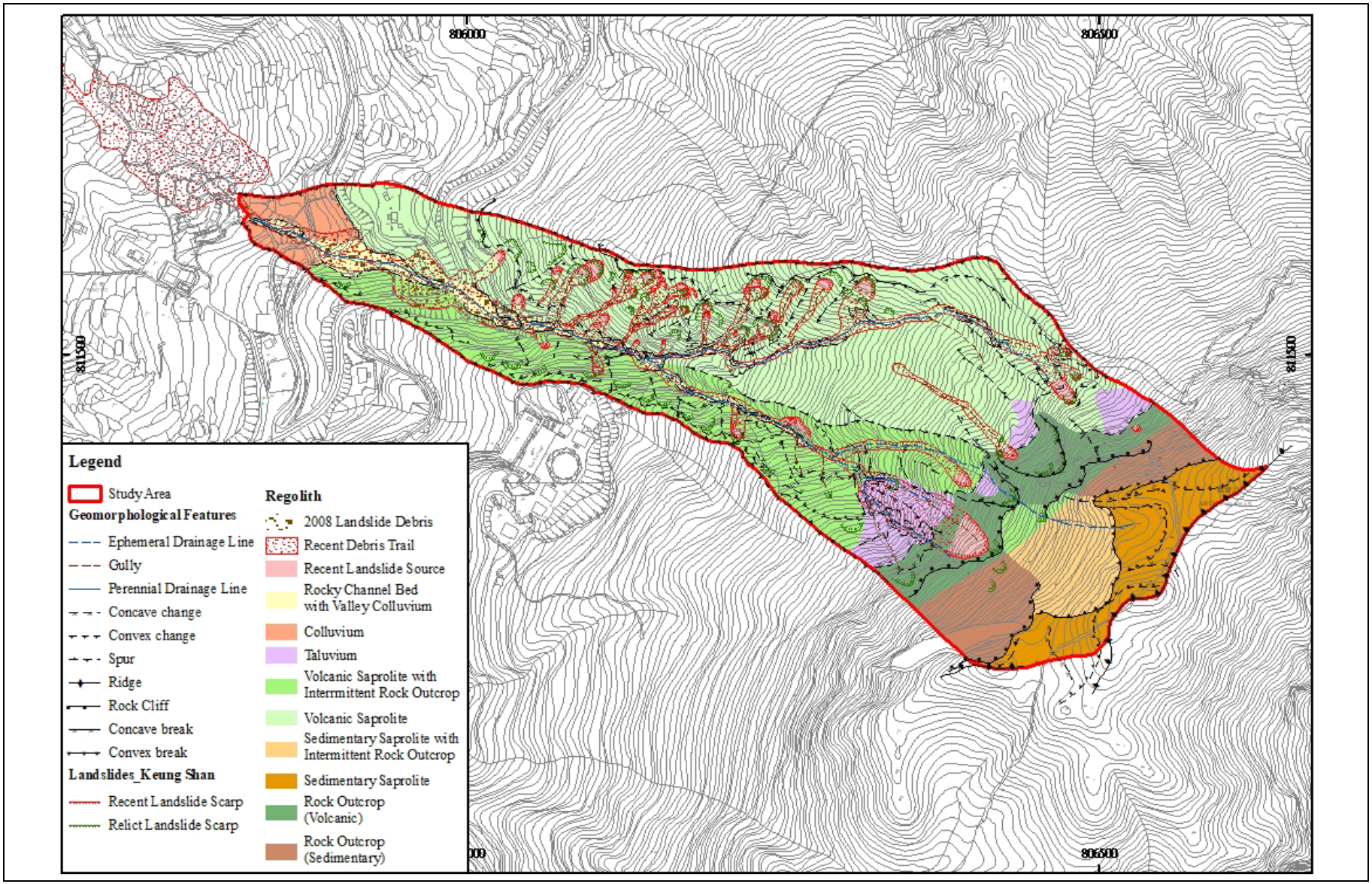

Figure F6.1 Regolith Map of the Study Area

Table F6.1 Regolith of Recent and Relict Landslides

Regolith Type	Area in Respect of the Entire Study Area (%)	Recent Landslides (49 nos.)	Relict Landslides (54 nos.)	All Landslides (103 nos.)
Rock Outcrop (Sedimentary)	6	0 (0%)	2 (4%)	2 (2%)
Rock Outcrop (Volcanic)	8	3 (6%)	7 (13%)	10 (10%)
Sedimentary Saprolite	7	0 (0%)	0 (0%)	0 (0%)
Sedimentary Saprolite with Intermittent Rock Outcrop	4	0 (0%)	0 (0%)	0 (0%)
Volcanic Saprolite	43	39 (80%)	29 (54%)	68 (66%)
Volcanic Saprolite with Intermittent Rock Outcrop	20	7 (14%)	15 (28%)	22 (21%)
Taluvium	5	0 (0%)	1 (2%)	1 (1%)
Colluvium	3	0 (0%)	0 (0%)	0 (0%)
Rocky Channel Bed with Valley Colluvium	4	0 (0%)	0 (0%)	0 (0%)

F.7 Terrain Unit

The Study Area was divided into seven terrain units based on geology, geomorphology, geomorphological process, regolith, etc., mainly based on site specific API (Figure F7.1). The distribution and characteristics of each terrain unit are described below.

F.7.1 Ridge Unit (TU1a)

Ridge Unit (TU1a) consists of saprolite terrain with smooth convex topography located along the ridgeline at the crest of the Study Area respectively. The gradient of ridge is generally less than 25°. The lower boundary of TU1a is generally marked by a distinct, sharp convex break-in-slope. No clear evidence of any landslide activity was noted within TU1a (Table F6.1) and soil development (i.e. weathering) was considered as the main process in TU1a.

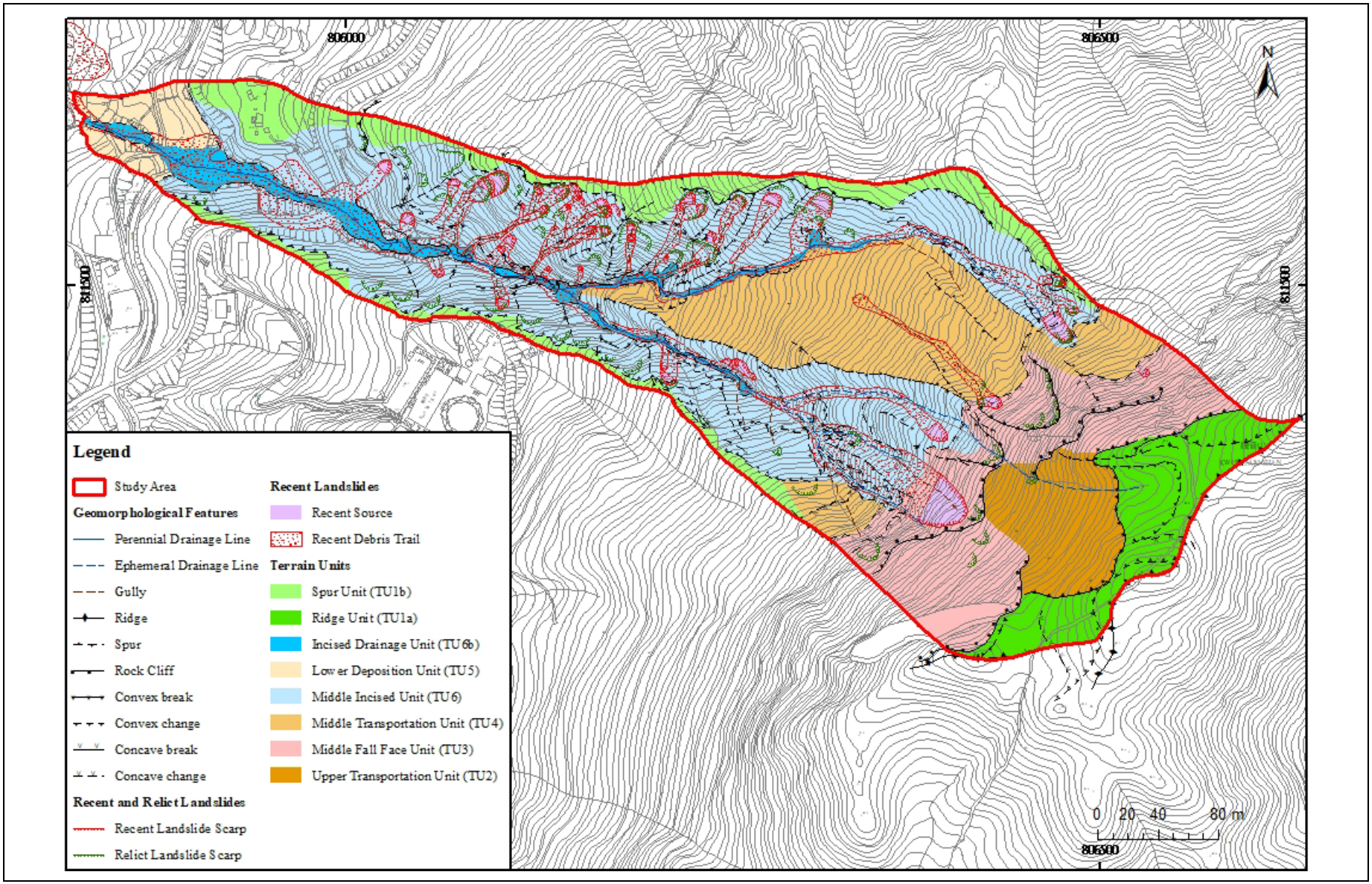

Figure F7.1 Terrain Unit Map of the Study Area

F.7.2 Spur Unit (TU1b)

Spur Unit (TU1b) consists of saprolite terrain with smooth convex topography located along the two spurs at the north and south of the Study Area respectively. The gradient of the two spurs are inclined at 20 - 35° respectively. The lower boundary of TU1b is generally marked by a distinct, sharp convex break-in-slope. No clear evidence of any landslide activity was noted within TU1b (Table F6.1) and soil development (i.e. weathering) was considered as the main process in TU1b.

F.7.3 Upper Transportation Unit (TU2)

Upper Transportation Unit (TU2) is characterised by a smooth concave topography located at the central portion of the upper slope, below a rounded convex break of the ridgeline. It comprises an ephemeral drainage line to the north and exhumed corestones were commonplace. The general gradient of TU2 is about 30 - 40°. The regolith interpreted for TU2 mainly includes sedimentary saprolite, with some volcanic saprolite at the lower portion. TU2 is considered as a valley head of an older landform. One relict landslide occurred in the lower portion of TU2 (Figure F6.1 and Table F6.1) and the main process within TU2 is slope degradation.

F.7.4 Middle Fall Face Unit (TU3)

The middle fall face unit (TU3) present in the upper portion of the mid-slopes of the Study Area. TU3 mainly comprises rock cliffs with very steep gradients (generally > 45°, locally up to 60°). The morphology varies from hummocky and irregular slopes to concave depressions. TU3 accounts for about 14% of the plan area of the Study Area and 12% of the landslides are located within this unit (Table F6.1). The relatively high percentage of landslide occurrence within this unit is considered related to the steep slope gradient and localised adverse orientation of geological structures. Also, the geomorphological setting with head of drainage lines just below this unit may also contributed in destabilising the toe of this unit and causing landslides.

F.7.5 Middle Transportation Unit (TU4)

The middle transportation unit (TU4) present in the upper mid-slopes of the Study Area and immediately below TU3 and the upper boundary is defined by a sharp concave break-in slope. This unit comprises moderately steep (predominantly 25 - 30° but locally up to 35°) open hillslope and is generally underlain by relative thin saprolite with considerable amount of exhumed rock outcrops or corestones. Taluvium is commonly present immediately below the rock crops. About 2% of the landslides occurred within this unit (Table F6.1). Slope degradation and transportation of mass wasting debris from upslope are the dominant process in this terrain unit.

F.7.6 Lower Deposition Unit (TU5)

The lower deposition unit (TU5) bounded by concave break-in-slope occupies the gentler foot slopes (< 20° in general) of the Study Area. It is interpreted to be underlain by

colluvial deposits. This terrain unit has been modified by man-made features and anthropogenic activities. No landslide is recorded within this unit (Table F6.1).

F.7.7 Middle Incised Unit (TU6a)

The middle incised unit (TU6a) occupies the largest plan area of the Study Area (approximately 40%). It is mainly delineated along the flanks of incised valley side slopes below the convex break of the spurs, with incising valley heads and valley side slopes below TU3 and TU4. The upper mid-slope of this unit comprises relatively open, moderately steep valley heads and side slopes (predominantly 30 - 35°) whereas the lower mid-slope is characterised by over-steepened side slopes that are associated with clusters of relict and recent landslide scars. PI observations, supported by detailed field mapping of the June 2008 landslides, suggest that this terrain unit is generally underlined by a thin layer of volcanic saprolite (less than 2 m) with colluvium drapes and recent landslide debris within concave breaks in slope and local depressions. About 85% of the landslides occurred within this unit (Table F6.1). Active erosion due to fluvial undercutting of steep saprolite slope at gully head and drainage side-slopes, periodic landslide and landslide reactivation are considered to be the main processes within TU6a.

F.7.8 Incised Drainage Channel Unit (TU6b)

The incised drainage channel unit (TU6b) includes the main incised drainage lines in the middle to lower slopes of the Study Area. It is delineated by concave breaks-in-slopes along the edges of valley floor. The drainage channels in this unit generally comprise V-shaped stepped rocky channel beds ranging from 3 - 15 m wide and bounded by steep side slopes. Channel gradients are of 20 - 25° at the upper mid-slope and become less inclined (< 20° in general) along the lower mid-slope. Detailed field mapping of the June 2008 landslides indicates that valley colluvium, recent landslide debris and alluvial deposits are mainly present within the confined drainage line at the lower mid-slope. No landslide is recorded within this unit (Table F6.1). Active processes with this unit include alluvial reworking of fines from previous landslides and fluvial undercutting.

Table F7.1 Terrain Units for Recent and Relict Landslides

Terrain Unit	Area in Respect of the Entire Study Area (%)	Recent Landslides (49 nos.)	Relict Landslides (54 nos.)	All Landslides (103 nos.)
Ridge Unit	8	0 (0%)	0 (0%)	0 (0%)
Spur Unit	9	0 (0%)	0 (0%)	0 (0%)
Upper Transportation Unit	5	0 (0%)	1 (2%)	1 (1%)
Middle Fall Face Unit	14	3 (6%)	9 (17%)	12 (12%)
Middle Transportation Unit	17	0 (0%)	2 (4%)	2 (2%)
Lower Deposition Unit	3	0 (0%)	0 (0%)	0 (0%)
Middle Incised Unit	40	46 (94%)	42 (78%)	88 (85%)
Incised Drainage Channel Unit	4	0 (0%)	0 (0%)	0 (0%)

F.8 Landslide Cluster

The 49 recent landslides were examined in a view to establish if the recent landslides are in cluster with other older landslides based on the eight-fold classification system proposed by Tang et al (2018). The result is presented in Table F8.1.

Table F8.1 Summary of Characteristics of Landslide (Recent) Cluster at the Study Area

Type of Landslide Cluster	No. of Recent Landslides	Range of Distance to the Closest Related Relict (Older) Landslides (m)
1	13 (27%)	0.5 - 6.5
2	10 (20%)	1 - 12
3	3 (6%)	0.5
4	9 (18%)	0.5 - 8
5	1 (2%)	0.5
6	0 (0%)	-
7	5 (10%)	N/A
8	2 (4%)	6 - 7.5
Not in Clusters	6 (12%)	N/A

The study has found that 72% of recent landslides in the Study Area were Types 1 to 4 clusters which were related to retrogressive failures, destabilised past landslide debris, over-steepened slopes at previous failure scars and/or topographic depressions. Thus, these Types 1 to 4 landslide clusters are considered more likely to be affected by adverse geomorphological settings, than to any underlying geological factors. For these 4 types of landslide clusters, the ranges of distance (crown to crown plan distance) to the closest related relict landslides are up to 12 m (Table F8.1).

In addition, 12% recent landslides were related to headward erosion at the head of drainage lines or to undercutting processes along drainage lines (i.e. Types 5 to 7 clusters). The distribution of these landslide clusters are thus considered to be related to the drainage pattern of the catchment, which in-turn might be indirectly related to the underlying geological structures (e.g. fault).

Of the 49 recent landslides, only two, of which the largest recent landslide (ENTLI no. 13NWB02728E) was one of these, are classified as Type 8 clusters. Based on the detailed landslide mapping report, the two failures were mainly controlled by the presence of adversely-oriented joints.

F.9 Conclusions

A review of the landslides within the natural terrain catchment above Keung Shan Road in west Lantau Island was carried out based on detailed site-specific API and the June 2008 landslides mapped by Lee et al (2010). All the landslides recorded in the ENTLI were verified and the potential geological and geomorphological factors that may contribute to concentration of landslide activities were examined. The geological and geomorphological settings of the Study Area have been refined with respect to the distribution of relict and recent landslides. The key observations are summarised below:

(a) The ENTLI features were verified and there are 49 nos. of recent landslides and 54 nos. of relict landslides confirmed within the Study Area. All the recent and relict landslides are shallow failures (< 2 m). About 94% of the recent landsides with estimated landslide volumes less than 150 m^3 (of which about 76% of them are less than 50 m^3), with two recent features up to around 350 m^3 and the largest one approximately 730 m^3.

(b) A regolith map for the Study Area was produced using API, supported by the detailed field mapping of the June 2008 landslides. The map reveals that majority of the Study Area (about 40%) is underlain by volcanic saprolite and volcanic saprolite with intermittent rock outcrop in which more than 85% of the landslides are located. The rest of the landslides mainly occur in intermittent volcanic rock outcrop, with a minimal portion occurring in sedimentary rock outcrop and taluvium.

(c) The delineation of terrain units indicated that the landslides were concentrated in the "Middle Incised" units. About 78% relict and 94% recent landslides occurred in this unit.

(d) Twenty-six landslides occurred in the Study Area in year 2008. These landslides are considered as representative, in terms of their size, source volumes and characteristics, of the recent landslides in this catchment. The largest recent landslide (ENTLI No. 13NWB2728E with volume of about 760 m^3 recorded in year 2008) occurred on the "Middle Fall Face" unit was controlled by adversely-oriented sheeting joints (Lee et al, 2010). The other smaller recent landslides occurred in 2008 were generally shallow failures at the boundary between thin colluvium/topsoil/completely decomposed volcanics and the underlying less weathered bedrock.

(e) Based on the review of the recent landslides using the eight-fold classification system, about 72% of the recent landslides were related to retrogressive failures, failure of

previous landslide debris, or over-steepened slopes or topographic depressions (Types 1 and 4). The distance between the recent landslide and the related relict landslide is in a range of 0.5 - 22 m. About 22% recent landslides were related to erosion/undercutting along drainage lines (i.e. Types 5 to 7). Only two recent landslides which may have been genuinely controlled by geological factors (i.e. Type 8), such as adversely oriented joints.

F.10 References

Geotechnical Engineering Office (GEO) (1995). *Shek Pik.* Hong Kong Geological Survey Sheet 13, Solid and Superficial Geology, 1:20,000 Series HGM20. Geotechnical Engineering Office, Hong Kong.

Langford, R.L., James, J.W.C., Shaw, R., Campbell, S.D.G, Kirk, P.A. & Sewell, R.J. (1995). *Geology of Lantau District. Hong Kong Geological Survey Memoir No. 6*. Geotechnical Engineering Office, Hong Kong, 173 p.

Lee, C.W., Ho, S.Y. & Shek, W.C. (2010). *2008 Landslide Field Mapping Records - Landslide Mapping Report at Kwun Yum Temple (Landslide No.LS08-0228).* Geotechnical Engineering Office, Hong Kong, 214 p.

So, W.F. (2010). *Geology of Shek Pik Area (Geological Report No. GR 11/2010)*. Geotechnical Engineering Office, Hong Kong, 122 p.

Appendix G

Multi-Distance Spatial Cluster Analysis of 80 Catchments and Fan Kam Road Catchment

Contents

List of Tables

Table G1 Multi-Distance Spatial Cluster Analysis of 80 Catchments (Page 1 of 4)

ID	Location	Geology (1:20,000 - scale) [1]	Minimum Clustering Distance (m) [2]		Shortlisted Catchment by the Planning Division	Catchment Indicates Clustering by Ripley's K Function
			Relict Landslide	Recent Landslide		
0	Hung Fa Leng, NENT	V	24	<3 landslides	No	Only Relict Landslides
1	Nam Hang Mei, NENT	V	No clustering	<3 landslides	No	No
2	Tiu Tang Lung, NENT	V	22	0	Yes	Yes
3	Luk Keng, NENT	S	56	12	Yes	Yes
4	Lo Lung Tin, NENT	V	No clustering	33	No	Only Recent Landslides
5	Lai Tau Shek, NENT	S & V	17	<3 landslides	No	Only Relict Landslides
6	Wu Kau Tang, NENT	S	No clustering	<3 landslides	No	No
7	Kang Mun Tsui, Tai Po	S	No clustering	<3 landslides	No	No
8	Kang Mun Tsui, Tai Po	S	N/A	<3 landslides	No	No
9	Sheung Miu Tin, NENT	S	No clustering	No clustering	No	No
10	Hung Shek Mun Leng, NENT	S & V	15	26	Yes	Yes
11	Shek Shui Kan, NENT	S	19	<3 landslides	No	Only Relict Landslides
12	North of Lung Shan, Tai Po	V	18	No clustering	No	Only Relict Landslides
13	Cheung Mei, NENT	S & V	26	<3 landslides	No	Only Relict Landslides
14	Chek Ma Tau, NENT	S	27	<3 landslides	No	Only Relict Landslides
15	Nai Tong Kok, Tai Po	S & V	No clustering	<3 landslides	No	No
16	Hok Tau Reservoir, NENT	V	40	28	Yes	Yes
17	Wang Leng, NENT	S	11	2	Yes	Yes
18	South of Lung Shan, Tai Po	V	44	<3 landslides	No	Only Relict Landslides
19	Lai Pek Shan, Tai Po	V	9	No clustering	No	Only Relict Landslides
20	Chung Pui, Tai Po	V	26	11	No	Yes
21	Cloudy Hill, Tai Po	V	No clustering	<3 landslides	No	No

Table G1 Multi-Distance Spatial Cluster Analysis of 80 Catchments (Page 2 of 4)

ID	Location	Geology (1:20,000 - scale) [1]	Minimum Clustering Distance (m) [2]		Shortlisted Catchment by the Planning Division	Catchment Indicates Clustering by Ripley's K Function
			Relict Landslide	Recent Landslide		
22	Lai Pek Shan, Tai Po	V	22	<3 landslides	No	Only Relict Landslides
23	Fu Tau Sha, Tai Po	S	24	<3 landslides	No	Only Relict Landslides
24	Sam Mun Shan, Tai Po	S	20	<3 landslides	No	Only Relict Landslides
25	Pak Tai To Yan, Tai Po	V	11 [3]	6 [3]	Yes	Yes
26	Chung Sha Teng, Tai Po	V	12	<3 landslides	No	Only Relict Landslides
27	Sheung Ma Shek, Tai Po	G	38	<3 landslides	No	Only Relict Landslides
28	Cham Shuen Wan, Sai Kung	V	No clustering	<3 landslides	No	No
29	Wong Nai Fai, Sha Tin	S	30	<3 landslides	No	Only Relict Landslides
30	Nam She Au, Tai Po	V	14	<3 landslides	No	Only Relict Landslides
31	Tai Mo Shan, Tai Po	V	53	<3 landslides	No	Only Relict Landslides
32	Ngau Wu Tun, Tai Po	V	No clustering	<3 landslides	No	No
33	Ma On Shan, Sha Tin	G	No clustering	<3 landslides	No	No
34	Nim Au, Sha Tin	V	27	1	No	Yes
35	Chat Wan, Sai Kung	V	No clustering	<3 landslides	No	No
36	Tai Mo Shan, Tai Po	V	12	<3 landslides	No	Only Relict Landslides
37	Tiu Shau Ngam, Sha Tin	S	No clustering	<3 landslides	No	No
38	Grassy Hill, Sha Tin	S	21	<3 landslides	No	Only Relict Landslides
39	Pyramid Hill, Sai Kung	V	N/A	<3 landslides	No	No
40	Needle Hill, Sha Tin	G	21	<3 landslides	No	Only Relict Landslides
41	Sheung Fa Shan, Tsuen Wan	V	N/A	<3 landslides	No	No
42	Sharp Island, Sai Kung	V	No clustering	<3 landslides	No	No
43	Lion Rock, Kowloon	G	17	<3 landslides	No	Only Relict Landslides
44	Sai Shan, Kwai Tsing	G	No clustering	<3 landslides	No	No

Table G1 Multi-Distance Spatial Cluster Analysis of 80 Catchments (Page 3 of 4)

ID	Location	Geology (1:20,000 - scale) (1)	Minimum Clustering Distance (m) (2)		Shortlisted Catchment by the Planning Division	Catchment Indicates Clustering by Ripley's K Function
			Relict Landslide	Recent Landslide		
45	Razor Hill, Sai Kung	V	No clustering	<3 landslides	No	No
46	Fei Ngo Shan, Kowloon	V	3 (3)	1 (3)	Yes	Yes
47	Mau Wu Shan, Sai Kung	V	26	<3 landslides	No	Only Relict Landslides
48	Mount Cameron, Wan Chai	V & G	No clustering	<3 landslides	No	No
49	Tai O, W Lantau	S	38	<3 landslides	No	Only Relict Landslides
50	Tai O, W Lantau	S	16(3)	32(3)	Yes	Yes
51	Sham Wat, W Lantau	V	37	8	Yes	Yes
52	Tai O, W Lantau	S	No clustering	No clustering	No	No
53	Nam Shan, W Lantau	G	No clustering	<3 landslides	No	No
54	Cheung Shan, W Lantau	V	23	No clustering	No	Only Relict Landslides
55	Upper Keung Shan, West Lantau	V	<3 landslides	<3 landslides	No	No
56	Keung Shan Road, W Lantau	V	17 (3)	1 (3)	Yes	Yes
56A			No clustering(3)	No clustering (3)	N/A (adjacent catchment)	No
57	Lower Keung Shan, W Lantau	V & S	No clustering	<3 landslides	No	No
58	Keung Shan Road, W Lantau	V	22 (3)	1 (3)	Yes	Yes
59	Kwun Yam Shan, W Lantau	V	17	12	Yes	Yes
60	Keung Shan, W Lantau	V	No clustering	No clustering	Yes	No
61	Keung Shan, W Lantau	V	28	<3 landslides	No	Only Relict Landslides
62	Kwun Yam Shan, W Lantau	V	No clustering	No clustering	Yes	No
63	Kai Kung Shan, W Lantau	V	29	No clustering	No	Only Relict Landslides
64	West of Shek Pik, W Lantau	V	No clustering	4	Yes	Only Recent Landslides
65	West of Shek Pik, W Lantau	V	18	2	Yes	Yes

Table G1 Multi-Distance Spatial Cluster Analysis of 80 Catchments (Page 4 of 4)

ID	Location	Geology (1:20,000 - scale) [1]	Minimum Clustering Distance (m) [2]		Shortlisted Catchment by the Planning Division	Catchment Indicates Clustering by Ripley's K Function
			Relict Landslide	Recent Landslide		
66	Yi O, W Lantau	V	21	34	Yes	Yes
67	West of Shek Pik, W Lantau	V	No clustering	<3 landslides	No	No
68	East of Shek Pik, W Lantau	V	No clustering	<3 landslides	No	No
69	East of Shek Pik, W Lantau	V	6	6	Yes	Yes
70	Kau Nga Ling, W Lantau	V	3	3	Yes	Yes
71	Yi O, W Lantau	V	14	<3 landslides	No	Only Relict Landslides
72	Tong Fuk, W Lantau	V	13	<3 landslides	No	Only Relict Landslides
73	Ling Wui Shan, W Lantau	V	32	16	No	Yes
74	South of Shek Pik, W Lantau	V	No clustering	N/A	No	No
75	West of Shek Pik, W Lantau	V	15	No clustering	Yes	Only Relict Landslides
76	East of Shek Pik, W Lantau	V	45	0	Yes	Yes
77	Tung Wan, W Lantau	V	No clustering	N/A	No	No
78	Sham Hang Lek, W Lantau	V	No clustering	N/A	No	No
79	Kau Ling Chung, W Lantau	V	No clustering	14	No	Only Recent Landslides
NA	Fan Kam Road, Tai Po	V	No clustering	4 [3]	N/A	Only Recent Landslides

Notes:
(1) Geology: “G” denotes granitic rocks; “S” denotes sedimentary rocks; “V” denotes volcanic rocks.
(2) Clustering distance: “< 3 landslides” indicates the number of landslide within the catchment is less than 3 and does not meet the minimum requirement for Ripley’s K function to perform. “No clustering” denotes no clustering of landslides within the catchment based on the results of Ripley’s K function analysis.
(3) Site-specific landslide inventory was adopted in the multi-distance spatial cluster analysis.

GEO PUBLICATIONS AND ORDERING INFORMATION
土力工程處刊物及訂購資料

An up-to-date full list of GEO publications can be found at the CEDD Website http://www.cedd.gov.hk on the Internet under "Publications". The following GEO publications can also be downloaded from the CEDD Website:

i. Manuals, Guides and Specifications
ii. GEO technical guidance notes
iii. GEO reports
iv. Geotechnical area studies programme
v. Geological survey memoirs
vi. Geological survey sheet reports

詳盡及最新的土力工程處刊物目錄，已登載於土木工程拓展署的互聯網網頁http://www.cedd.gov.hk 的"刊物"版面之內。以下的土力工程處刊物亦可於該網頁下載：

i. 指南、指引及規格
ii. 土力工程處技術指引
iii. 土力工程處報告
iv. 岩土工程地區研究計劃
v. 地質研究報告
vi. 地質調查圖表報告

Copies of some GEO publications (except geological maps and other publications which are free of charge) can be purchased either by:

Writing to
Publications Sales Unit,
Information Services Department,
Room 626, 6th Floor,
North Point Government Offices,
333 Java Road, North Point, Hong Kong.

or

- Calling the Publications Sales Section of Information Services Department (ISD) at (852) 2537 1910
- Visiting the online Government Bookstore at http:// www.bookstore.gov.hk
- Downloading the order form from the ISD website at http://www.isd.gov.hk and submitting the order online or by fax to (852) 2523 7195
- Placing order with ISD by e-mail at puborder@isd.gov.hk

讀者可採用以下方法購買部分土力工程處刊物(地質圖及免費刊物除外):

書面訂購
香港北角渣華道333號
北角政府合署6樓626室
政府新聞處
刊物銷售組

或

- 致電政府新聞處刊物銷售小組訂購 (電話：(852) 2537 1910)
- 進入網上「政府書店」選購，網址為 http://www.bookstore.gov.hk
- 透過政府新聞處的網站 (http://www.isd.gov.hk) 於網上遞交訂購表格，或將表格傳真至刊物銷售小組 (傳真：(852) 2523 7195)
- 以電郵方式訂購 (電郵地址：puborder@isd.gov.hk)

1:100 000, 1:20 000 and 1:5 000 geological maps can be purchased from:

Map Publications Centre/HK,
Survey & Mapping Office, Lands Department,
23th Floor, North Point Government Offices,
333 Java Road, North Point, Hong Kong.
Tel: (852) 2231 3187
Fax: (852) 2116 0774

讀者可於下列地點購買1:100 000、1:20 000及1:5 000地質圖：

香港北角渣華道333號
北角政府合署23樓
地政總署測繪處
電話: (852) 2231 3187
傳真: (852) 2116 0774

Any enquires on GEO publications should be directed to:

Chief Geotechnical Engineer/Standards and Testing,
Geotechnical Engineering Office,
Civil Engineering and Development Department,
Civil Engineering and Development Building,
101 Princess Margaret Road,
Homantin, Kowloon, Hong Kong.
Tel: (852) 2762 5351
Fax: (852) 2714 0275
E-mail: ivanli@cedd.gov.hk

如對本處刊物有任何查詢，請致函：

香港九龍何文田公主道101號
土木工程拓展署大樓
土木工程拓展署
土力工程處
標準及測試部總土力工程師
電話: (852) 2762 5351
傳真: (852) 2714 0275
電子郵件: ivanli@cedd.gov.hk